SPORE GERMINATION IN THE FUNGUS

Syncephalastrum racemosum

(Electron micrographs, graphs, tables and diagrams)

Volume Two

Thesis submitted in accordance with the regulations of the University of Kent at Canterbury for the degree of

Doctor of Philosophy

by

Jan Adam Hobot

1977

CONTENTS

KEY

PS - phase contrast micrograph

SEM - scanning electron micrograph (bar represents 1 μm)

SR - surface replica micrograph

FF - freeze fracture micrograph

TS - thin section micrograph

MS - metal shadow micrograph

ELECTRON MICROGRAPHS

A - spore/germ tube wall

B - " " " "

C - " " " "

D - " " " "

D_1 - " " " "

D_2 - " " " "

Am - amorphous layer

Cy - cytoplasm

EM - electron microscope

H - vegetative hypha

Ha - aerial hypha

IP - intermediate particle

M - mitochondria

N - nucleus

P - plasmamembrane

R - nucleolus

S - surface rodlet layer

Sd - spore with depression

Sp - spherical spore

Sr - rectangular spore

St - terminal spore

Sw - swollen spore

T - nuclear membrane

W - spore wall

X - breakpoint

Y - point of attachment

a - ampulla/sporangium

b - wrinkled bumps

d - crystal-like deposits

g - germ tube

m - merosporangia

mf - microfibrils

p - hyphal apex

GRAPHS/TABLES

dw - dry weight ($mg.ml^{-1}$)

f - frequency in population (%)

G.L.C. - gas liquid chromatography

%gt - percentage germ tube emergence

R_t - retention time (minutes)

sd - average spore diameter (m)

sdc - spore diameter classes (m)

sdw - sterile distilled water

t - time after inoculation (hours)

temp (^{o}C) - temperature (^{o}C)

tg - time in glucose medium before transfer (hours)

CHAPTER ONE

Fig. 1

SEM of vegetative hyphae. Lateral branching gives rise to hyphae with side-branches at some distance back from the tip (bar = 1μm)

Fig. 2

SR of vegetative hyphae. The mycelium is seen as an interwoven net of criss-crossing hyphae (H). These vegetative hyphae have smooth outer walls (x2000).

10μ

Fig. 3

SR of vegetative hyphae. The smooth outer surface of the hyphae is again evident. Near the apex of the hyphae (p), small pock marks are discernable (x2600).

Fig. 4

SR of vegetative hyphae. Higher magnification of a hyphal apex showing more clearly the small pock marks as being small depressions or craters just around the tip (p)(x20200).


p
H
p


p

Fig. 5

SEM of aerial hyphae (Ha) with the sporangium or ampulla (a) at the tip. Small sac-like protrusions (the merosporangia,m) are just beginning to develop. Crystal-like deposits (d) are seen on both the aerial hyphae and sporangium surfaces (Bar = 1 μm)

Fig. 6

SEM of the sporangium. The merosporangia (m) elongate as development proceeds. Crystal-like deposits (d) are seen on the sporangium surface. (Bar = 1 μm)

Fig. 7

SEM of the sporangium. Further extension of the merosporangia (m) is noticeable. The base of the sacs are smaller in diameter than the rest of the structure (arrows). Crystal-like deposits (d) are seen both on the aerial hypha and sporangium (Bar = 1 μm)

۱μ

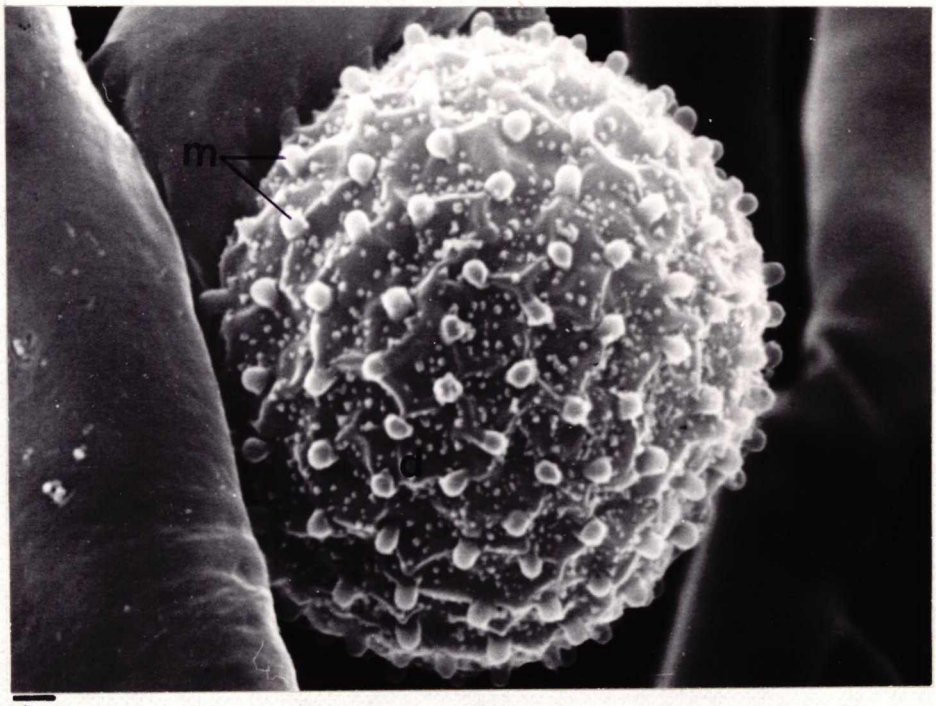

۱μ

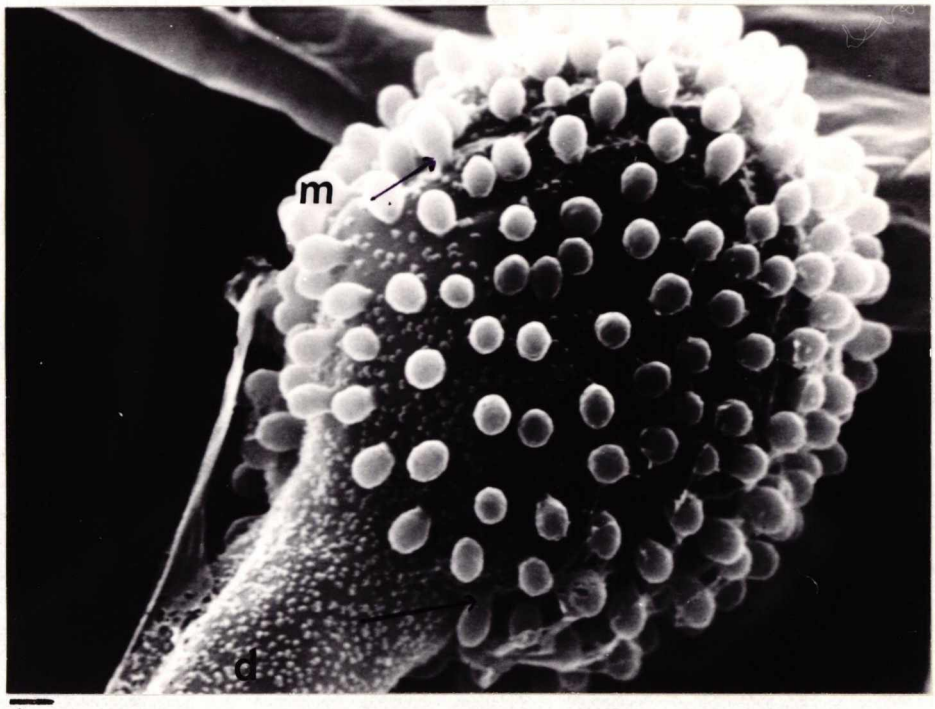

۱μ

Fig. 8

SEM of aerial hypha (Ha) bearing developing merosporangia (m). The merosporangia (m) now have a tubular appearance (Bar = 1μm)

Fig. 9

SEM of fully developed merosporangia (m). Crystal-like deposits are seen on the aerial hyphal surfaces (Bar = 1μm)

10μ

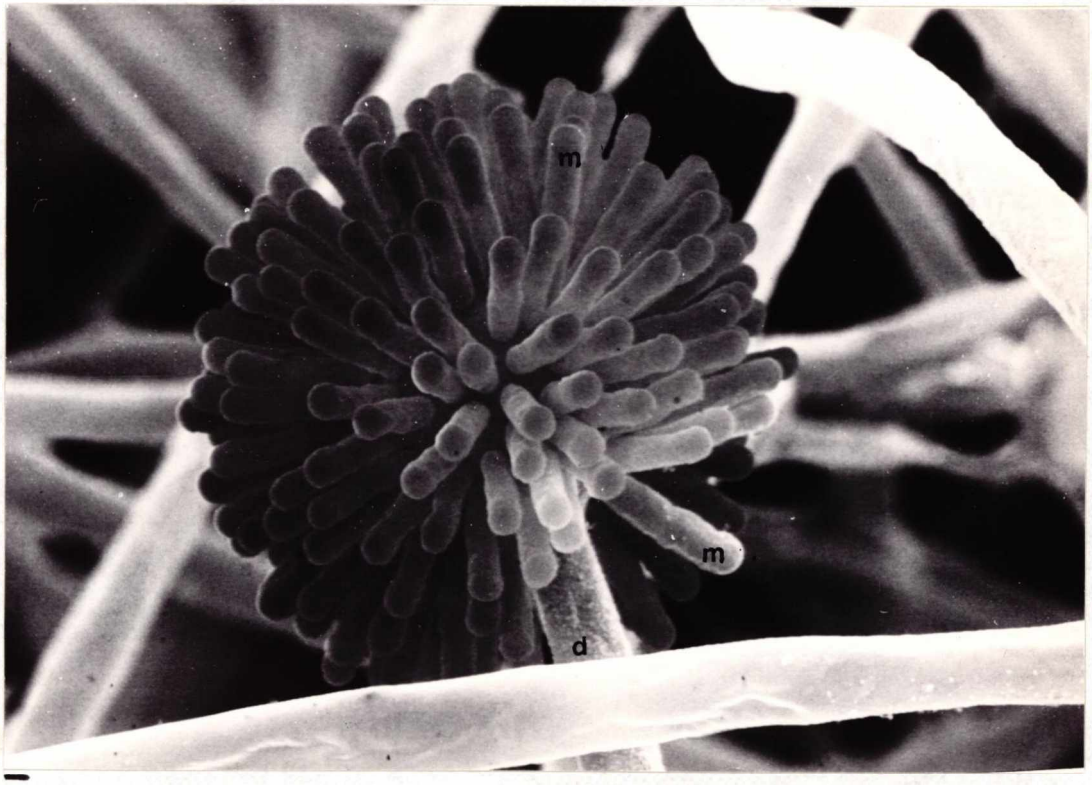

4

Fig.10

SR of sporangium. Rectangular crystal-like deposits are noticeable (d) on both the sporangium (a) and aerial hyphal (Ha) surface. The small circular structures (c) are probably the sites of attachment of the merosporangia (x 4800)

Fig.11

SR of sporangium surface. Higher magnification of the ampulla shows more clearly the rectangular shape of the crystal-like deposits (d) and also the circular structure (c). The sporangium surface has a rodlet pattern (S) (x21300)

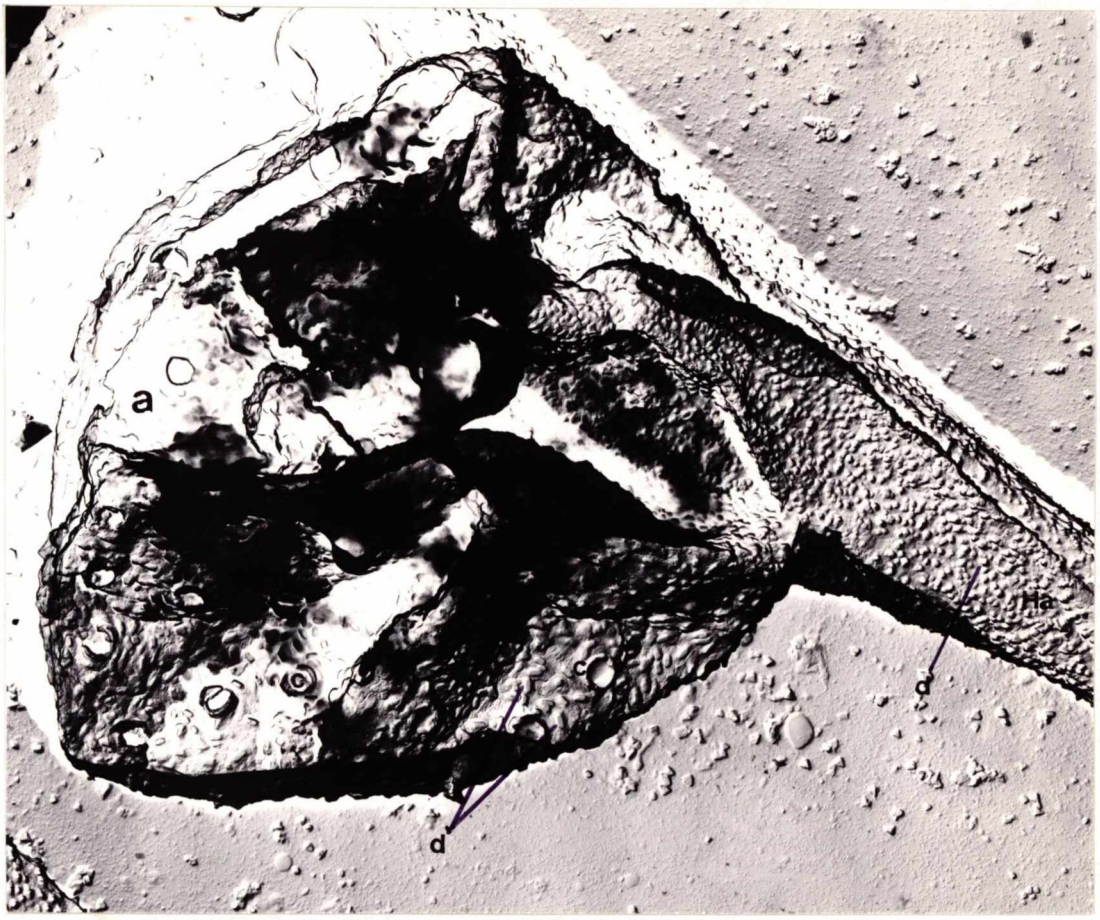
a
d
d

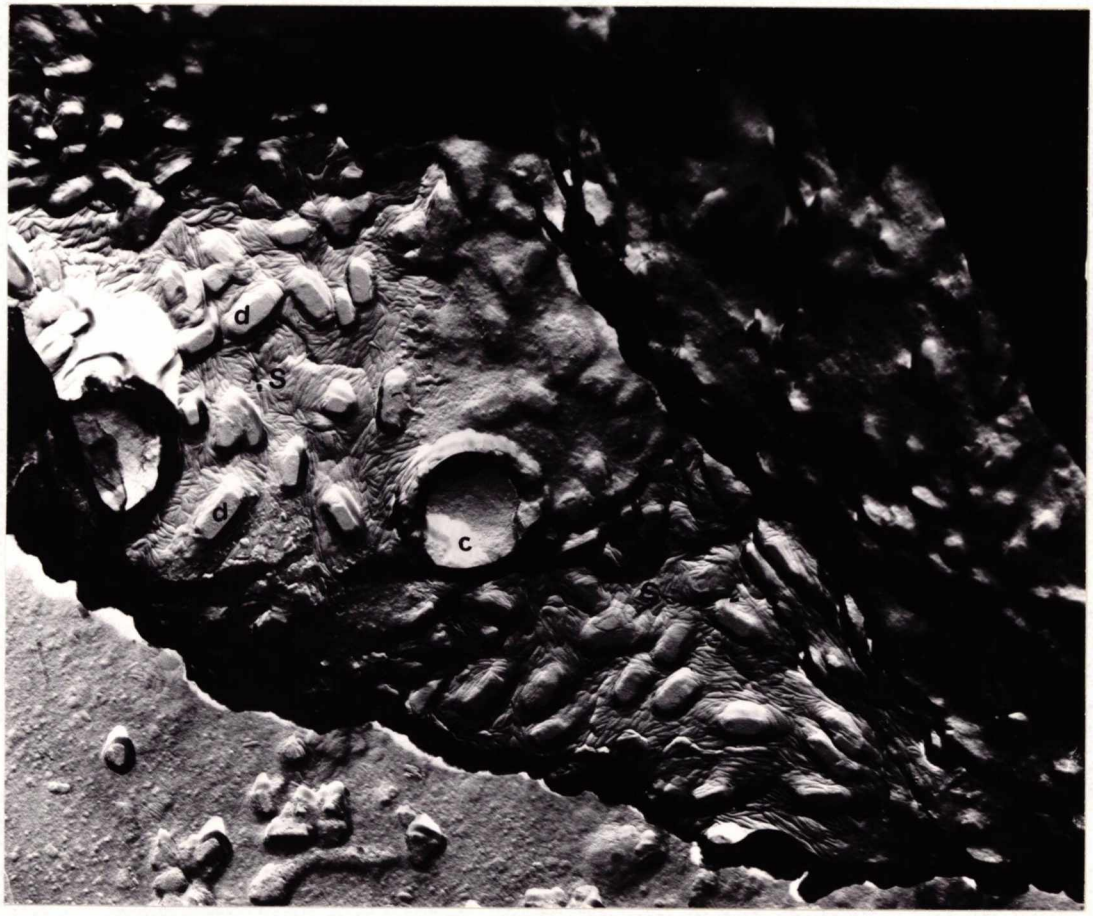
d
S
d
c

Fig. 12

SR of an aerial hypha or sporangiophore. The surface rodlet pattern (S) is covered with numerous crystal-like deposits (d) (x27500)

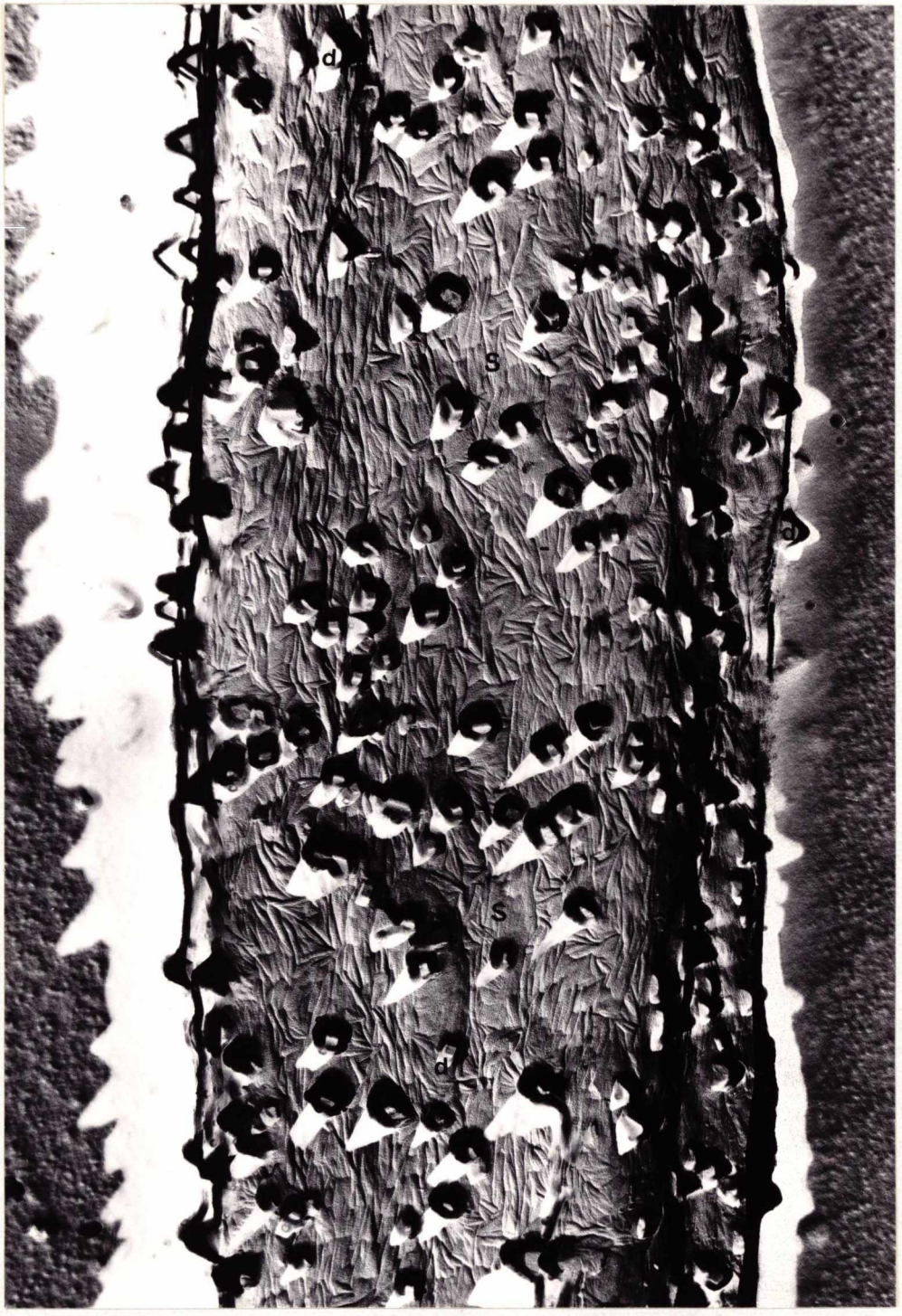
d
S
d
S
d

Fig. 13

SR of dormant spores. There are nine mature spores in the chain, each having a rectangular shape, except the terminal spore (St) which is rounded at one end (x7900)

Fig.14

SR of dormant spores. Besides rectangular-shaped spores, the terminal spore (St) rounded at one end is also seen (x12200)

Fig. 15

SR of dormant spores. A diversity of spore shapes is observable: rectangular (Sr); spherical (Sp), with or without depressions (Sd) (x1900)

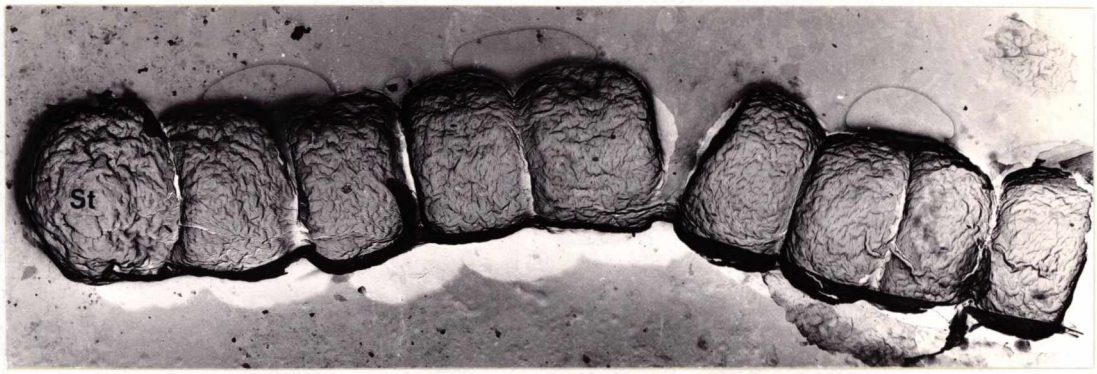
St


St
Sr
St

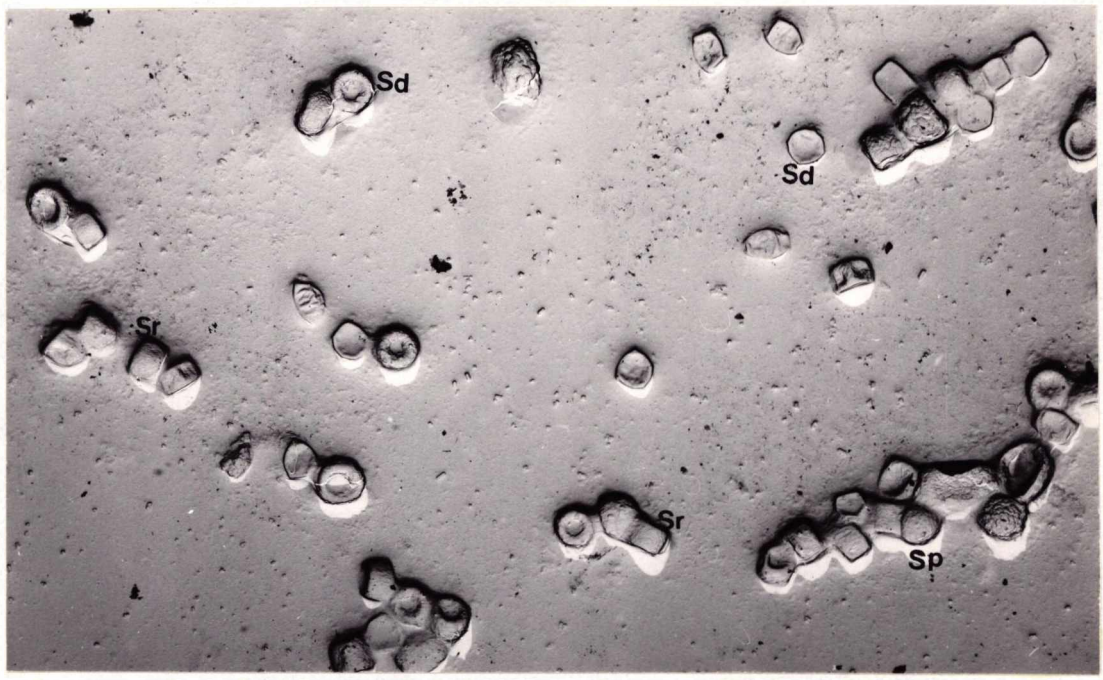
Sd
Sd
Sr
Sr
Sp

Fig. 16

SR of dormant spores. The spherical spore on the left has a circular, central depression which is free of any surface ornamentation. The surface ornamentation is also noticeable on the other two rectangularly-shaped spores (x15100)

Fig. 17

SR of a long, dormant spore. The surface ornamentation is a surface layer arranged in a criss-cross pattern of small groups of rodlets (S) (x15200)

Fig. 18

FF of a dormant spore, revealing surface layer of rodlets, arranged in a criss-cross pattern of small groups of rodlets (x36100)

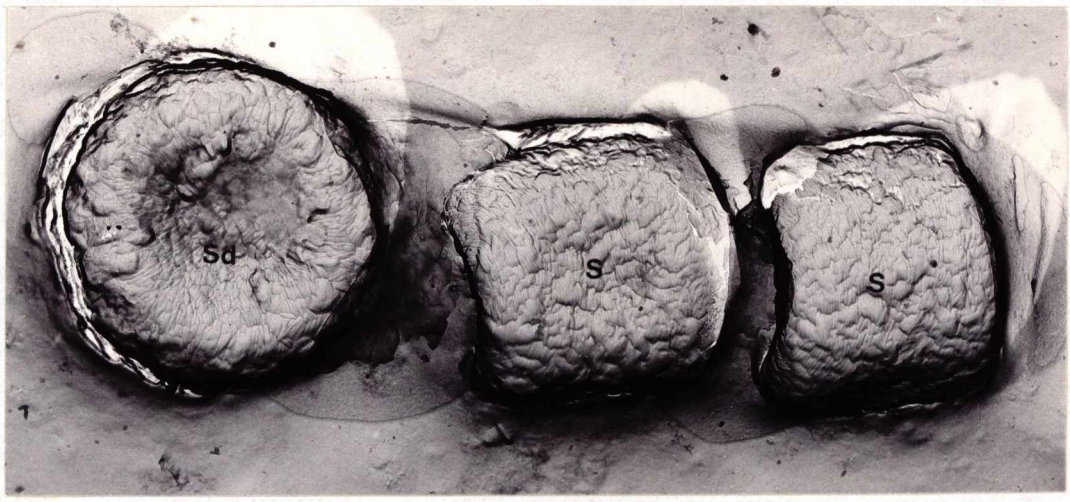
Sd
S
S

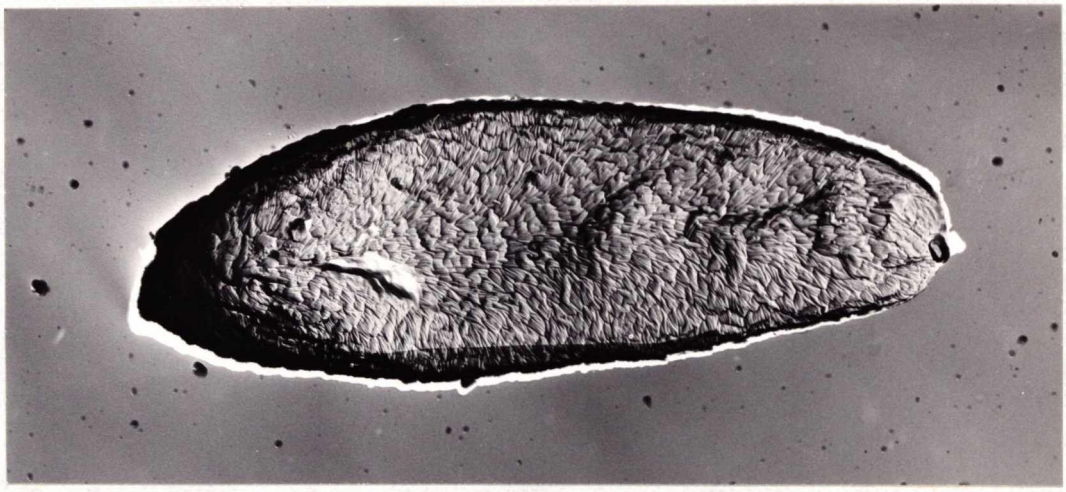

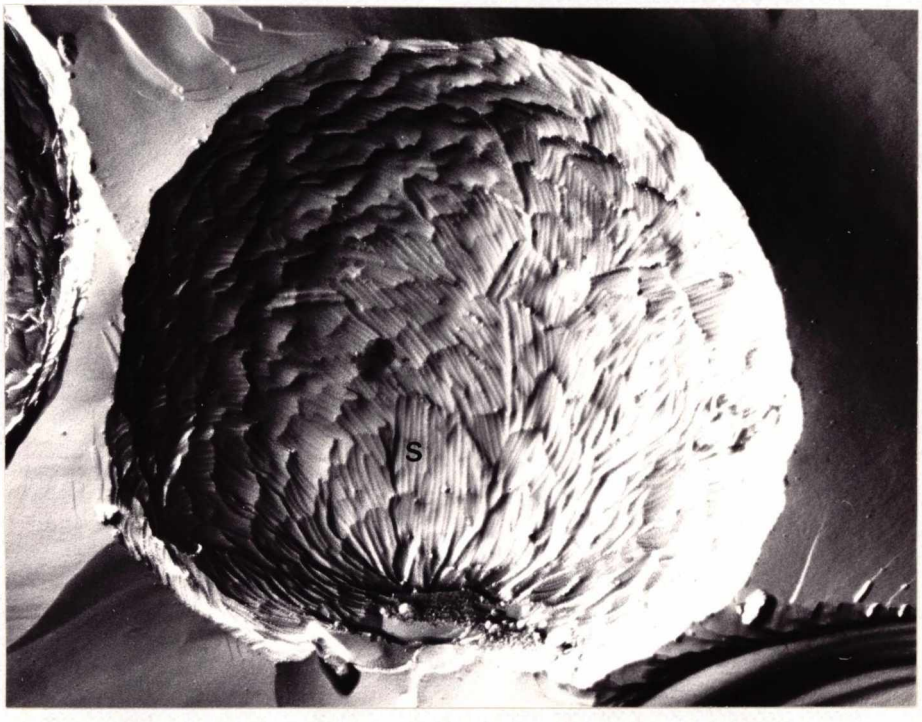
S

Fig. 19

SR of aerial hypha. Crystal-like deposits (d) and a surface layer of rodlets (S) are both present. This contrasts sharply with the smooth outer wall of vegetative hyphae seen in the next figure (x50000)

Fig. 20

SR of vegetative hypha. The hyphae of the mycelial mat, as represented by the hypha in this micrograph, have smooth outer walls with no crystal-like deposits being present (x5500)

Fig. 21

SR of an empty merosporangial sac. The surface of the sac appears smooth, although it is possible that a surface rodlet layer is present (arrows) (x14400)

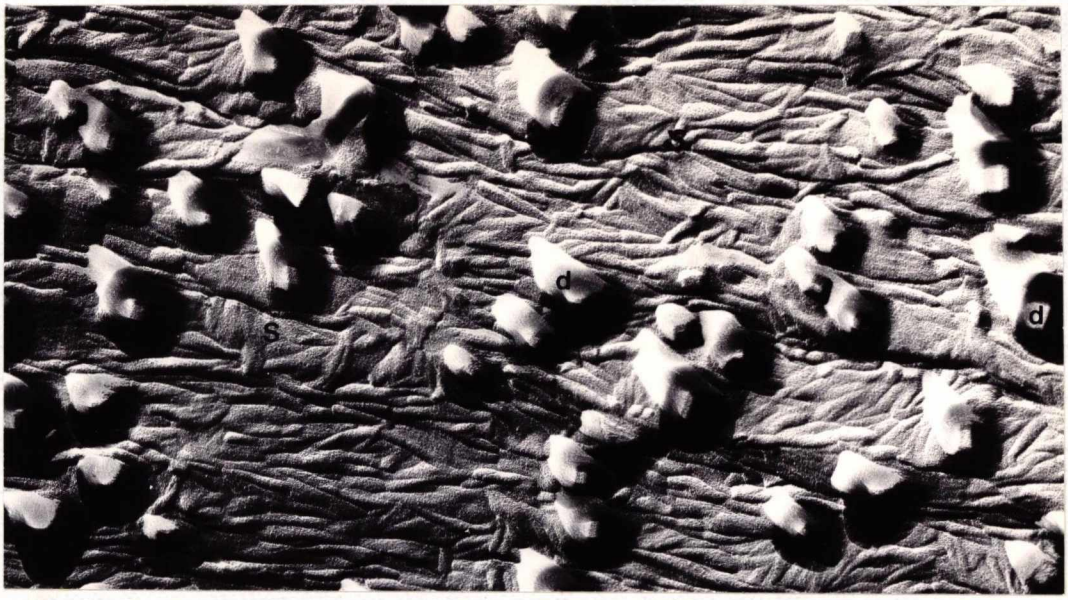
S
d
d
d


H

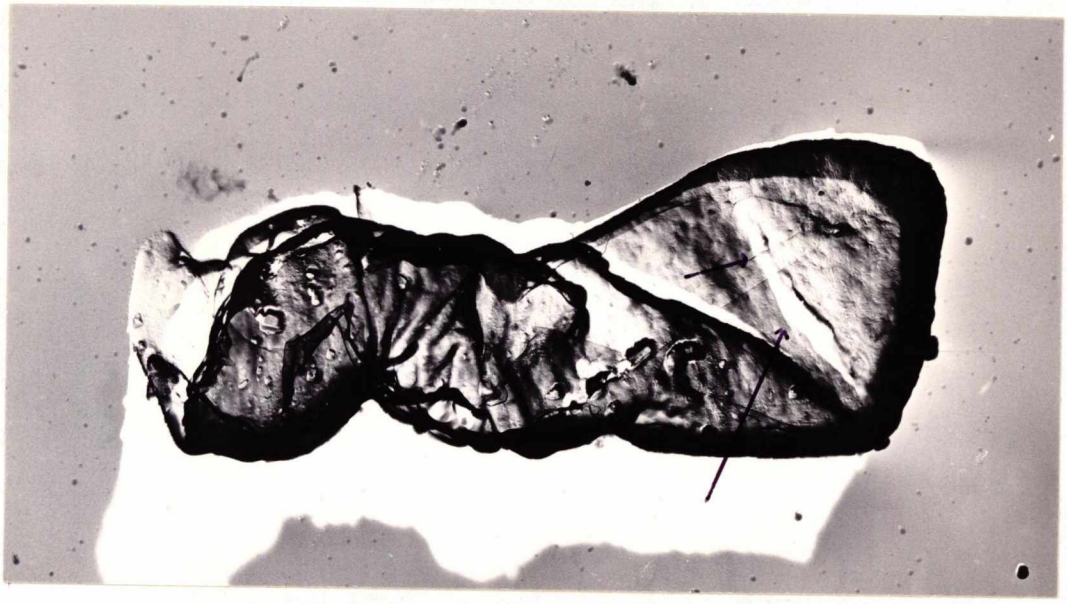

Fig. 22

SEM of a swollen spore. The spore is spherical in shape (Bar = 1μm)

Fig. 23

SEM of spore with germ tube. A possible breakpoint (X) is noticeable between the spore (Sp) and germ tube (g) (Bar = 1 μm)

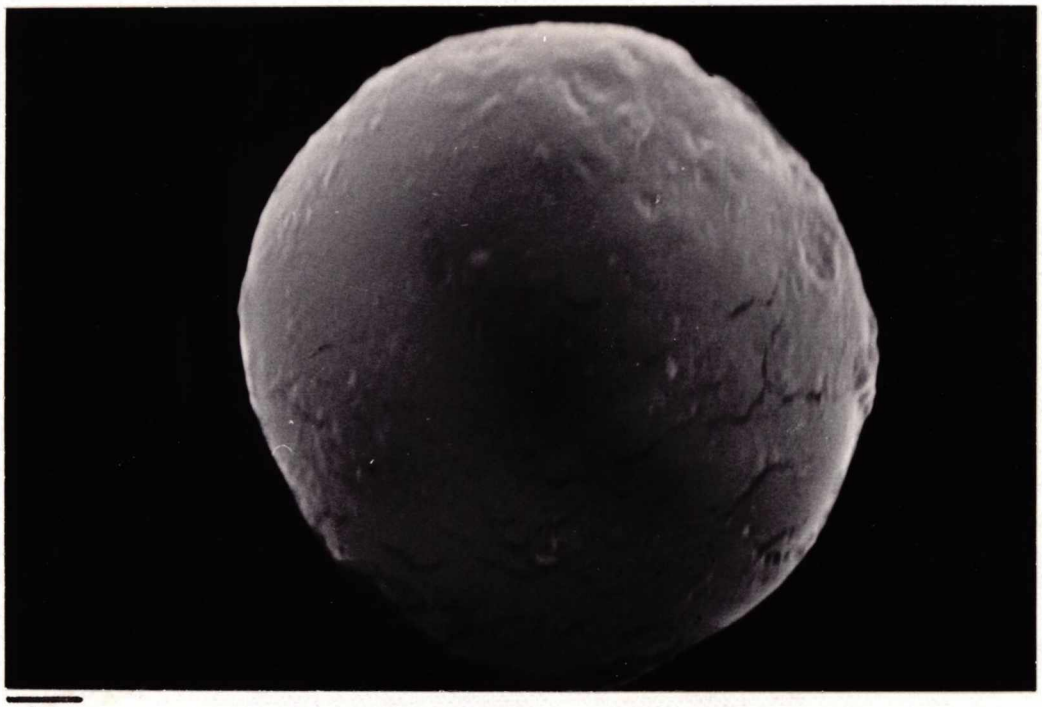

1μ

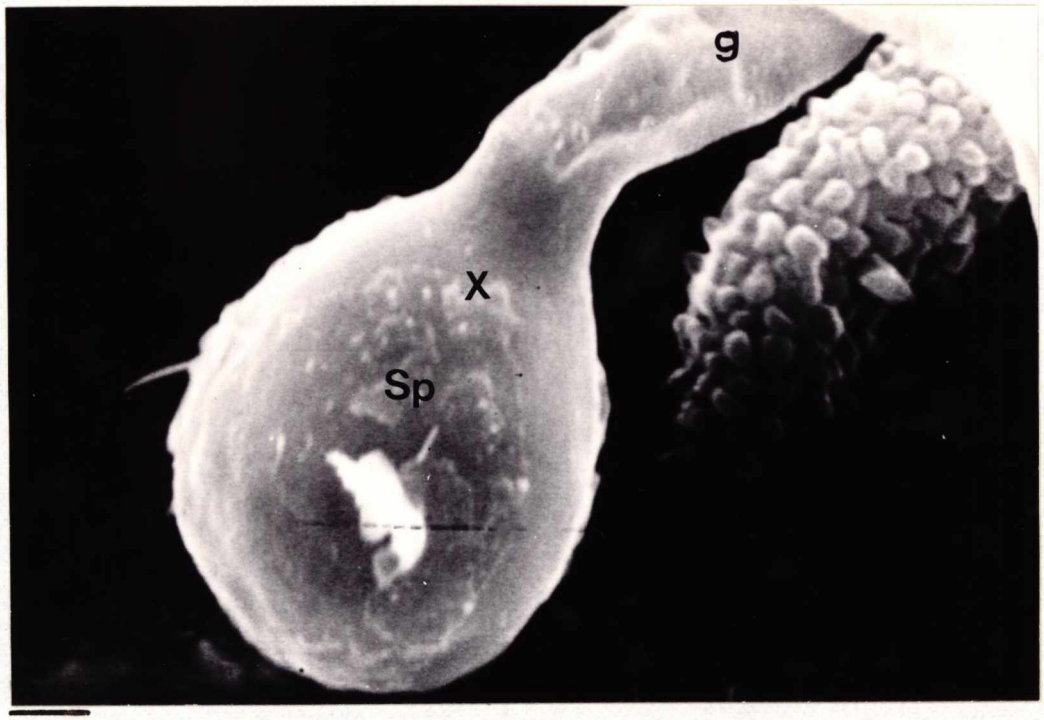

1μ

CHAPTER TWO

Fig. 24

Photograph of the Batch Fermenter System.

1 - Rotameter

2 - air in

3 - sterile air filter

4 - IL Quickfit pot

5 - stainless steel propeller shaft

6 - teflon stopper

7 - point of attachment to overhead electric motor

8 - sampling port

9 - sampling bottle

10 - inoculation port

11 - air out

12 - condenser

13 - air filter (glass wool)

14 - silicon tubing

15 - stainless steel tubing

The pot was mounted in a water bath heated to 37.5°C. This gave a temperature of 37°C inside the pot.

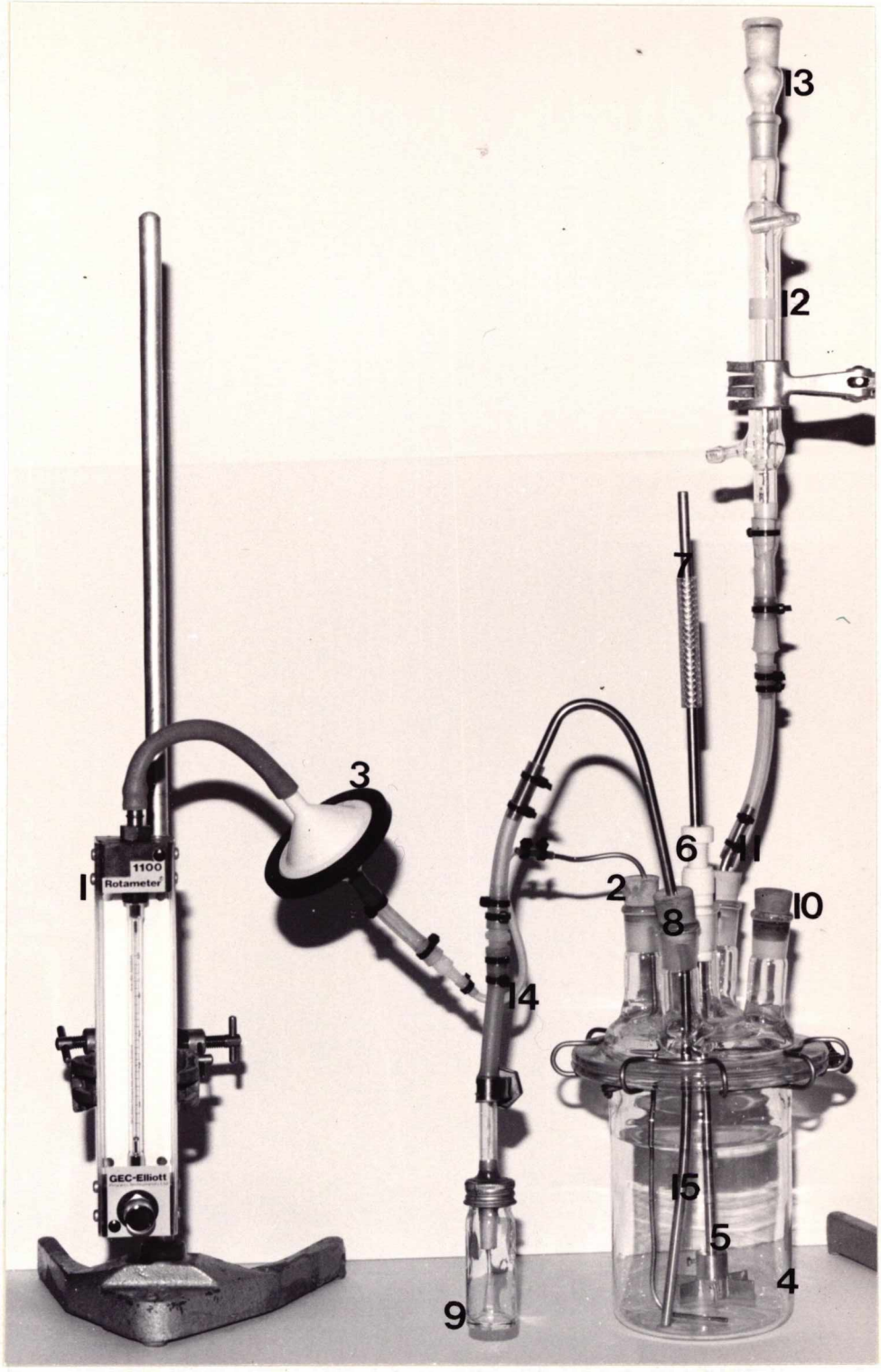
13
12
7
3
6
1
1100
Rotameter
2
8
10
14
GEC-Elliott
15
5
4
9

Fig. 25

PS of dormant spores. They have a refractile appearance (x920)

Fig. 26

PS of swollen spores. The spores have lost some of their refractility (x860)

Fig. 27

PS of spore with young, emergent germ tube. The germ tube is in its first stages of development (x1460)

Fig. 28

PS of spore with germ tube. The young germ tube has already formed its first lateral branch (x1030)

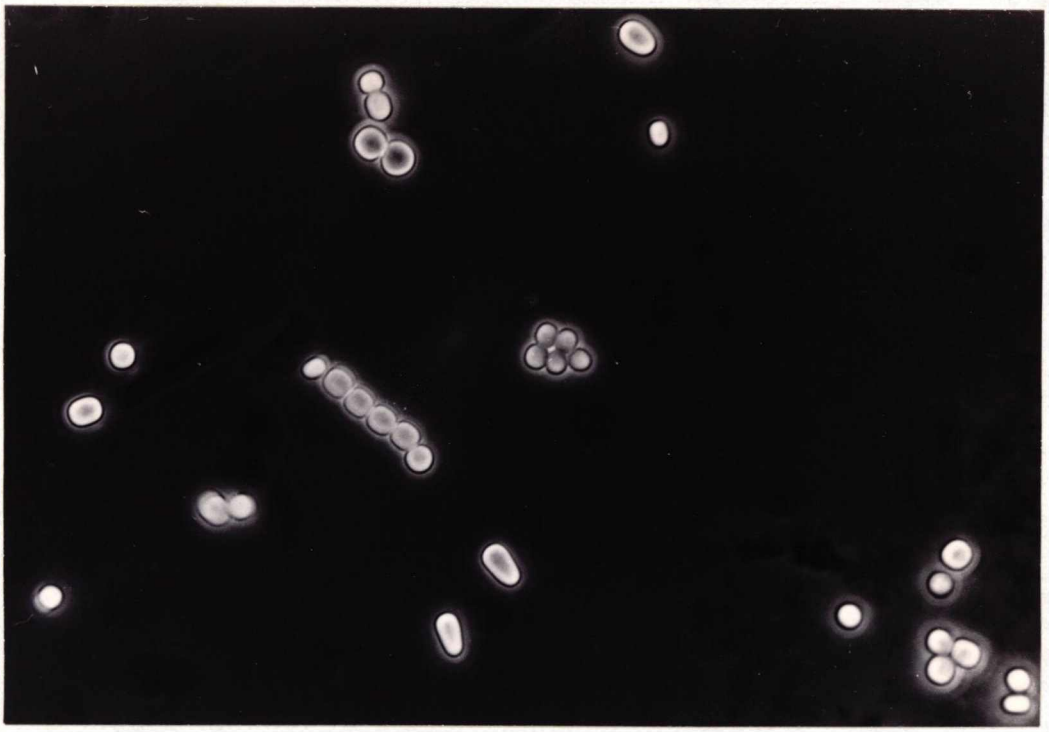

27

28

Fig. 29

Effect of temperature on the Colony Radial Growth Rate (CRGR).

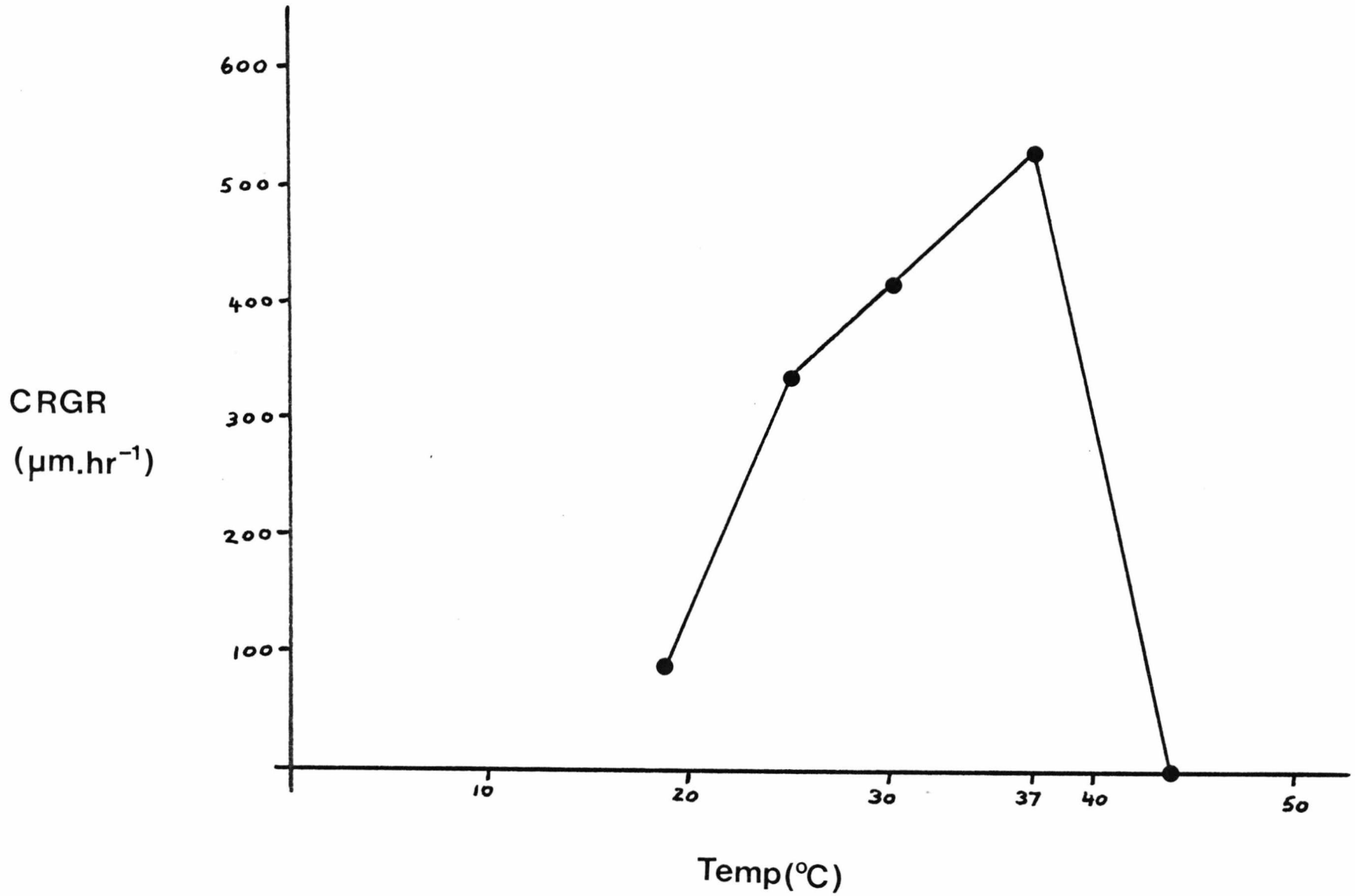
CRGR
(μm.hr⁻¹)
600
500
400
300
200
100
10
20
30
37
40
50
Temp(°C)

Fig. 30

Effect of different carbon sources on germ tube emergence. The concentration of all the carbon sources was 1% (w/v).

● galactose.

o glucose.

□ fructose.

■ sucrose.

△ succinate/citrate.

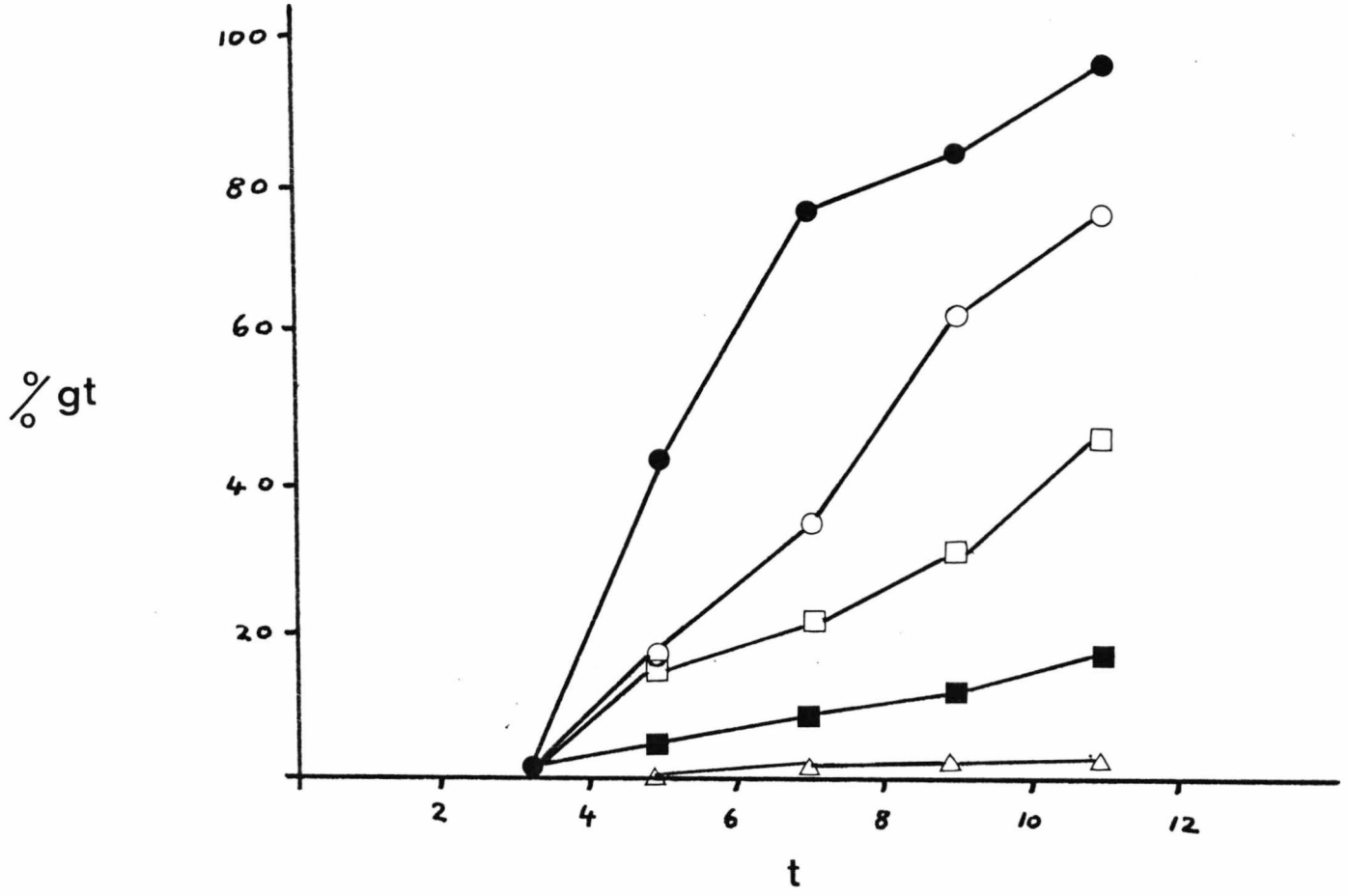
%gt
100
80
60
40
20
2
4
6
8
10
12
t

Fig. 31

Germination of spores in glucose defined medium supplemented with either succinate or citrate (0.01M).

● glucose-containing medium.

■ supplemented with succinate.

▲ supplemented with citrate.

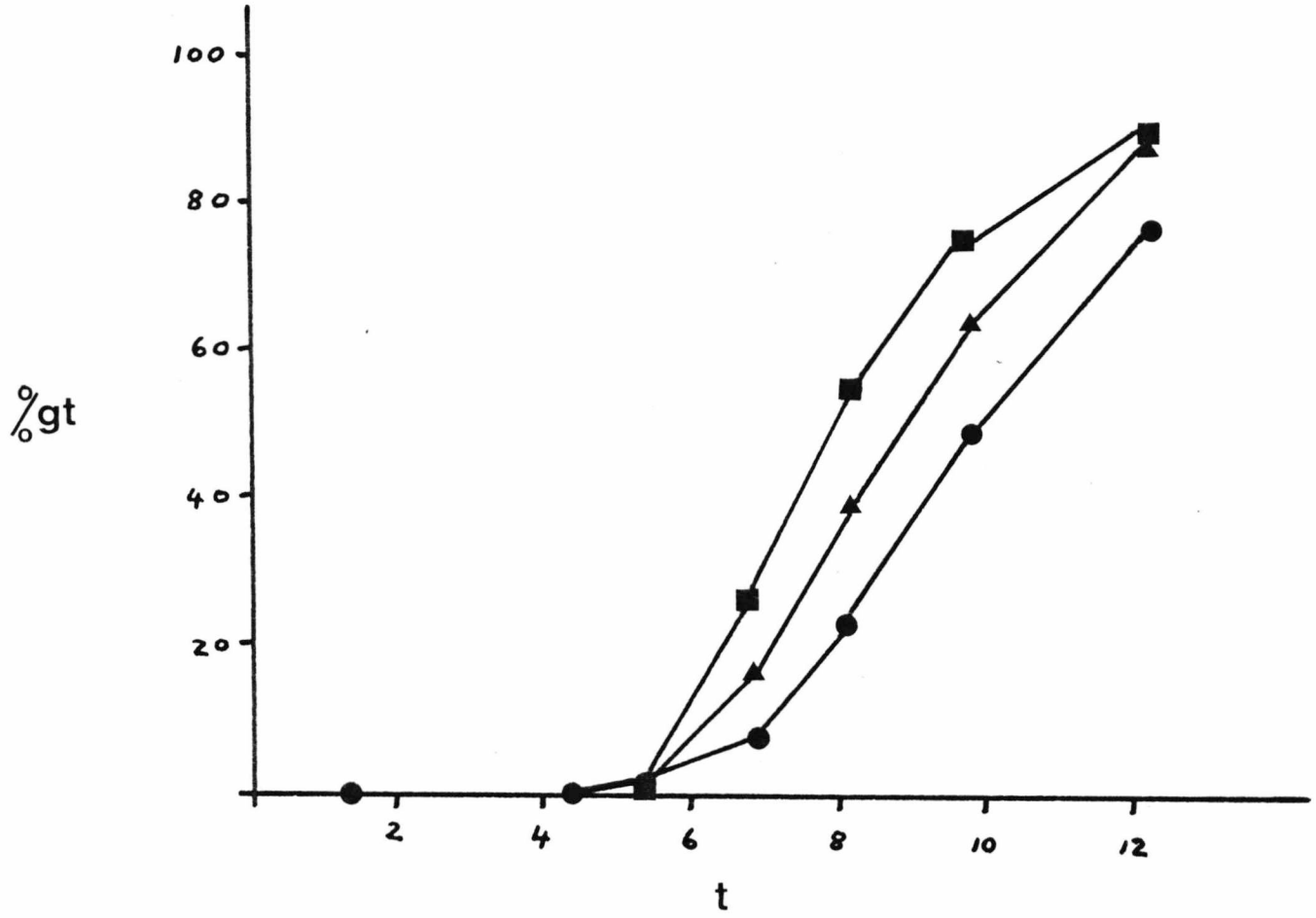
%gt
100
80
60
40
20
2
4
6
8
10
12
t

Fig. 32

Germination of spores in a typical batch fermenter culture.

● percentage germ tube emergence.

■ average spore diameter.

▲ dry weight.

The concentration of spores was 1.5×10^6 per ml. of culture medium.

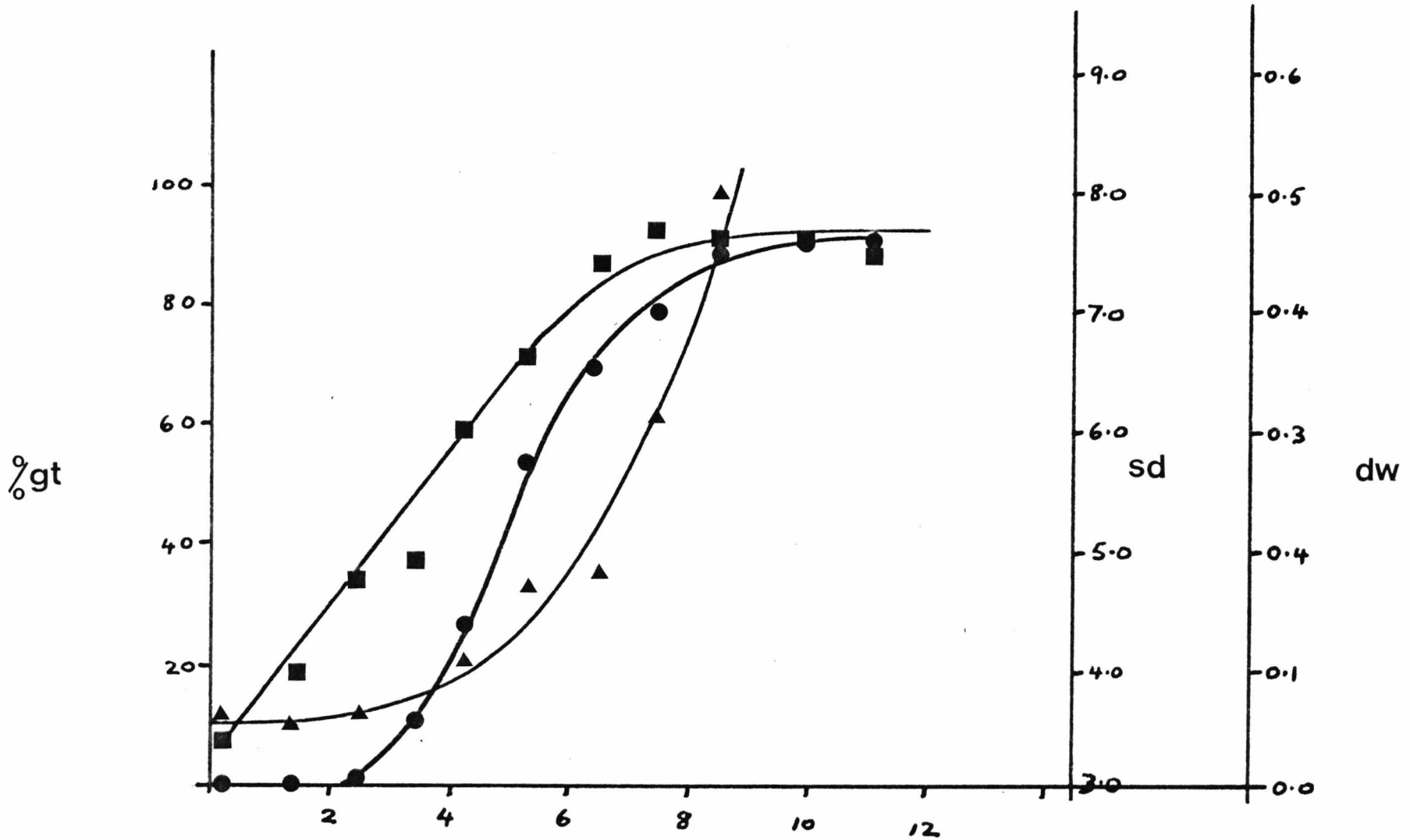
%gt
100
80
60
40
20
2
4
6
8
10
12
9·0
8·0
7·0
6·0
5·0
4·0
3·0
sd
0·6
0·5
0·4
0·3
0·4
0·1
0·0
dw

Fig. 33

Histogram of frequency of different sized spores in the population:

(A) Oh after inoculation; average spore diameter 3.4 μm; percentage germ tube emergence 0.

(B) 2.5h after inoculation; average spore diameter 4.8μm; percentage germ tube emergence 0.5%.

(C) 11.25h after inoculation; average spore diameter 7.5μm; percentage germ tube emergence 92.0%.

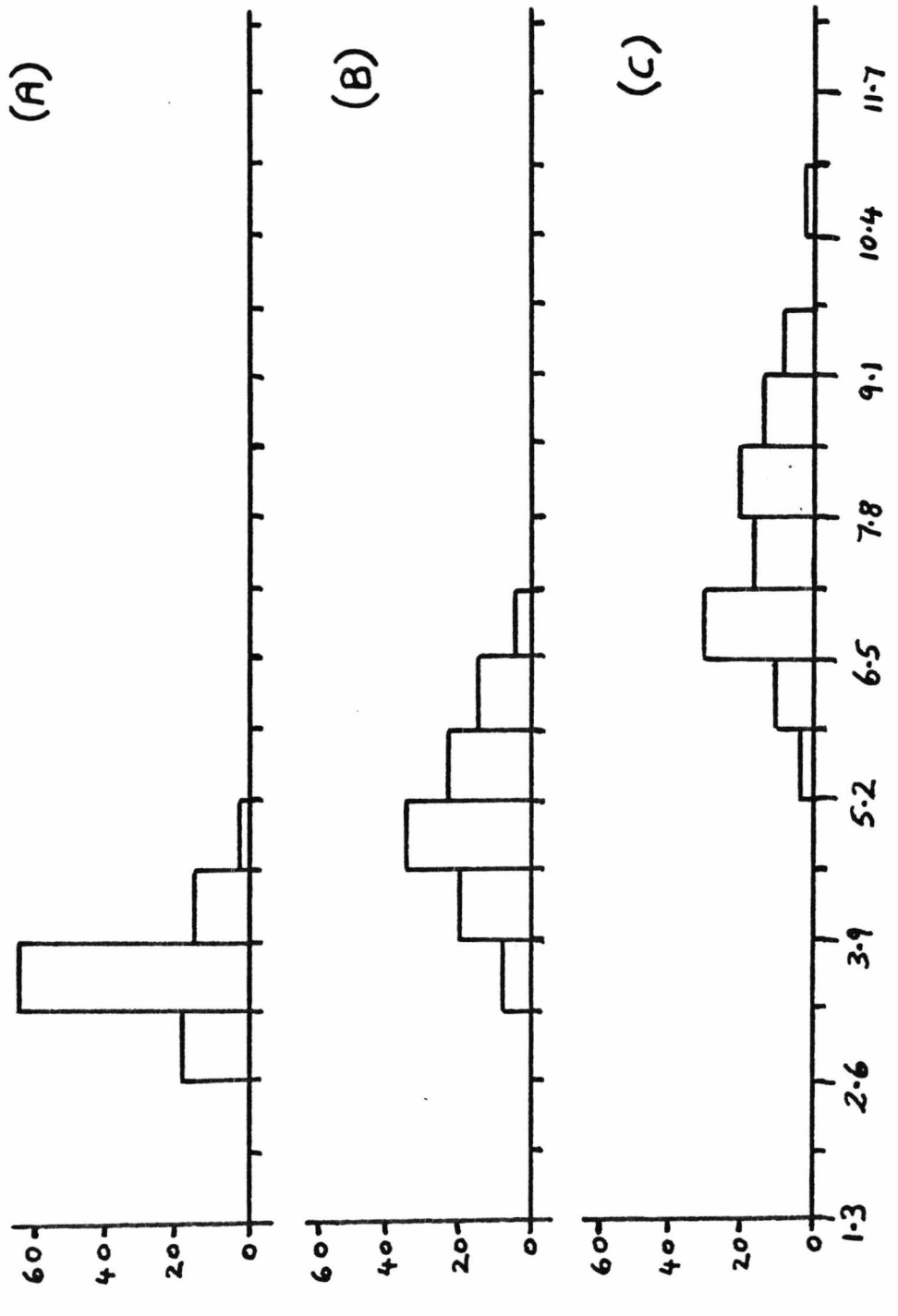
(A)
(B)
(C)
60
40
20
0
1·3
2·6
3·9
5·2
6·5
7·8
9·1
10·4
11·7
f
s d c

Fig. 34

Effect of glucose deprivation on germ tube emergence and swelling on S.racemosum spores.

- ● percentage germ tubes in a control culture containing 1% (w/v) glucose.
- O percentage germ tube emergence in the glucose-free medium.
- ■ average spore diameter in glucose grown cultures.
- □ average spore diameters in glucose-free cultures.

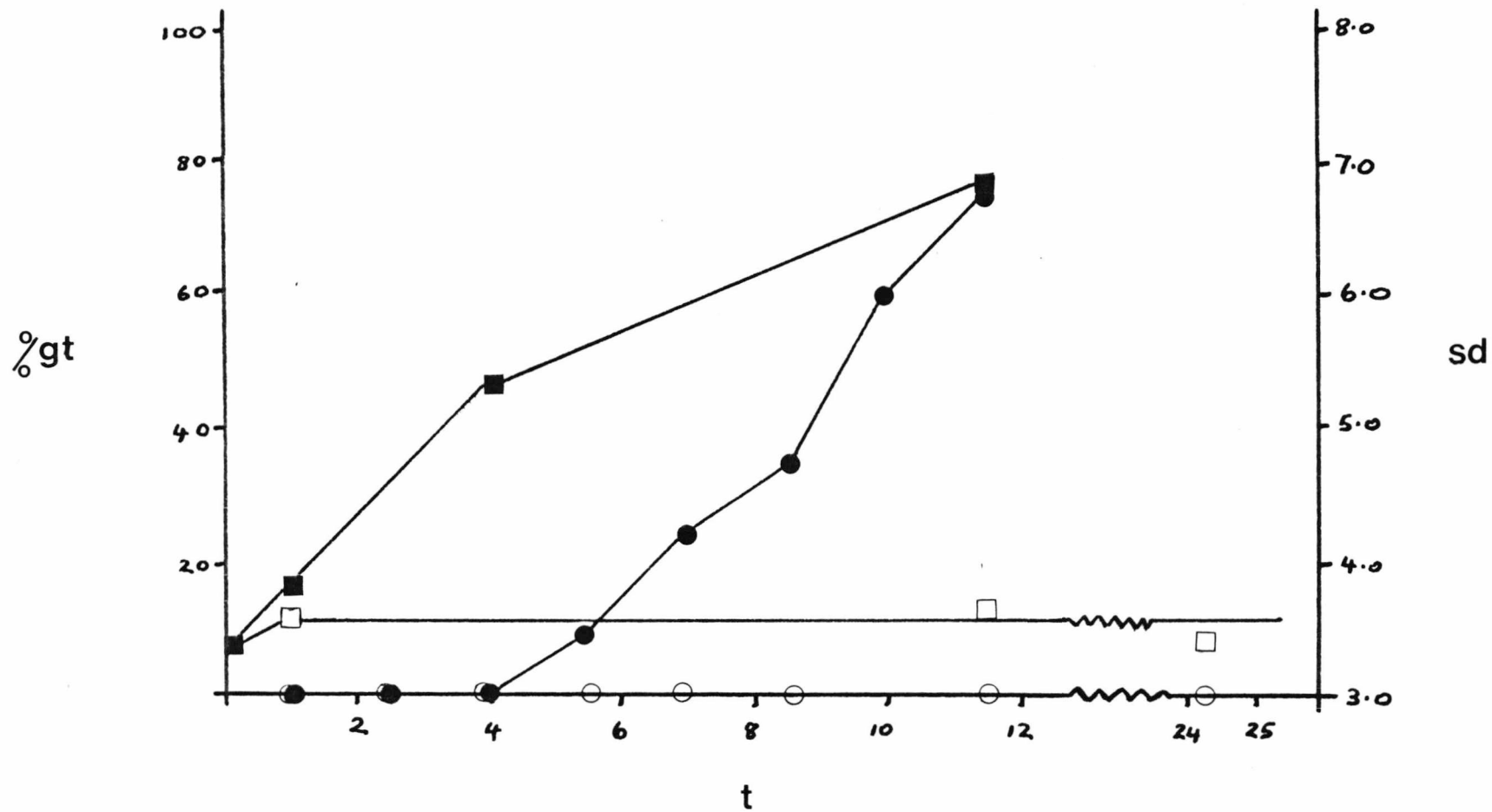
%gt
100
80
60
40
20
8·0
7·0
6·0
5·0
4·0
3·0
sd
2
4
6
8
10
12
24
25
t

Fig. 35

Effect of various glucose concentrations (G, % (w/v)) on the outgrowth of germ tubes.

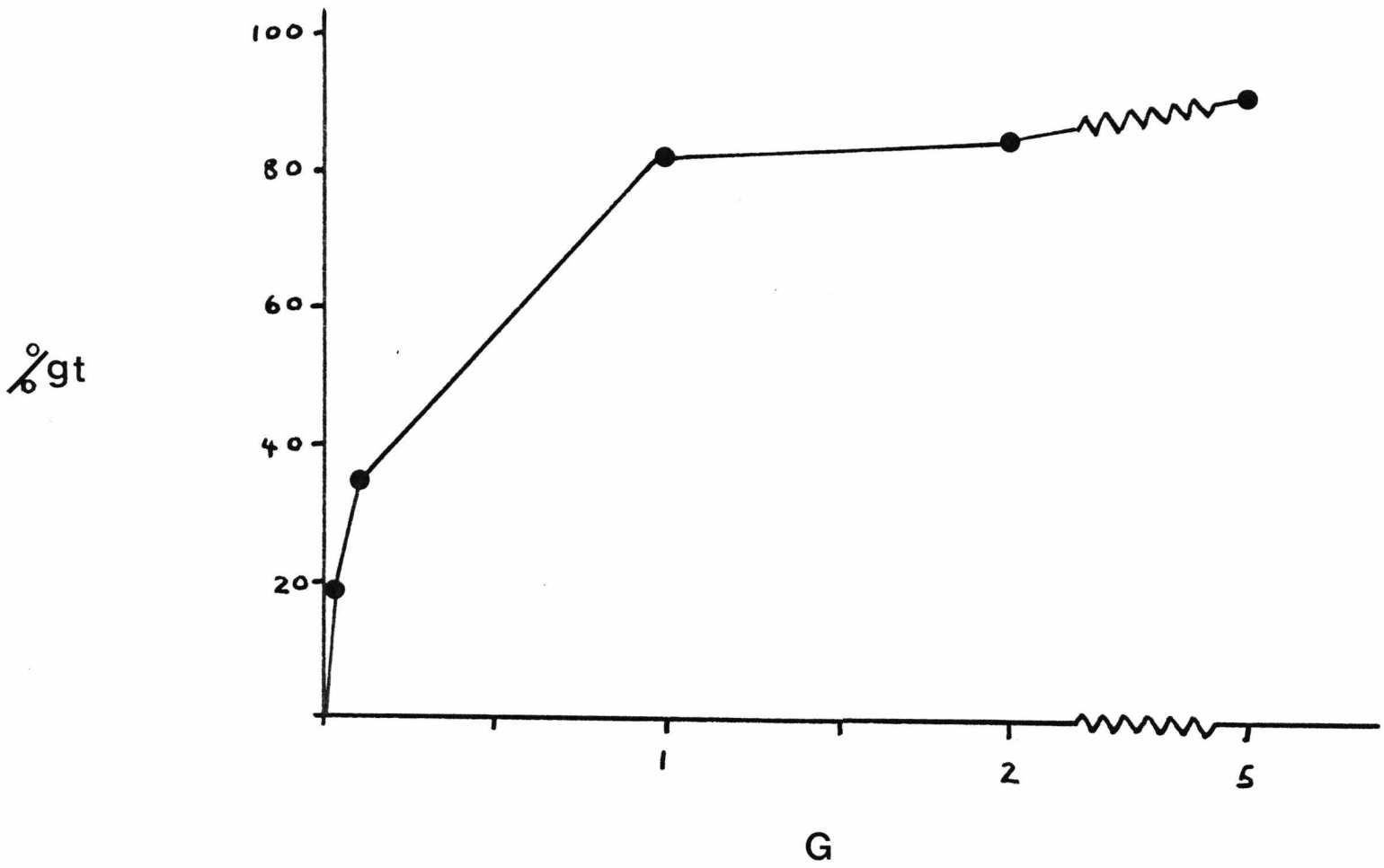
%gt
100
80
60
40
20
1
2
5
G

Fig. 36

Effect of glucose removal (shift-down) during germination on the average spore diameter. Samples were transferred from a glucose-containing medium to a glucose-free medium at hourly intervals up to 6h after inoculation.

○ control glucose grown culture.

◆ glucose-free medium.

■ shift down at 1h.

▲ shift down at 2h.

● shift down at 3h.

◇ shift down at 4h.

□ shift down at 5h.

△ shift down at 6h.

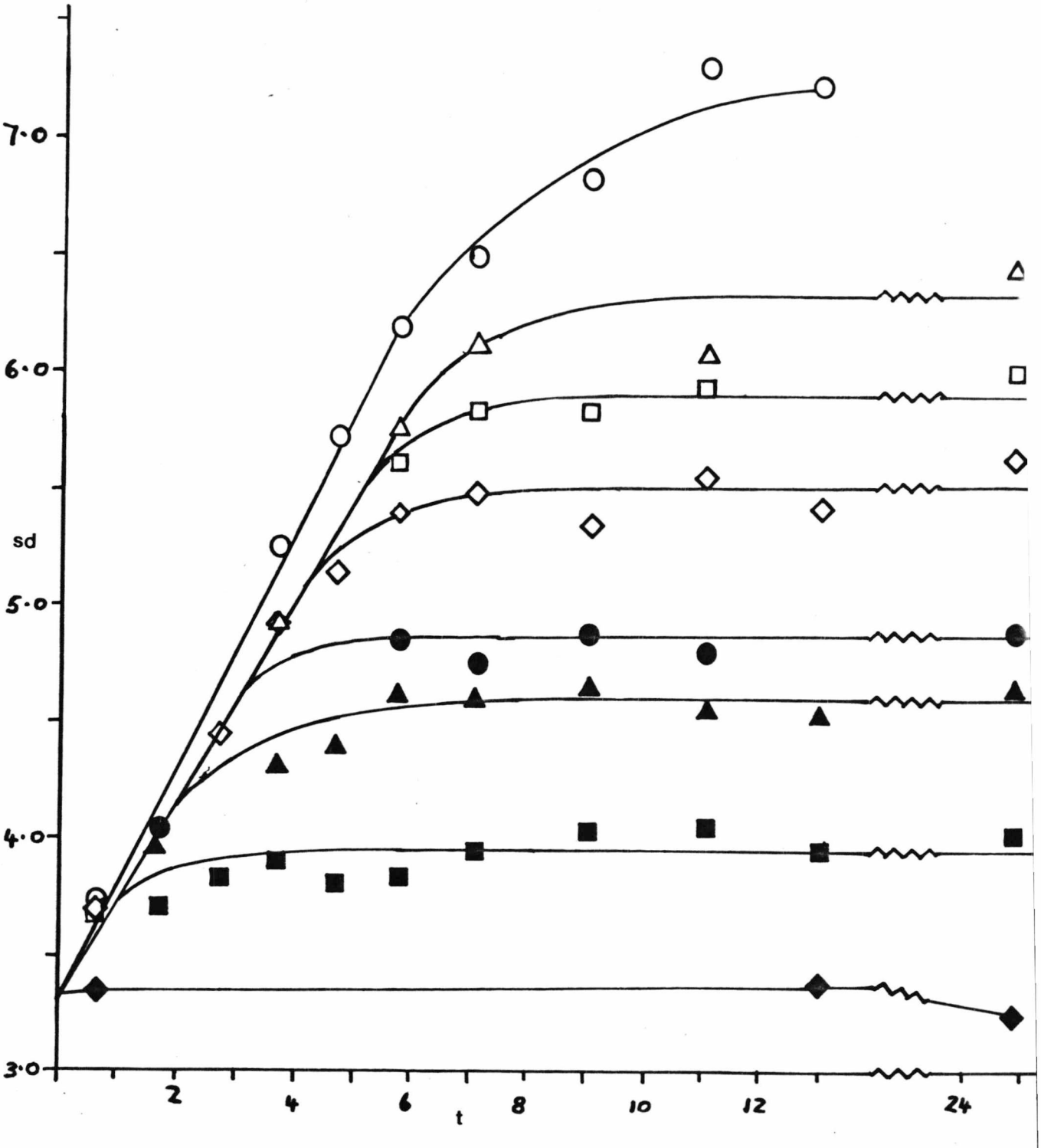
7·0
6·0
sd
5·0
4·0
3·0
2
4
6
8
10
12
24
t

Fig. 37

Compilation of the results from shift-down experiments. Spores were shifted down to a glucose-free medium at hourly intervals and the average spore diameter assessed at 12h, ●. Control curve for a culture that was not shifted down, ○.

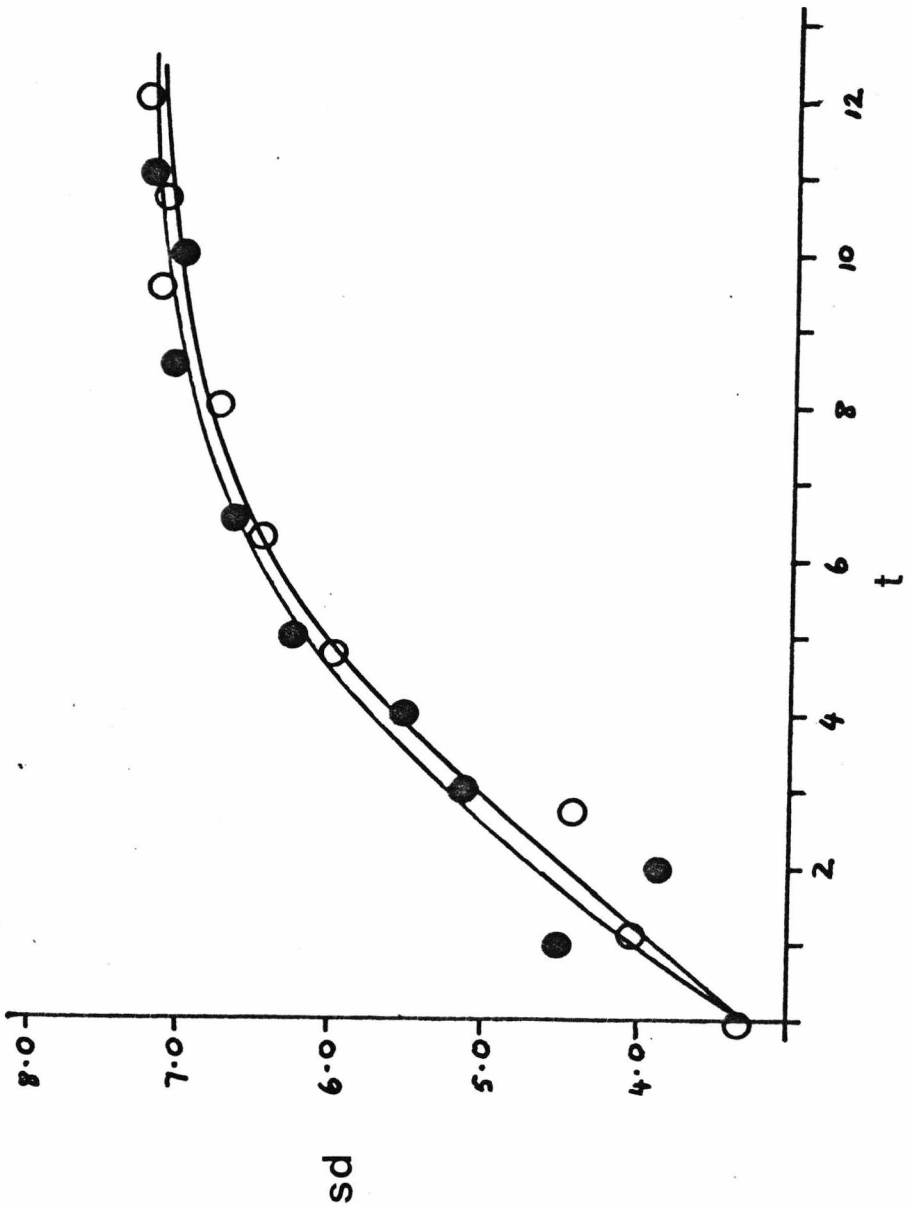
8·0
7·0
6·0
5·0
4·0
sd
2
4
6
8
10
12
t

Fig. 38

Compilation of results from shift-down experiments for germ tube emergence. Spores were shifted down to glucose-free medium at hourly intervals and the percentage germ tube emergence was assessed at 12h, o . Control curve for a culture that was not shifted down, ● .

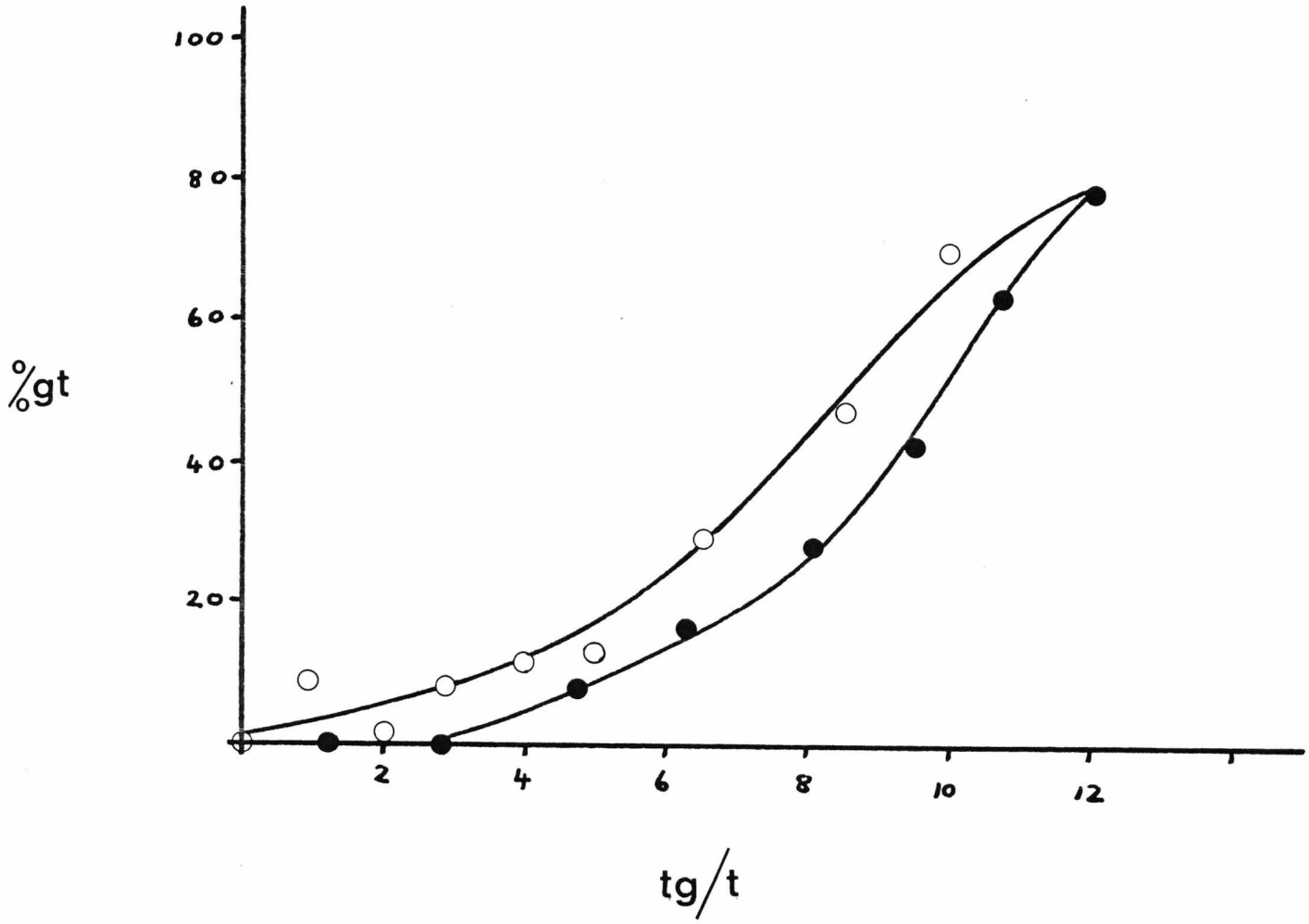
%gt
100
80
60
40
20
2
4
6
8
10
12
tg/t

Fig. 39

Histograms of the frequency of spore diameter classes in the total population (unshaded area, outlined in thick lines) and amongst those spores with germ tubes (shaded area).

(A) 1.2h after inoculation; average spore diameter 4.0μm; percentage germ tube emergence 0.

(B) 4.75h after inoculation; average spore diameter 6.0μm; percentage germ tube emergence 7.5%; average diameter of spores with germ tubes 7.4 μm.

(C) 12.0h after inoculation; average spore diameter 7.3μm; percentage germ tube emergence 78%; average diameter of spores with germ tubes 7.5μm.

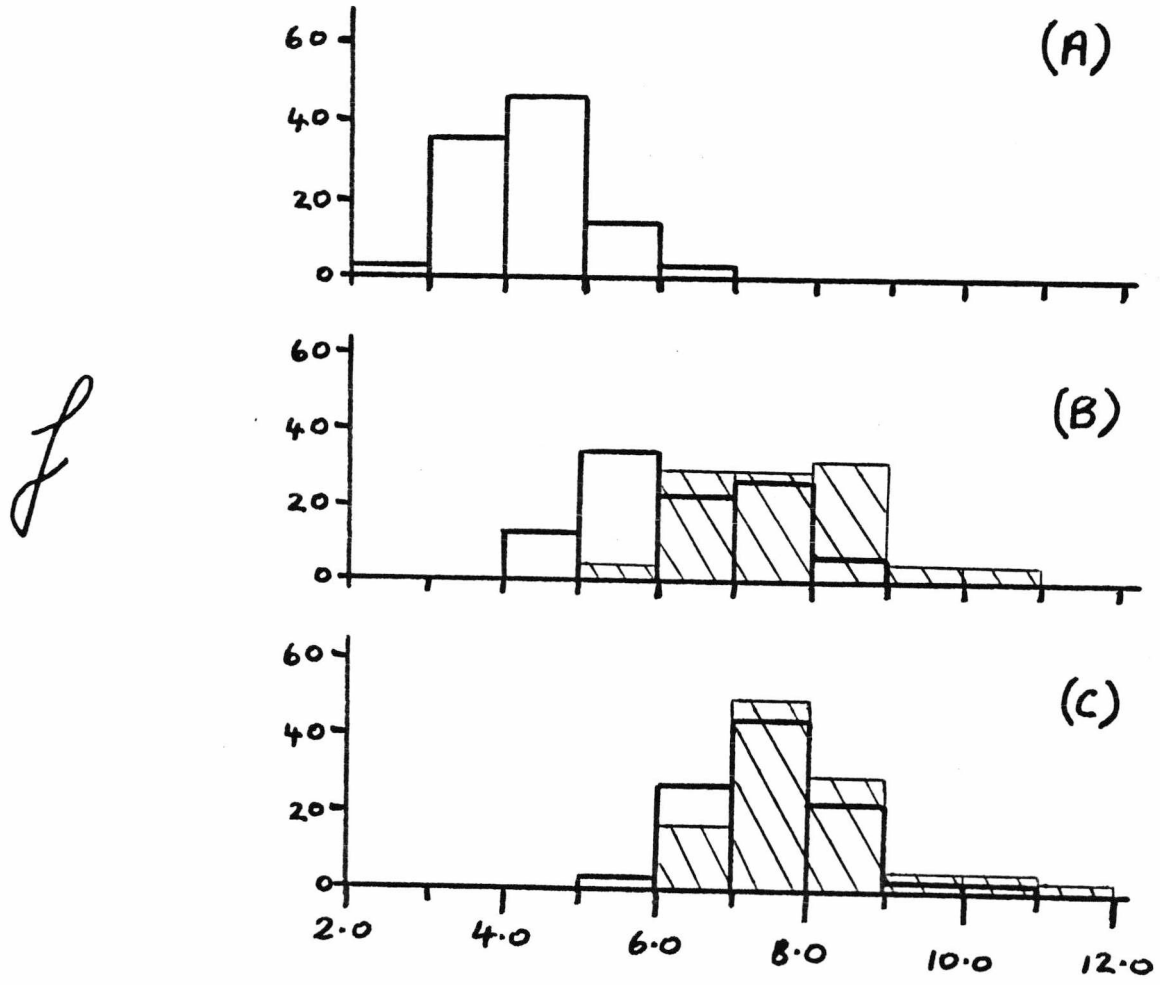
f
60
40
20
0
(A)
60
40
20
0
(B)
60
40
20
0
(C)
2·0
4·0
6·0
8·0
10·0
12·0
s d c

Fig. 40

Histograms of the frequency of spore diameter classes in the total population (unshaded areas, outlined in thick lines) and amongst those spores with germ tubes (shaded areas). In this experiment spores were sized at 12h, but had spent varying times in glucose before a shift-down to a glucose-free medium.

(A) Time spent in glucose medium 1h; percentage germ tube emergence at 12h 8.5%; average spore diameter at 12h 4.5μm; average diameter of spores with germ tubes 5.1μm.

(B) Time spent in glucose medium 5h; percentage germ tube emergence at 12h 13.5%; average spore diameter at 12h 6.3μm; average diameter of spores with germ tubes 7.7μm.

(C) Time spent in glucose medium 12h; percentage germ tube emergence at 12h 78%; average spore diameter at 12h 7.3μm; average diameter of spores with germ tubes 7.5μm.

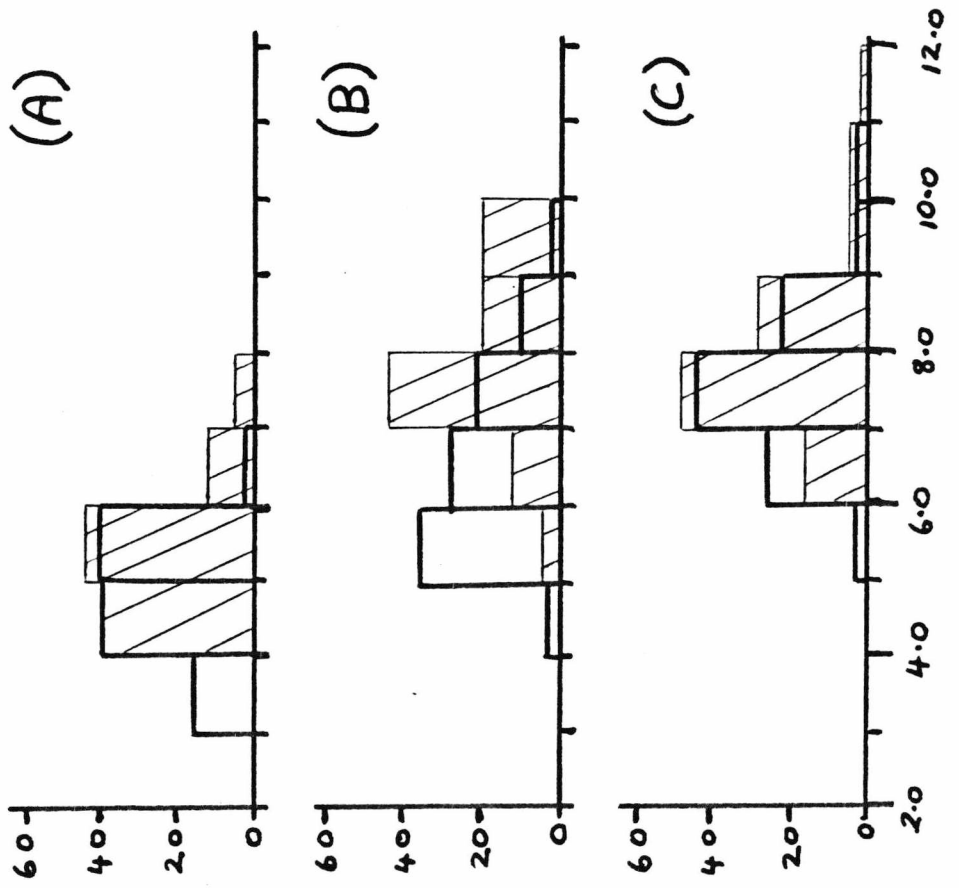
(A)
(B)
(C)
60
40
20
0
2.0
4.0
6.0
8.0
10.0
12.0
sdc

Fig. 41

Spores were shifted down to a glucose free medium at 3 h or 6h and shifted back to glucose medium 24h later.

○ control spores in glucose medium.

▲ spores in glucose-free medium shifted up to glucose medium at 24h.

■ spores shifted down to glucose-free medium at 6h.

△ spores shifted down to glucose-free medium at 6h and shifted back at 30h.

□ spore shifted down to glucose-free medium at 3h.

● spores shifted down to glucose-free medium at 3h and shifted back at 27h.

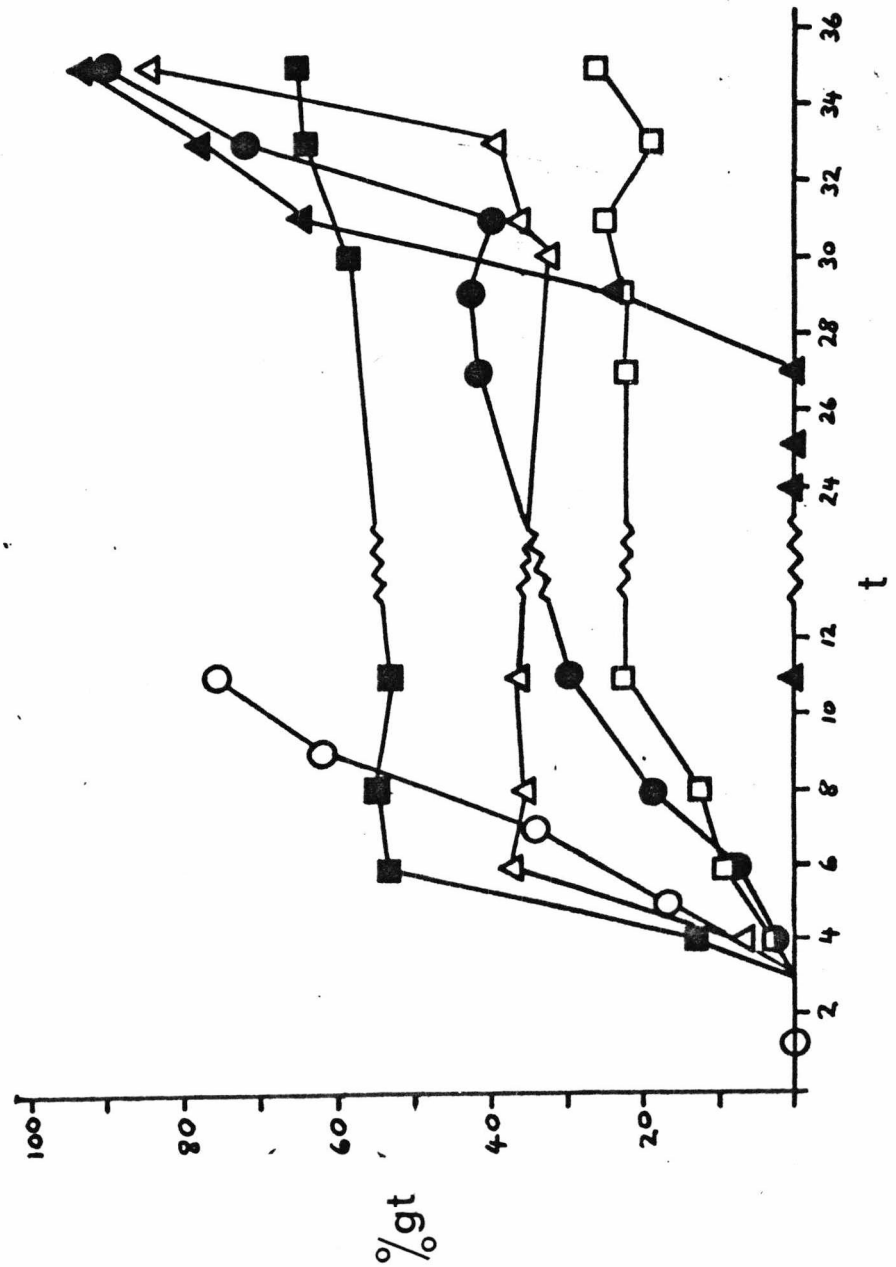
100
80
60
40
20
%gt
2
4
6
8
10
12
24
26
28
30
32
34
36
t

CHAPTER THREE

Fig. 42

Effect of different spore concentrations on germ tube emergence. (■ , □ , Runs 6 and 7 respectively).

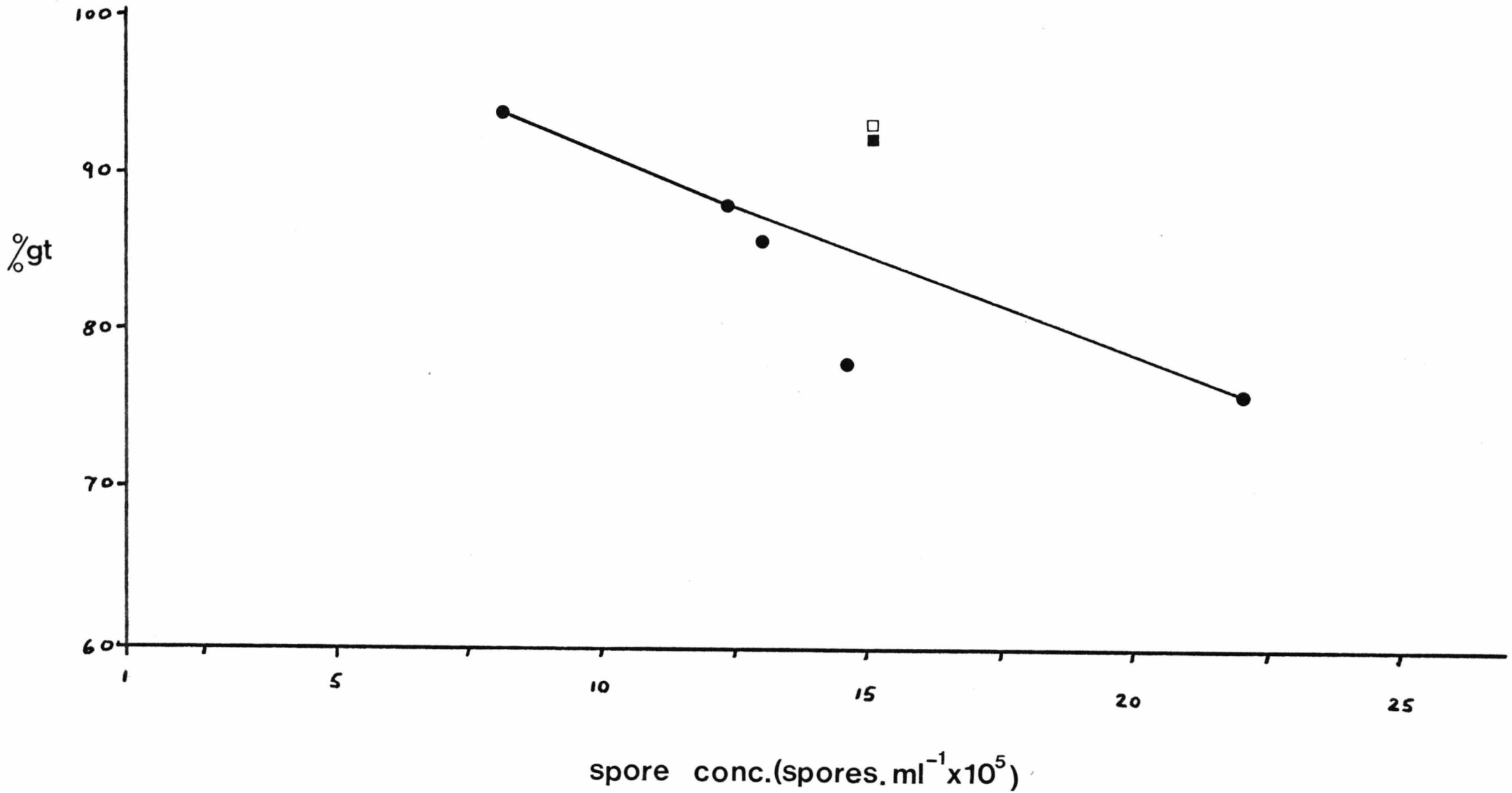
100
90
80
70
60
%gt
1
5
10
15
20
25
spore conc.(spores. ml^{-1}x10^{5})

Table 1

Compilation of data from several batch fermenter runs with different spore concentrations in the cultures, showing the effect of varying the spore concentration on germ tube emergence at 11h after inoculation.

Fermenter run no.	Spore conc. in culture (spores. $ml.^{-1}$).	% germ tube emergence at 11h.	No. of spore washes prior to inoculation
1	8×10^5	94	2
2	1.22×10^6	88	2
3	1.3×10^6	86	2
4	1.46×10^6	78	2
5	2.2×10^6	76	2
6	1.5×10^6	92	6
7	1.5×10^6	93	6

Fig. 43

G.L.C. scans of water washings (1), nonanoic acid standard (2), and diethylether standard (3).

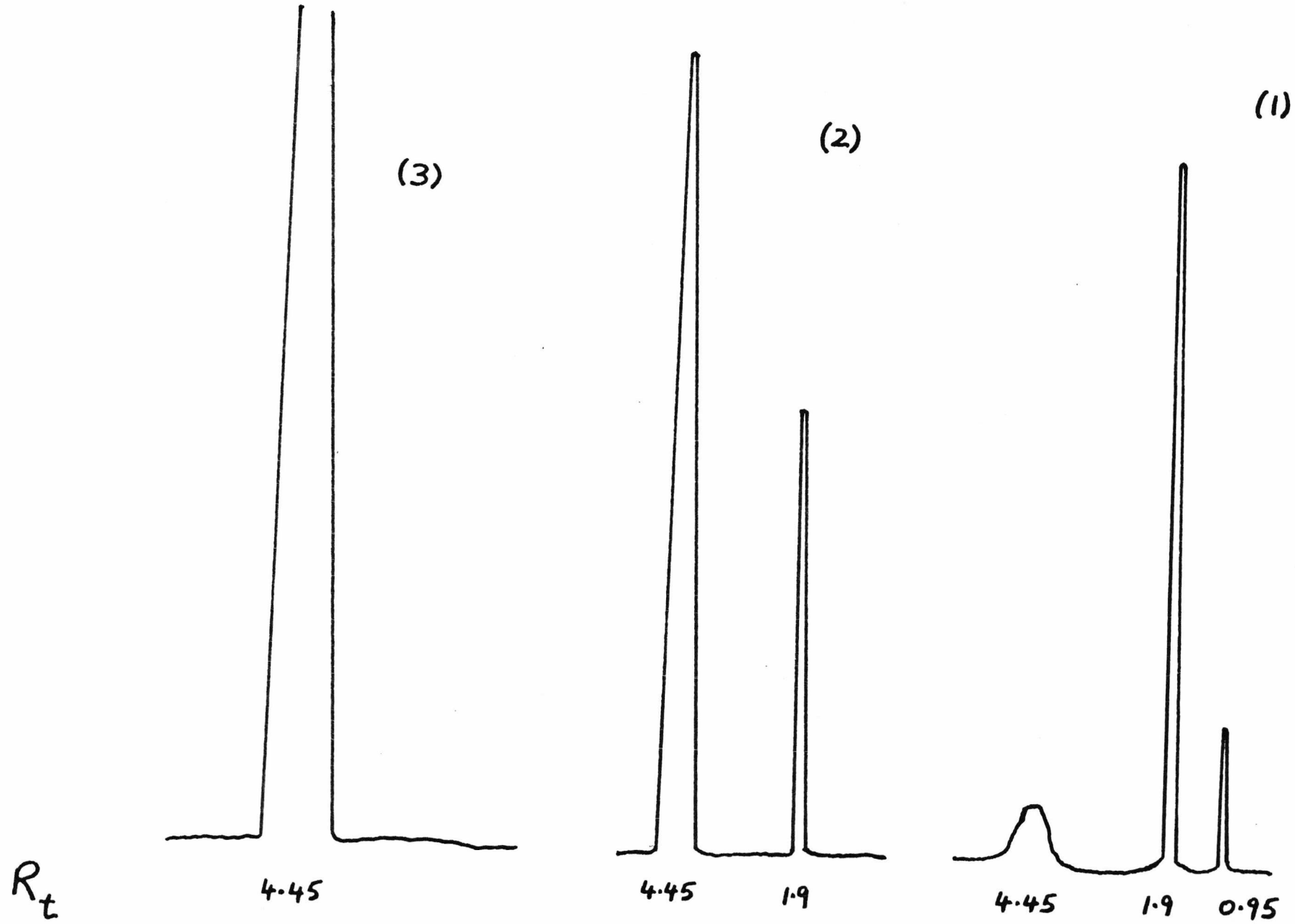
(3)
(2)
(1)
R_t
4·45
4·45
1·9
4·45
1·9
0·95

Fig. 44

Effect of various nonanoic acid concentrations on the outgrowth of germ tubes.

● control + acetone.

○ 10μg.ml^{-1} nonanoic acid.

■ 25μg.ml^{-1} nonanoic acid.

□ 50μg.ml^{-1} nonanoic acid.

▲ 100μg.ml^{-1} nonanoic acid.

△ 150μg.ml^{-1} nonanoic acid.

◆ 200μg.ml^{-1} nonanoic acid.

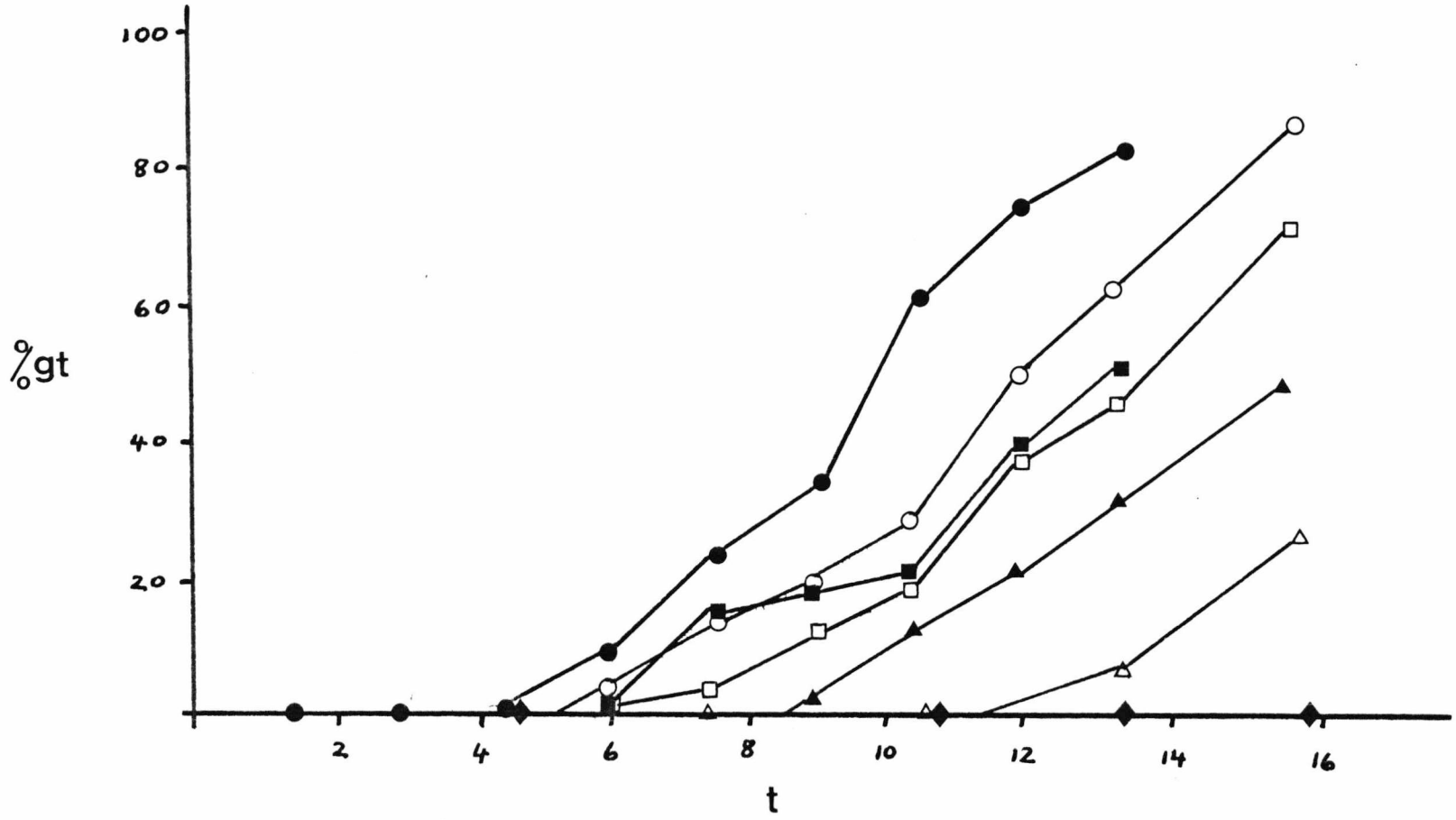
100
80
60
40
20
%gt
2
4
6
8
10
12
14
16
t

Fig. 45

Effect of various nonanoic acid concentrations on spore swelling.

● control + acetone.

■ 50μg.ml^{-1} nonanoic acid.

▲ 150μg.ml^{-1} nonanoic acid.

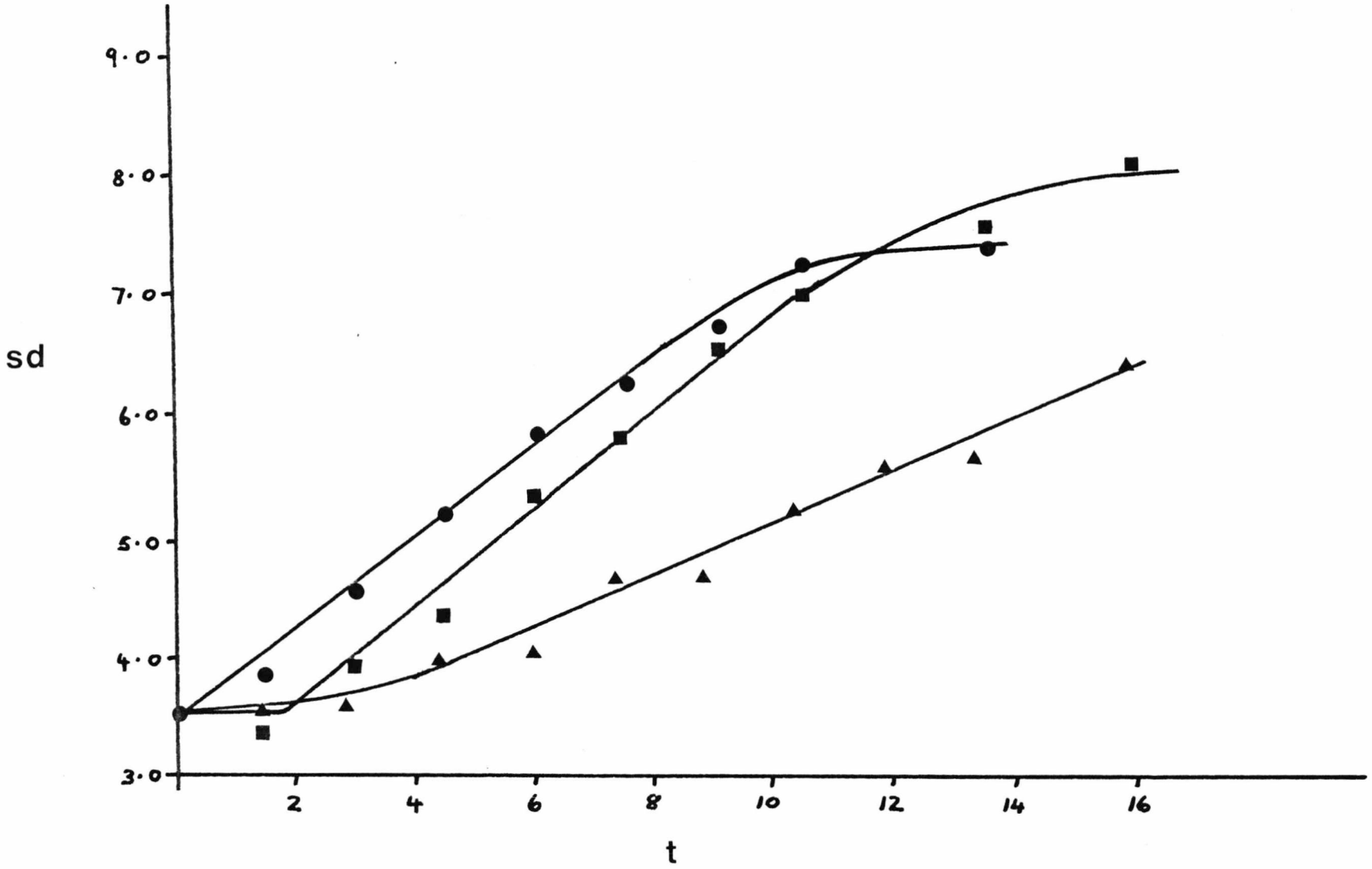
sd
9·0
8·0
7·0
6·0
5·0
4·0
3·0
2
4
6
8
10
12
14
16
t

Fig. 46

Effect of various nonanoic acid concentrations on percentage germ emergence at 13.5h. after inoculation.

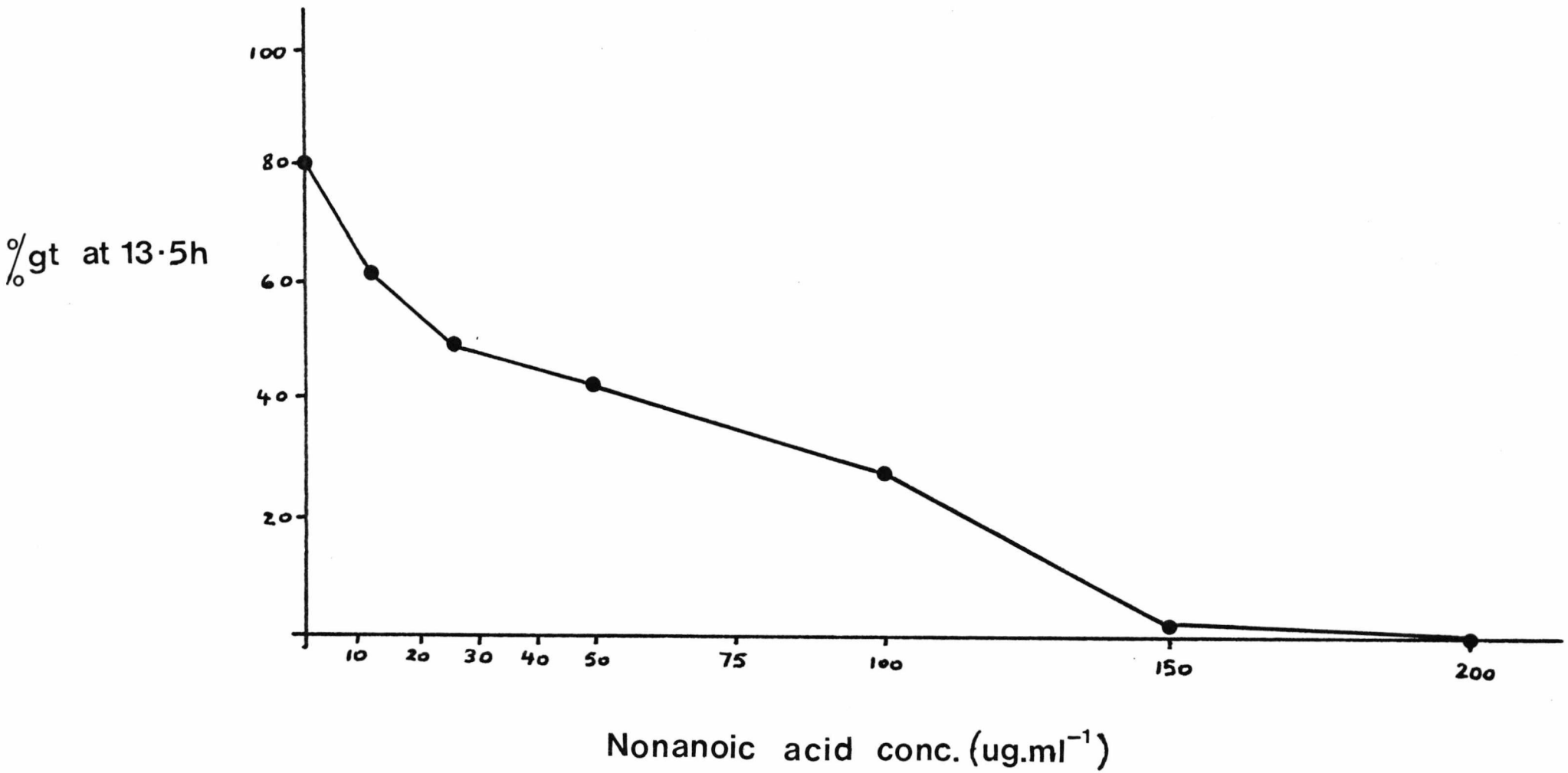
%gt at 13·5h
100
80
60
40
20
10
20
30
40
50
75
100
150
200
Nonanoic acid conc. (ug.ml^{-1})

Fig. 47

Stability of nonanoic acid in culture medium.

● Control, inoculated on Day 1.

○ Nonanoic acid ($200\mu g.ml^{-1}$) culture inoculated on Day 1.

▲ Control, prepared on Day 1, inoculated on Day 2.

△ Nonanoic acid ($200\mu g.ml^{-1}$) culture, prepared on Day 1, inoculated on Day 2.

■ Control, prepared and inoculated on Day 2.

□ Nonanoic acid ($200\mu g.ml^{-1}$) culture, prepared and inoculated on Day 2.

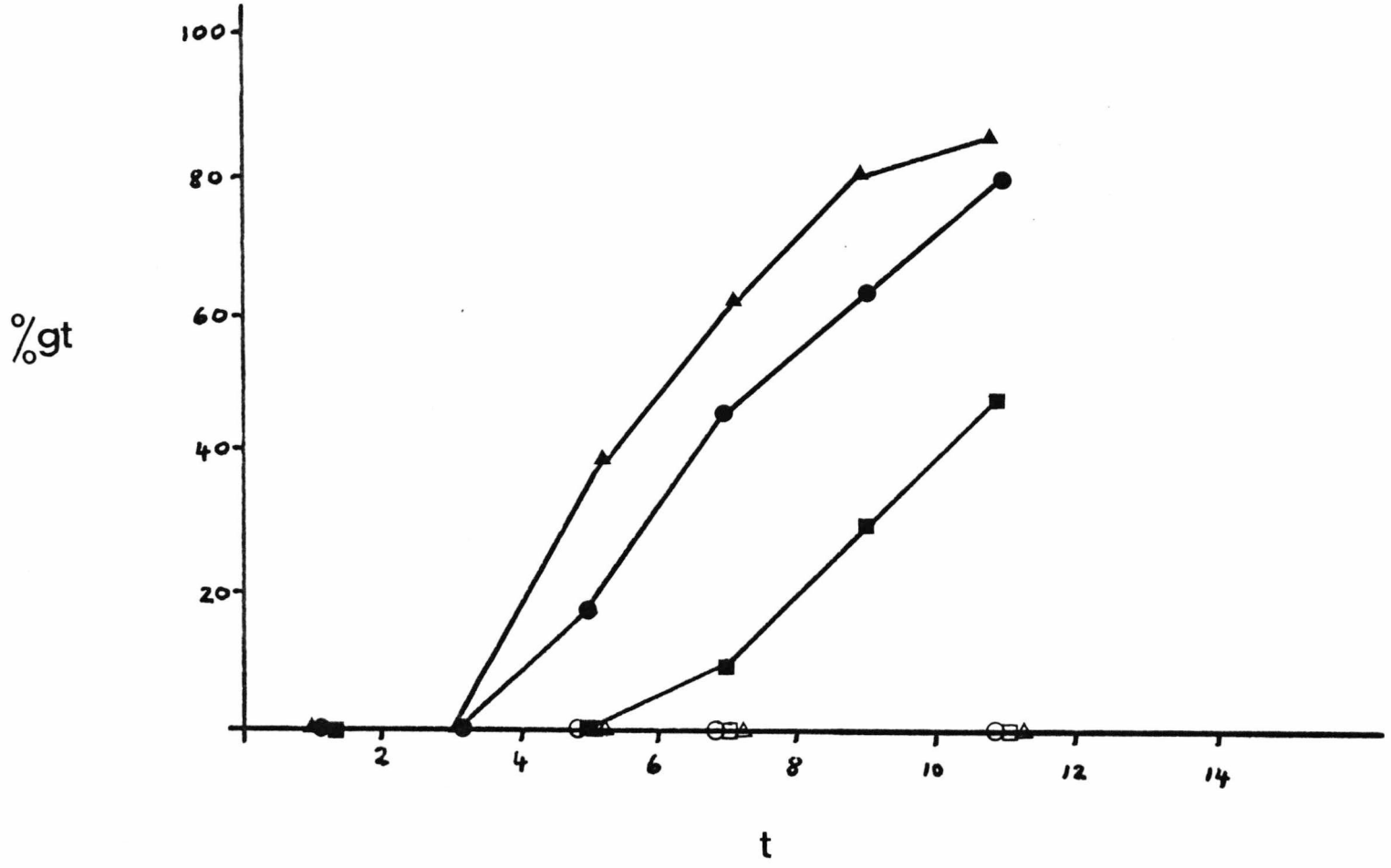
%gt
100
80
60
40
20
2
4
6
8
10
12
14
t

CHAPTER FOUR

Table 2

Outline of sequential chemical treatments to which spores were subjected, and extraction procedures for obtaining pellets (1), (2) and (B).

EM - material for electron microscope observation.

sdw - sterile distilled water.

EtOH - ethanol.

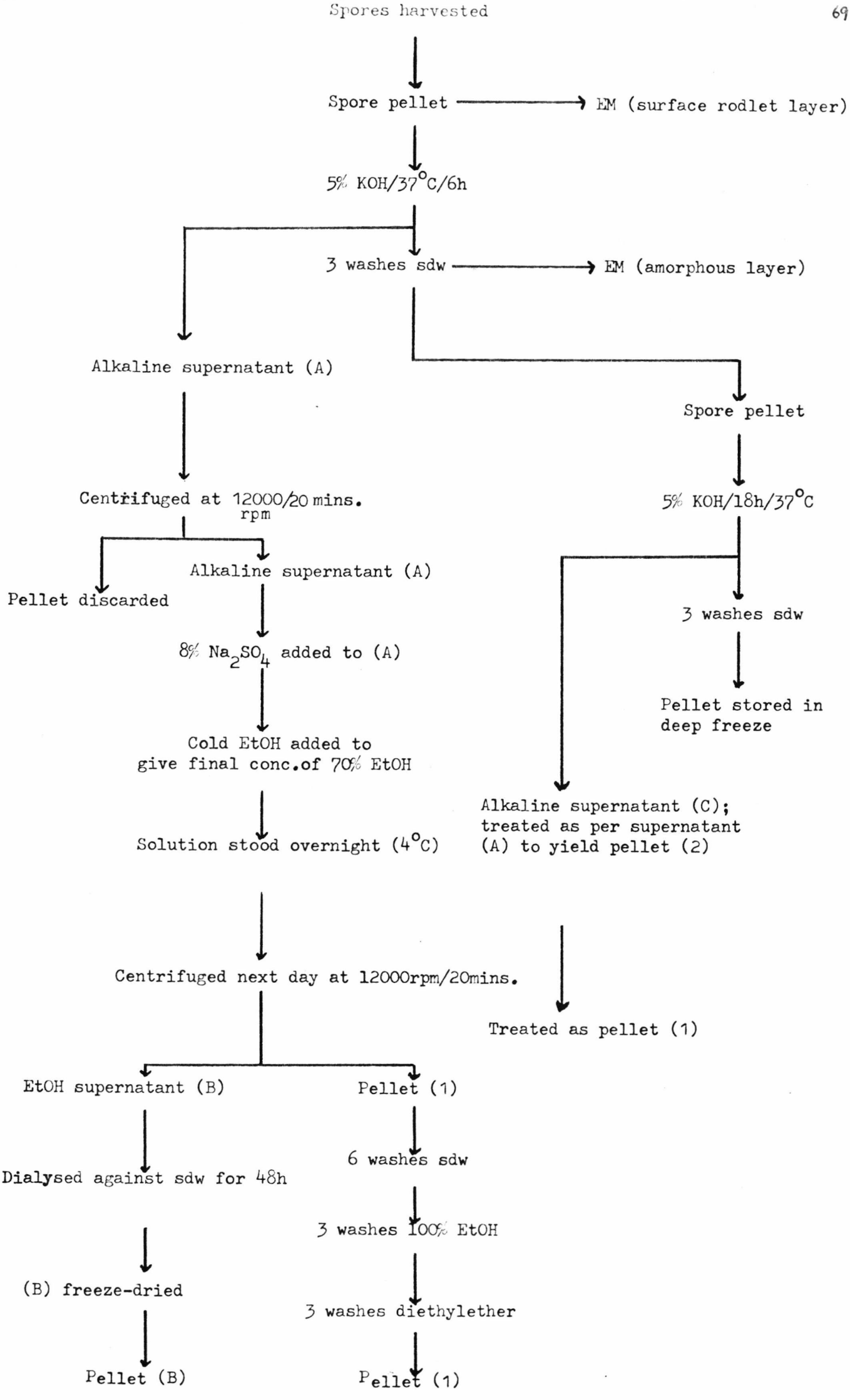
Spores harvested
Spore pellet
EM (surface rodlet layer)
5% KOH/37°C/6h
3 washes sdw
EM (amorphous layer)
Alkaline supernatant (A)
Spore pellet
Centrifuged at 12000/20 mins. rpm
5% KOH/18h/37°C
Alkaline supernatant (A)
Pellet discarded
3 washes sdw
8% Na2SO4 added to (A)
Pellet stored in deep freeze
Cold EtOH added to give final conc.of 70% EtOH
Alkaline supernatant (C); treated as per supernatant (A) to yield pellet (2)
Solution stood overnight (4°C)
Centrifuged next day at 12000rpm/20mins.
Treated as pellet (1)
EtOH supernatant (B)
Pellet (1)
6 washes sdw
Dialysed against sdw for 48h
3 washes 100% EtOH
(B) freeze-dried
3 washes diethylether
Pellet (B)
Pellet (1)

Fig. 48

FF of untreated dormant spore. The surface layer of a criss-cross network of rodlets is clearly seen in this micrograph and subsequent figures as well (x50000)

Fig. 49

FF of untreated dormant spore. The rodlets have a mean periodicity of 25nm. (x35100)

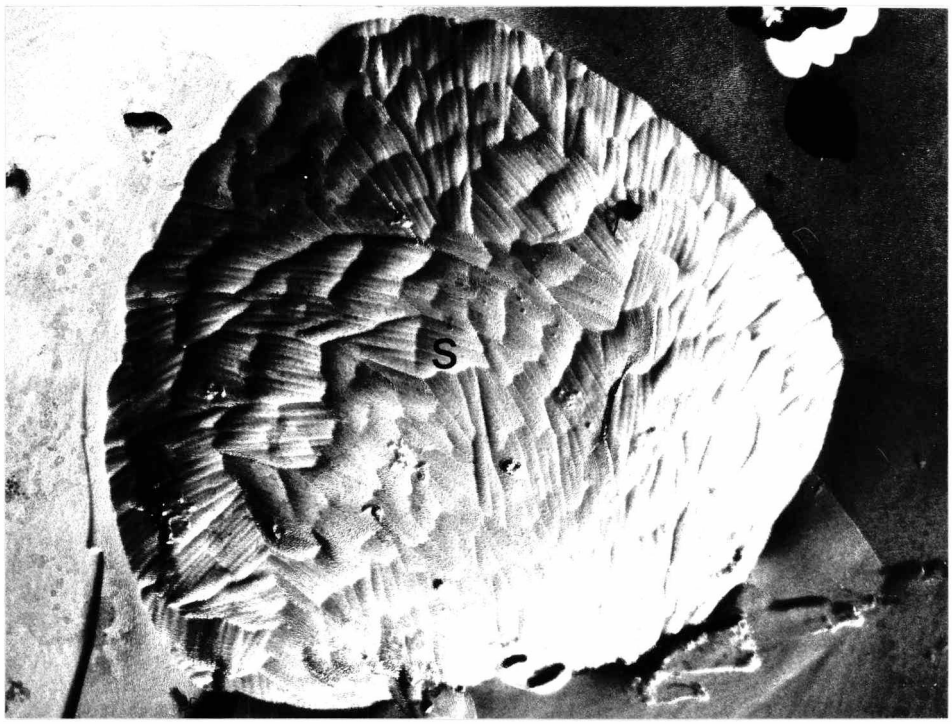
S


S

Fig. 50

SR of untreated dormant spore. The surface layer of rodlets is clearly visible by this technique. (x37500)

Fig. 51

SR of untreated dormant spore. The criss-cross pattern is seen as an interlaced network of groups of rodlets. (x43300)

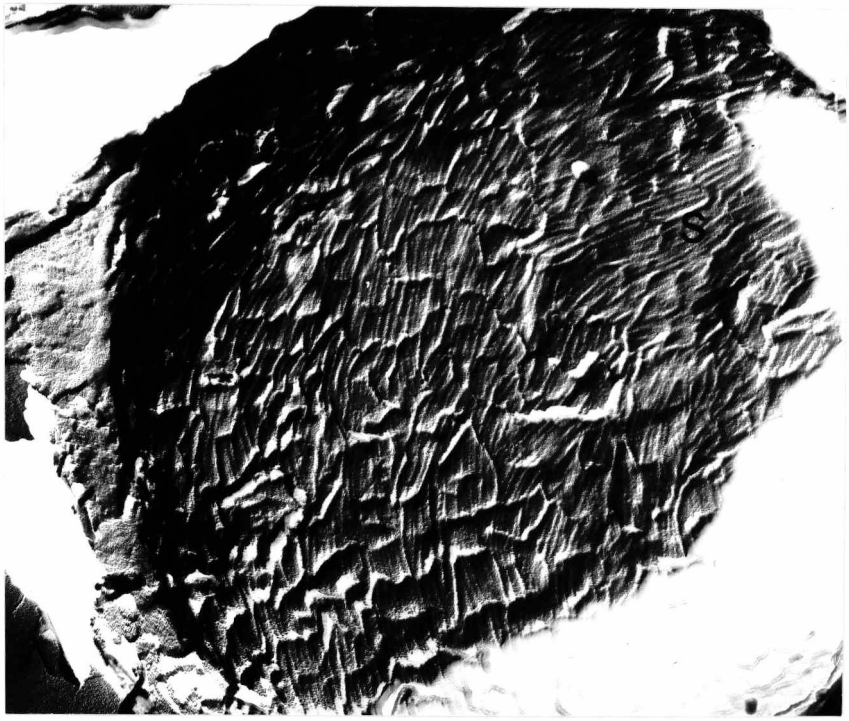
S


S

Fig. 52

SR of untreated dormant spore. Higher magnifications of the surface rodlet layer in both this micrograph and the following one show in more detail the interlaced network of groups of rodlets.(x44800)

Fig. 53

SR of untreated dormant spore. (x84100)

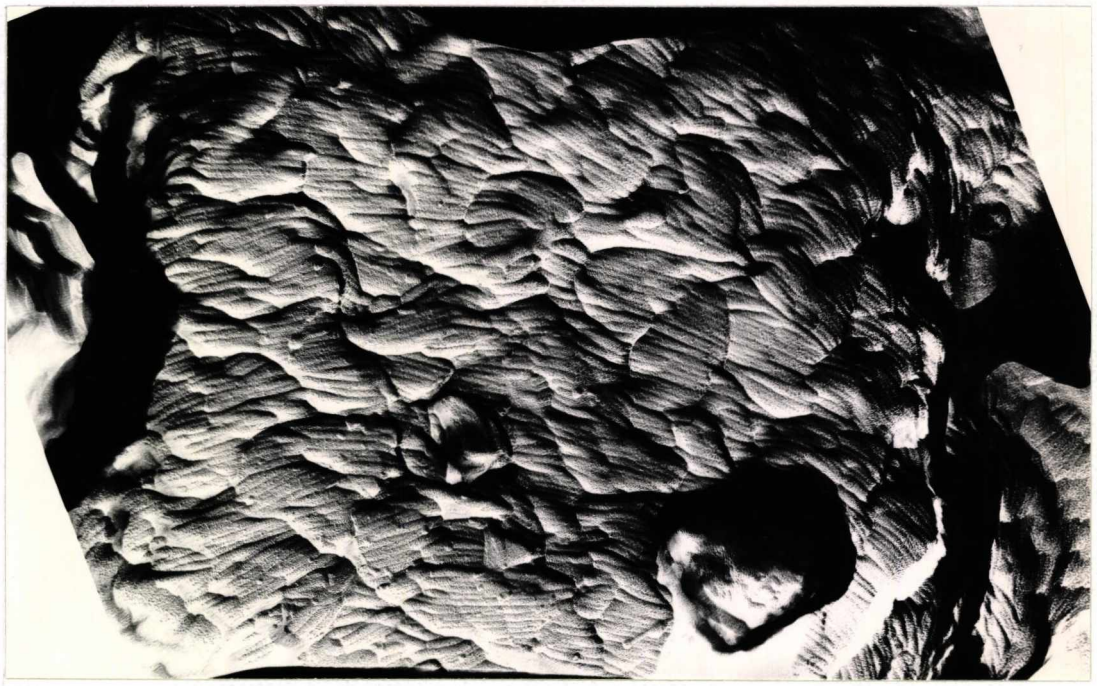

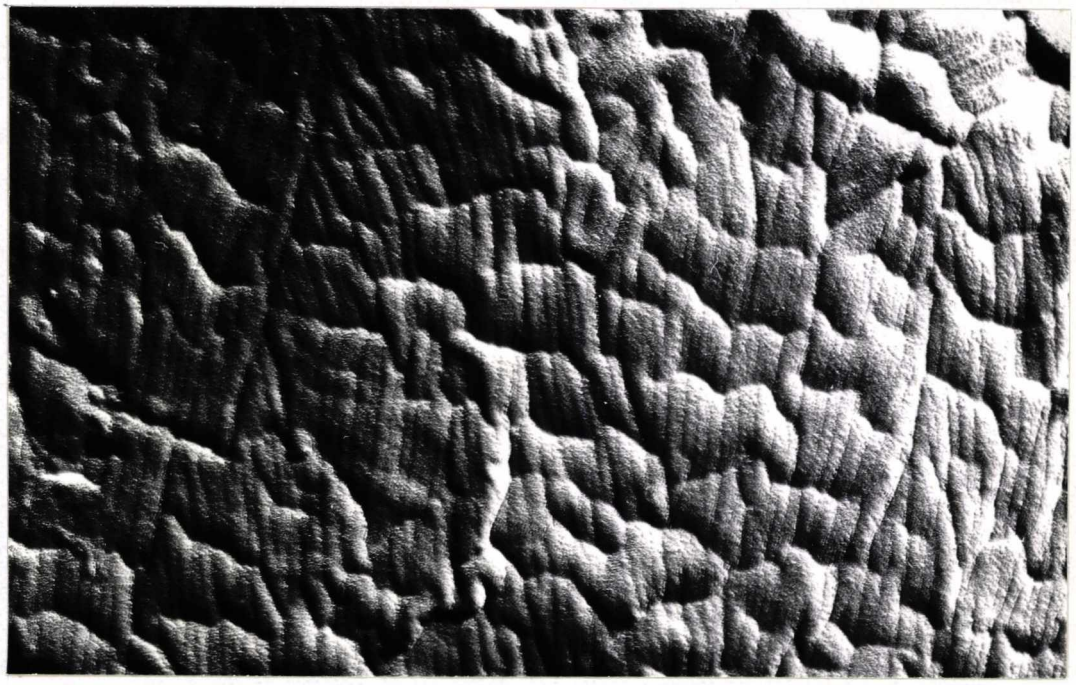

Fig. 54

FF of untreated dormant spore. Figures 54 and 55 show that freeze-fractured spore surfaces have an interlaced pattern of groups of rodlets as seen by the surface replica technique in the preceding two micrographs (x70000)

Fig. 55

FF of untreated dormant spore (x66100)

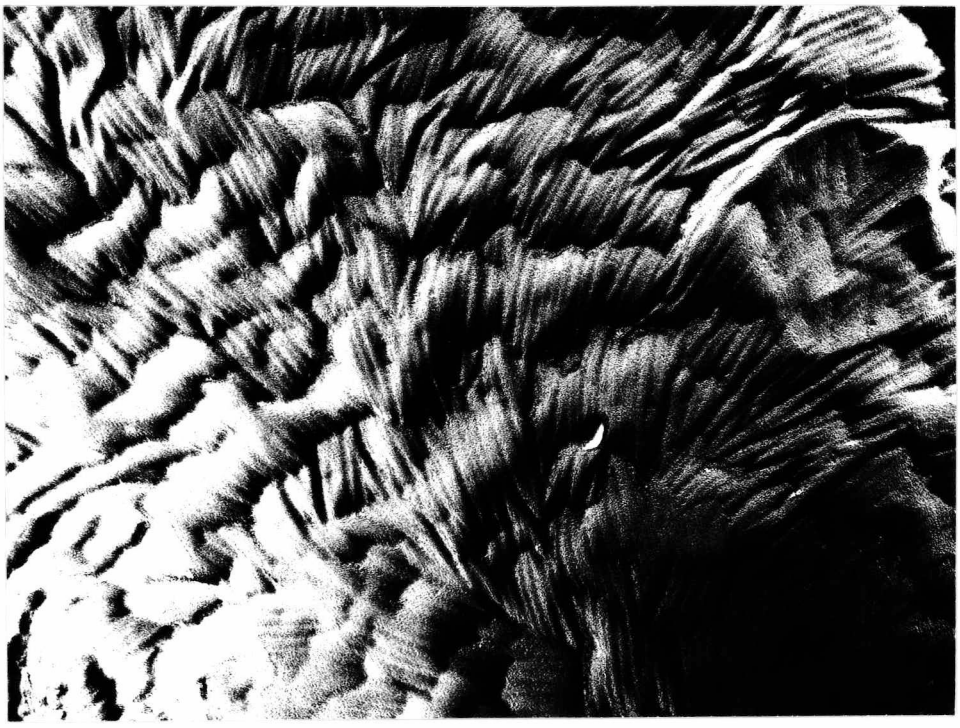

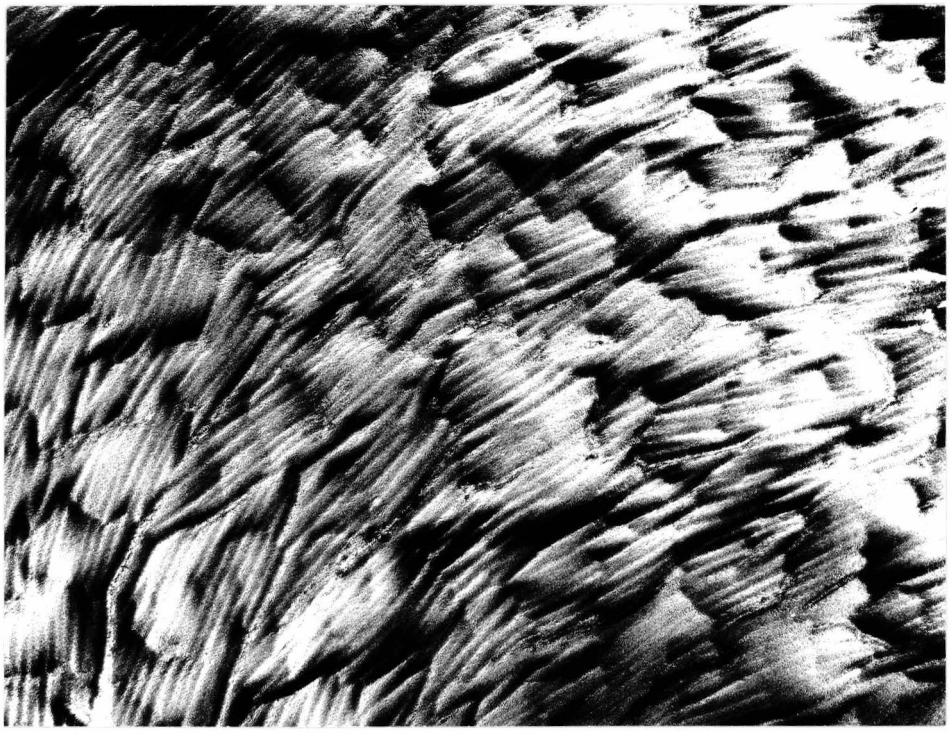

Fig. 56

SR of dormant spores after incubation with 5% KOH for 6h. The surface rodlet layer has been completely removed to reveal an underlying amorphous layer (x15100)

Fig. 57

SR of dormant spore after incubation with 5% KOH for 6h. Higher magnifications of the spore surface after KOH treatment revealed the complete absence of the surface rodlet layer. The micrographs, Figures 57-63, show the presence of an amorphous layer (x34100)

Fig. 58

SR of dormant spore after 6h 5% KOH treatment (x38000)


Am

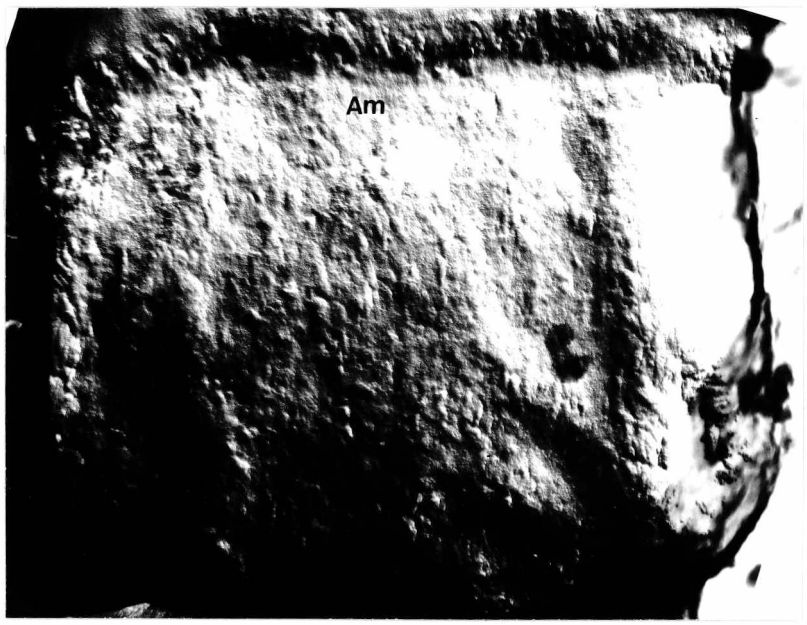
Am

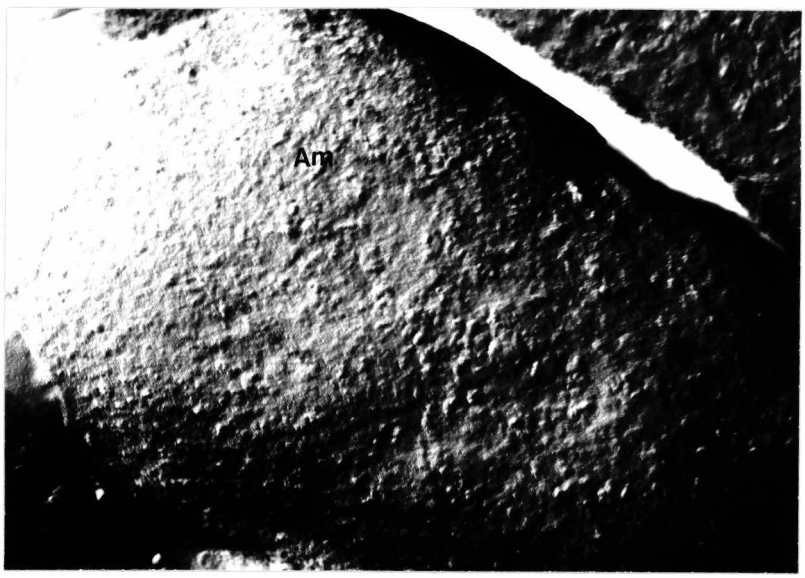
Am

Fig. 59

SR of dormant spore after 6h 5% KOH treatment. (x38200)

Fig. 60

SR of dormant spore after 6h 5% KOH treatment. (x38000)

Fig. 61

SR of dormant spore after 6h 5% KOH treatment. (x37500)

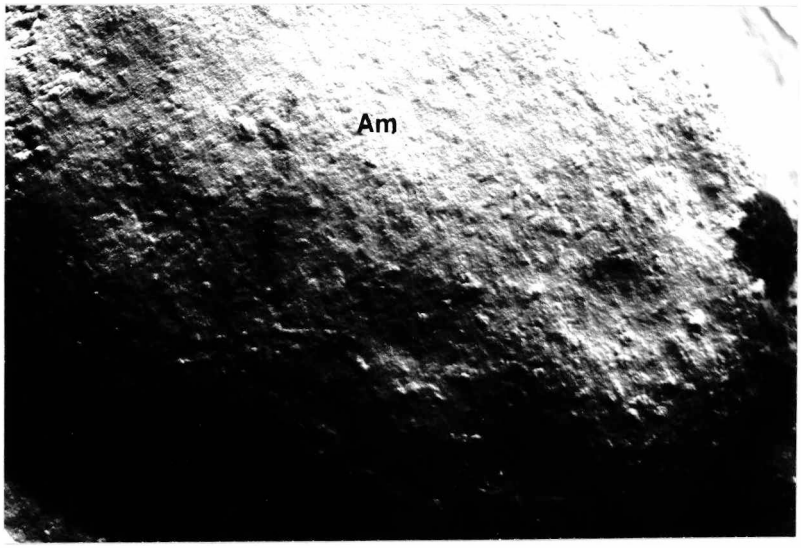
Am

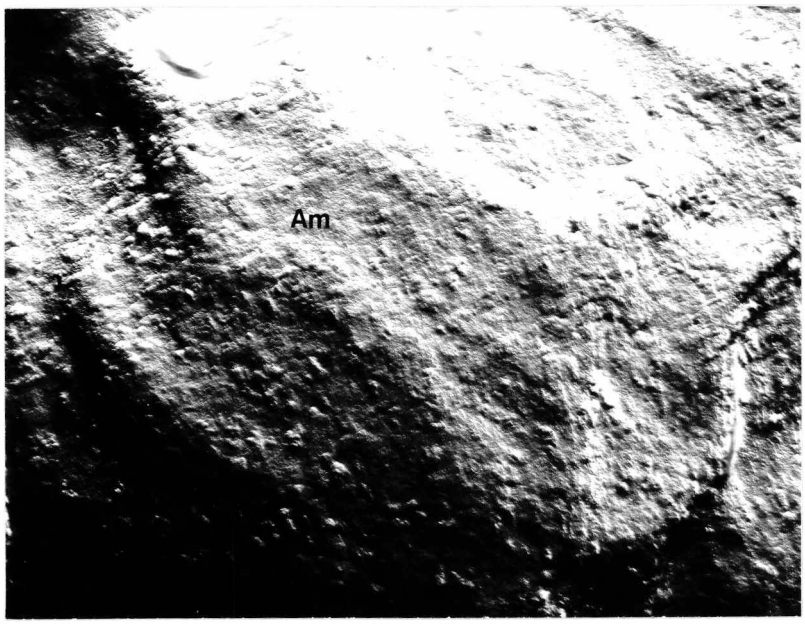
Am

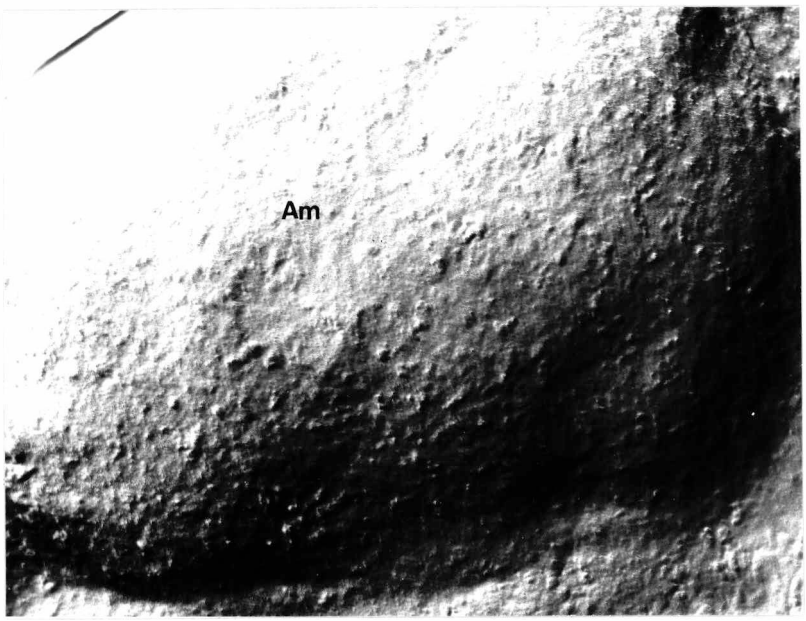
Am

Fig. 62

SR of dormant spore after 6h 5% KOH treatment (x64000)

Fig. 63

SR of dormant spore after 6h 5% KOH treatment (x60000)

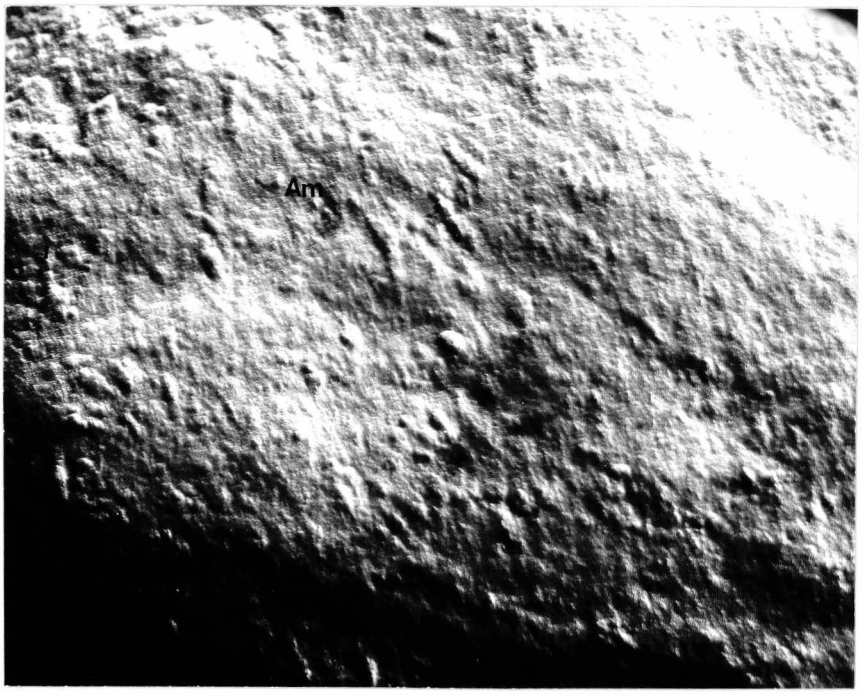
Am

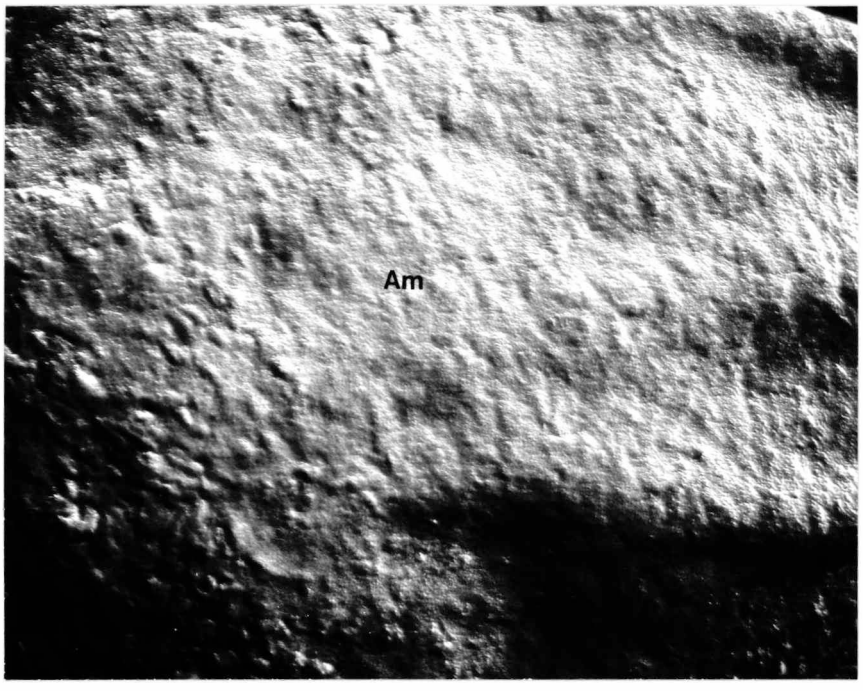
Am

Fig. 64

Photographs of 7.5% polyacryalmide gels.

(A) Pellet (B),

(B) α-1,3 glucan from Aspergillus nidulans,

(C) S-glucan from Schizophyllum commune.

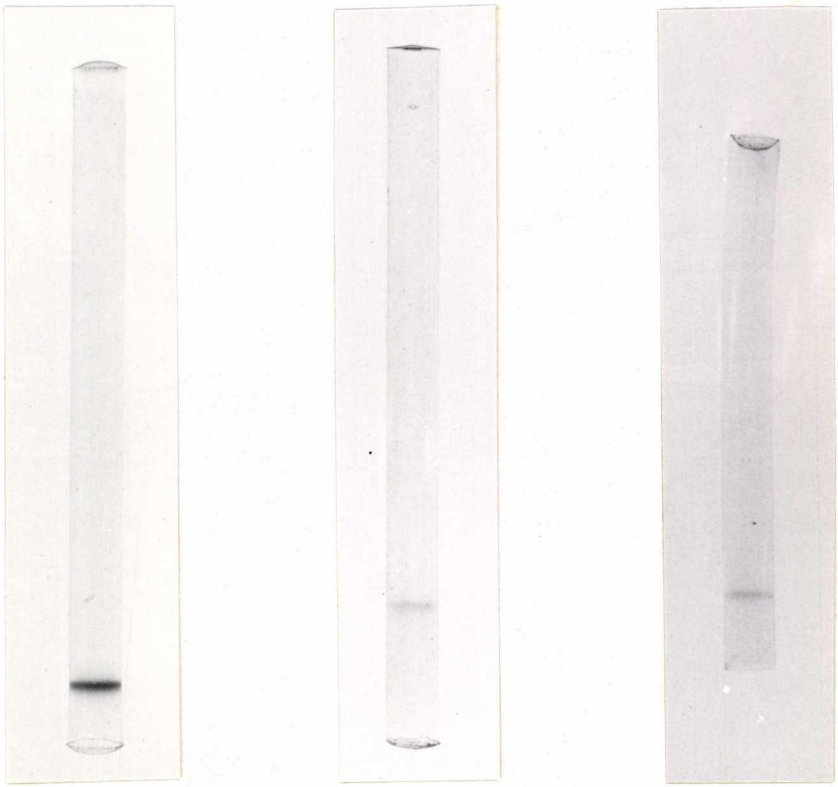

A B C

Table 3

Amino acid analysis data of pellet (B).

AMINO ACIDS	PERCENTAGE (Residues /100)
Aspartate + Asparagine	11.1
Threonine	6.1
Serine	11.4
Glutamate + Glutamine	8.1
Proline	6.2
Glycine	10.8
Alanine	8.8
Cystein (as Cysteic Acid)	2.7
Valine	4.8
Methionine	1.6
Isoleucine	3.1
Leucine	5.4
Tyrosine	3.7
Phenylalanine	4.4
Histidine	2.9
Lysine	4.8
Arginine	3.9

Fig. 65

Diagrammatic representation of sugar spots on chromatogram after total hydrolysis of pellet (1).

A - glucose

B - galactose

C - mannose

D - pellet (1)

E - galactose/glucose/mannose

F - mannose

G - galactose

H - glucose


A
B
C
D
E
F
G
H

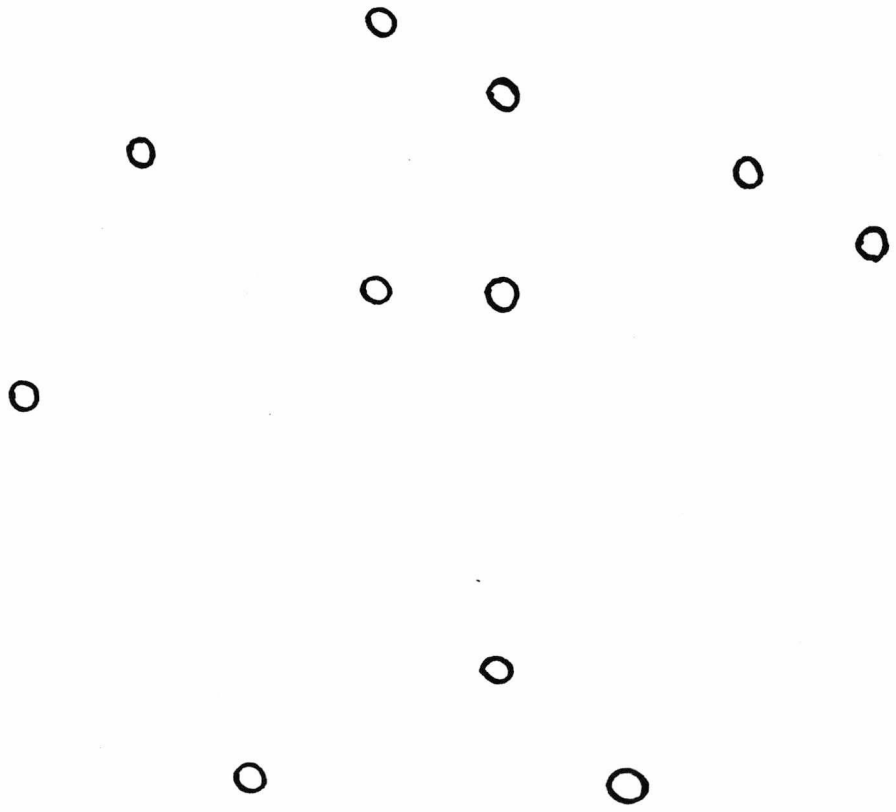

Table 4

R_G values, calculated from Figure 65, for the sugar spots obtained after total hydrolysis of pellet (1). R_G values were based upon the glucose spot run at E (Fig. 65).

SUGAR	R_G VALUE
A - glucose	1.12
B - galactose	0.87
C - mannose	1.49
D - pellet (1)	0.74/1.0
E - galactose	0.80
E - glucose	1.0
E - mannose	1.37
F - mannose	1.48
G - galactose	0.88
H - glucose	0.95

Fig. 66

Infra-red scans of (A) pellet (1); (B) pellet (2);

(C) pellet (3).

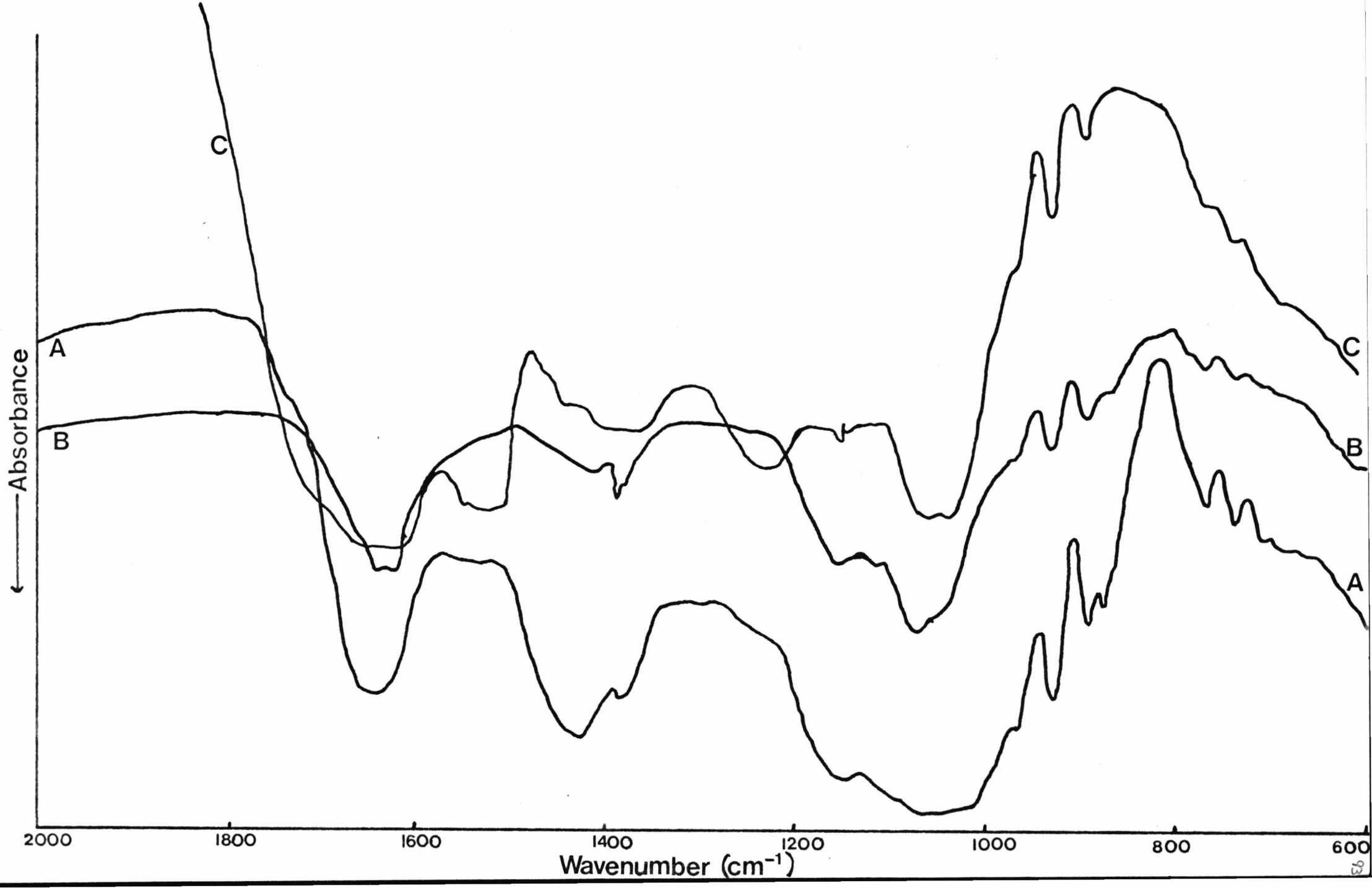
C
A
B
Absorbance
2000
1800
1600
1400
1200
1000
800
600
Wavenumber (cm⁻¹)
C
B
A

Fig. 67

Ultraviolet scans in the range 650-350nm for (A) pellet (3); (B) Aspergillus nidulans melanin; (C) Sepia melanin.

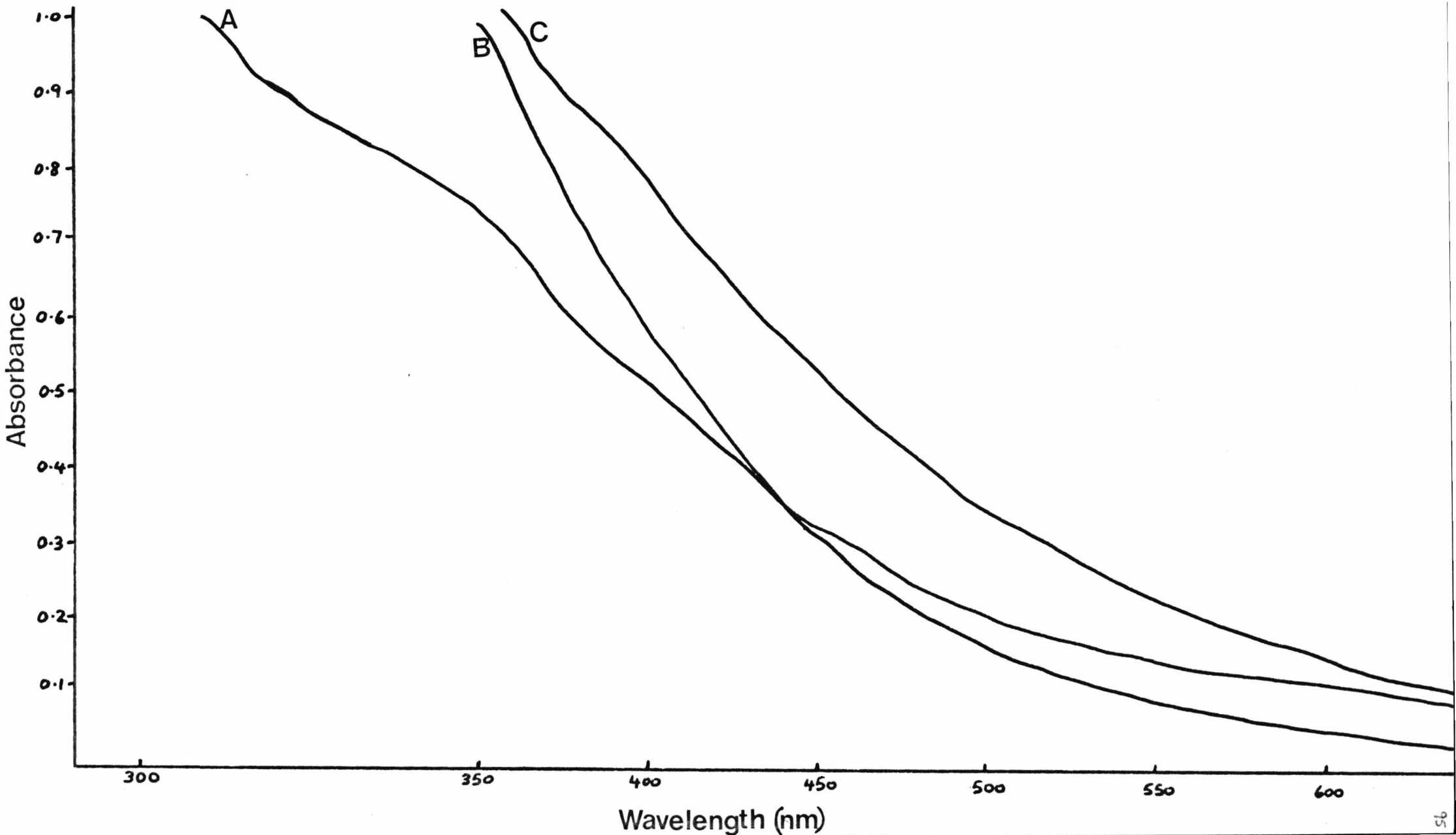
A
B
C
1·0
0·9
0·8
0·7
0·6
0·5
0·4
0·3
0·2
0·1
Absorbance
300
350
400
450
500
550
600
Wavelength (nm)

Fig. 68

Plots of log absorbance vs. wavelength for:

■ pellet (3),

▲ Aspergillus nidulans melanin,

● Sepia melanin.

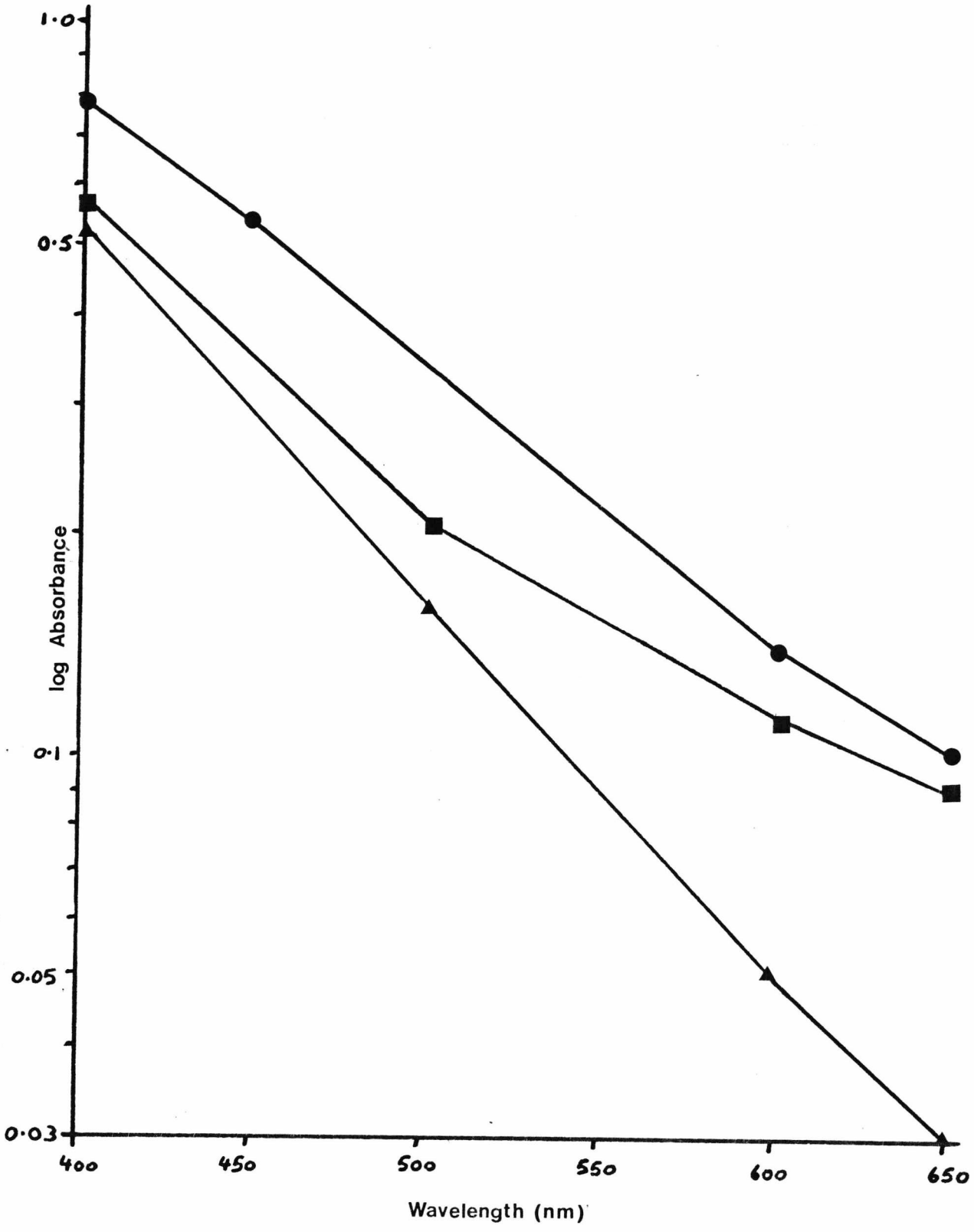
1·0
0·5
0·1
0·05
0·03
log Absorbance
400
450
500
550
600
650
Wavelength (nm)

Table 5

Comparison of melanins from various fungal sources with pellet (3).

(1) Bartnicki-Garcia & Reyes (1964).

(2) Ellis & Griffiths (1974).

FUNGAL SOURCE OF MELANIN	GRADIENT OF LOG ABSORBANCE vs. WAVELENGTH
Pellet (3)	-0.0030
Aspergillus nidulans	-0.0027
Sepia melanin	-0.0032
Mucor rouxii[1]	-0.0026
Amorphotheca resinae[2]	-0.0025
Epiccocum nigrum[2]	-0.0015
Humicola grisea[2]	-0.0030
Collectotrichum coccodes[2]	-0.0026
Verticillium dahliae[2]	-0.0015

Table 6

Comparison of amino acid analysis data for various fungal and bacterial structural wall proteins.

(1). Somerville, Delafield & Rittenberg (1970).

(2). Sleytr & Thorne (1976).

(3). Mitani & Kadota (1976).

(4). Kitajima & Nozawa (1975).

(5). Hashimoto, Wu-Yuan & Blumenthal (1976).

(A) Acidic amino acids.

(B) Amino acids with small side-chain (R) groups.

(C) Other amino acids.

	AMINO ACID	ORGANISM (VALUES ARE MOL% OR RESIDUES/100)										
		Pellet (B)	Bacillus thuringiensis(1)	Bacillus cereus(1)	Bacillus megaterium(1)	Bacillus subtilis(1)	Clostridium roseum(1)	Clostridium thermosulfuricum(2)	Clostridium thermosaccharolyticum(2)	Bacillus subtilis(3)	Epidermophyton floccosum(4)	Trichophyton metagrophytes(5)
A	Aspartate	11.1	11.2	10.6	10.5	10.3	10.9	14.16	17.46	9.5	10.5	15.67
	Glutamate	8.1	10.2	9.2	7.3	10.9	8.6	6.19	7.28	7.7	13.3	8.26
B	Glycine	10.8	10.9	11.3	10.6	12.0	13.3	7.90	8.15	13.9	17.0	9.02
	Serine	11.4	6.5	7.1	7.1	8.7	5.4	6.97	8.11	7.1	8.0	3.99
	Alanine	8.8	9.4	9.2	9.5	12.0	7.0	8.71	9.32	7.1	10.1	6.97
C	Threonine	6.1	8.6	8.9	10.5	6.1	9.4	10.01	9.96	4.8	9.4	5.10
	Proline	6.2	2.4	4.8	6.9	5.5	7.3	4.47	3.17	4.1	0.0	3.38
	Leucine	5.4	8.9	8.8	8.1	7.6	6.8	6.41	5.89	5.3	9.6	7.40
	Valine	4.8	8.9	8.0	7.4	7.4	7.7	10.71	10.55	4.9	4.1	7.47
	Lysine	4.8	4.0	3.5	3.9	3.6	5.2	7.18	5.74	8.5	2.4	7.86

CHAPTER FIVE

Table 7

Some common linkages found in fungal wall glucans.

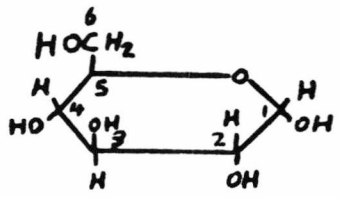

D-glucose (numbers refer to C-atom positions)

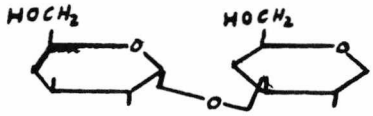

α-1,3 linkage

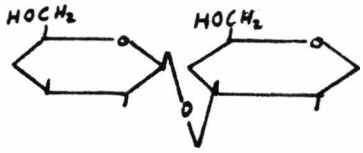

β-1,3 linkage

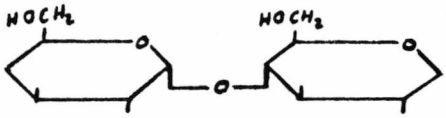

α-1,4 linkage

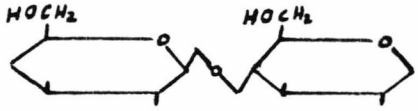

β-1,4 linkage

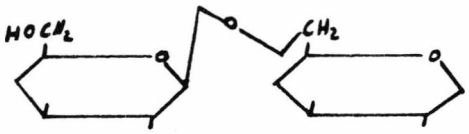

β-1,6 linkage

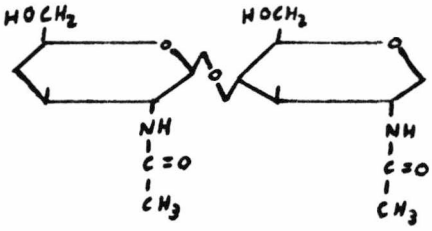

Chitin - a polymer of N-acetylglucosamine molecules linked by a β-1,4 bond

Table 8

Some of the techniques employed in fungal wall analysis. The table lists some of the experimental methods used currently in fungal wall analysis. The best studies should contain (conditions of work, such as yields of material, taken into account), as many of these different analytical procedures as is possible.

Table 8

Infra-red spectroscopy.	Identification of α/β wall glucans. If α-linked, comparison with standards may help in deducing nature of α-linkage.
Methylation analysis.	Provides data as to nature of linkages between the sugar units.
NMR spectra.	Signals can be confined to α/β configuration. Comparison with known standards may give information as to bonding.
X-ray powder diagrams.	Comparisons with known standards leads to possible identification of wall polymer.
Total macromolecular analysis.	Provides information on total carbohydrate, lipid, protein.
Electron microscope techniques, (e.g. metal shadowing, surface replicas, freeze-fracturing, negative staining, thin sectioning) coupled with chemical and/or enzyme dissection studies.	Provides information about ultrastructure of the wall and possible analysis of the wall layers.

EXPERIMENTAL TECHNIQUE	POSSIBLE DEDUCTIONS
Total hydrolysis.	Chromatography of hydrolysates reveal basic neutral/amino sugar composition of polymer.
Partial hydrolysis.	Chromatography of hydrolysates reveal partial breakdown products of wall polymers. Comparison with known standards can lead to identification of wall component present.
Enzyme digestion.	Action of specific enzymes (purity a most important criterion) against wall layers. Can lead to identification of the wall component present.
Periodate oxidation.	Reveals whether 1,3-glucosidic linkages are present or not.

Table 9

Outline of the sequential chemical treatments that spores were subjected to, and the points at which samples were taken for electron microscopic observation.

CHEMICAL TREATMENTS	E.M. OBSERVATIONS
Spores harvested	→ Surface layer of rodlets
↓	
5% KOH/6h/37°C	
↓	
3 washes sdw	→ Rodlet layer removed
↓	
5% KOH/18h/37°C	
↓	
3 washes sdw	→ More roughened appearance of spores
↓	
Autoclaved in 1:1(v/v) H_2O_2 + CH_3COOH	
↓	
3 washes sdw	→ Layer of thick microfibrils and plate-like layer
↓	
5% KOH/1h/100°C	
↓	
	→ Supernatant (A)
↓	
3 washes sdw	→ Layer of thin microfibrils

Table 10

Outline of the procedure used to extract the layer of thick microfibrils from supernatant (A) (cf. Table 9).

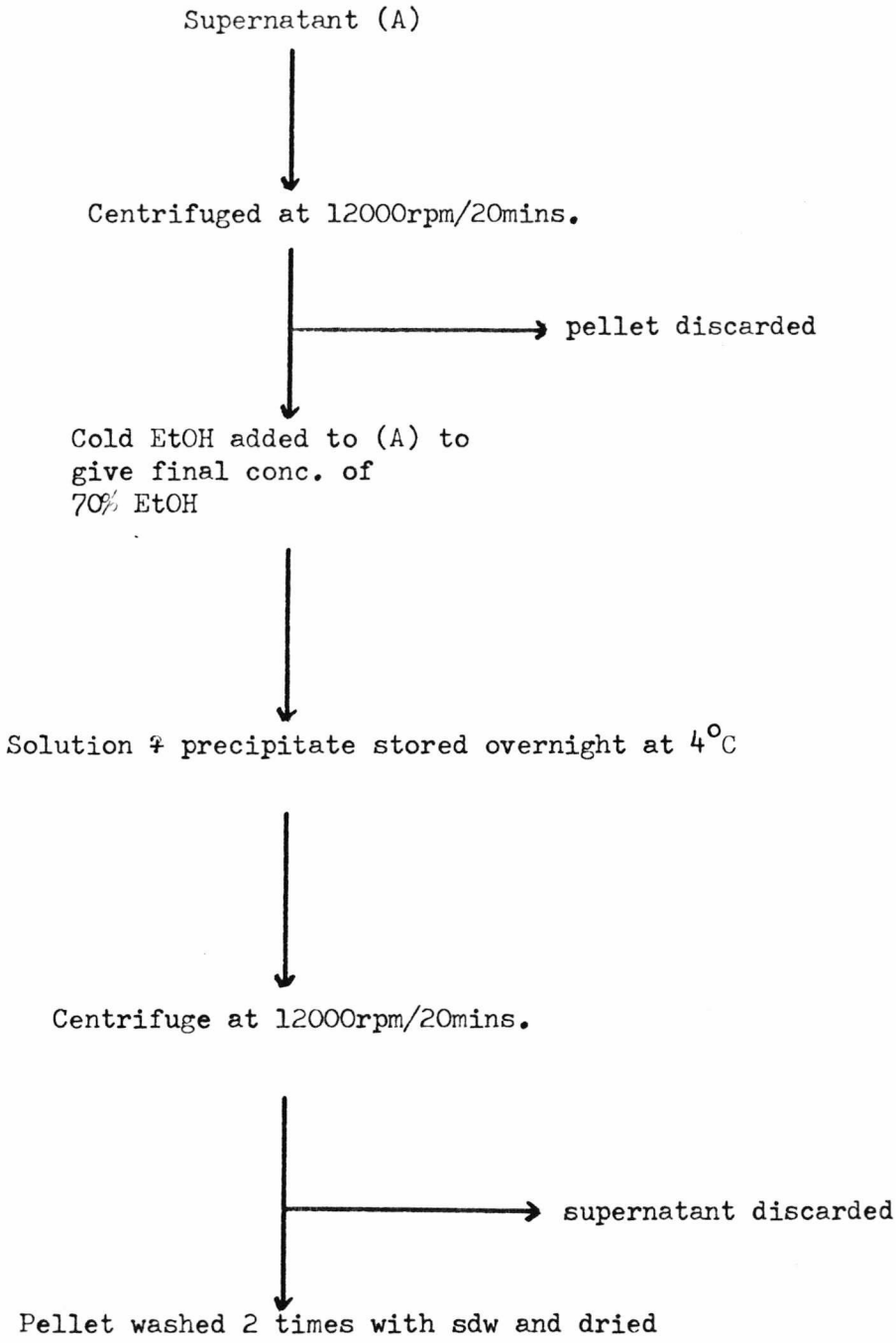
Supernatant (A)
Centrifuged at 12000rpm/20mins.
pellet discarded
Cold EtOH added to (A) to give final conc. of 70% EtOH
Solution + precipitate stored overnight at 4°C
Centrifuge at 12000rpm/20mins.
supernatant discarded
Pellet washed 2 times with sdw and dried

Fig. 69

SR of untreated dormant spore. Note the criss-cross pattern of surface rodlets (x71100)

Fig. 70

SR of dormant spore after 6h 5% KOH treatment. The surface layer of rodlets has been removed to reveal an underlying amorphous layer. (x40600)

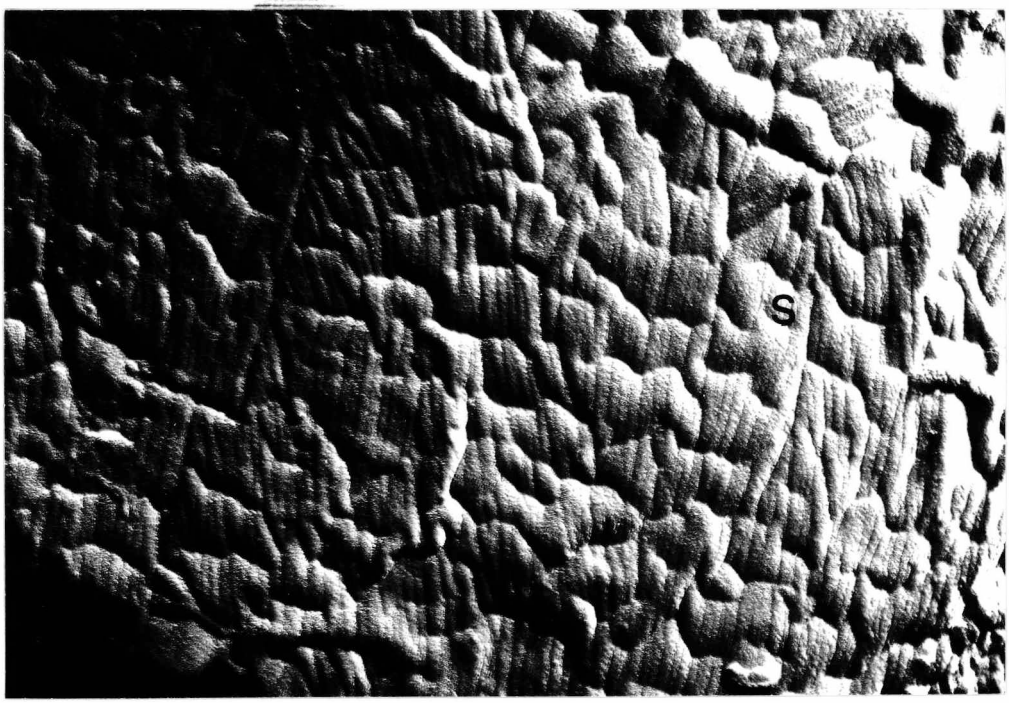
S

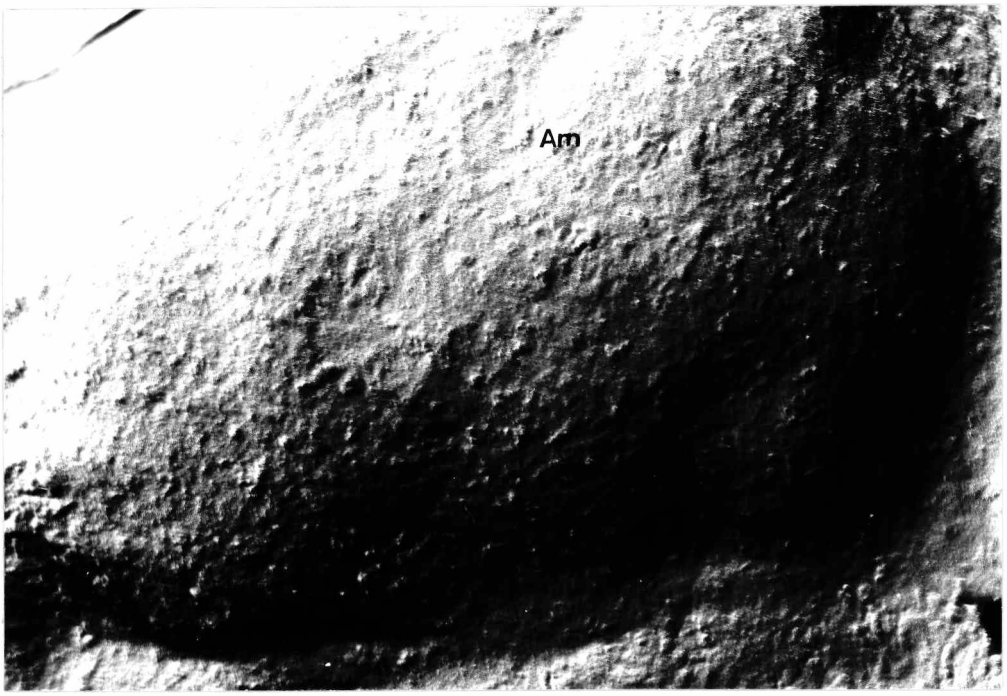
Am

Fig. 71

SR of dormant spores after (1) 6h 5% KOH and (2) further 18h in 5% KOH. The smooth nature of the wall seen in Figure 70 has been removed revealing a more roughened view of the spores. Microfibrils seeming to be located beneath the rugose layer can be observed at the edge of certain spores. (x7900)

Fig. 72

SR of dormant spores after (1) 6h 5% KOH and (2) further 18h in 5% KOH. Higher magnifications (Figs. 72-75) of the new wall layer show it to be covered with many wrinkled bumps. The spores still maintain (cf. Fig. 71) their structural integrity. (x20000)

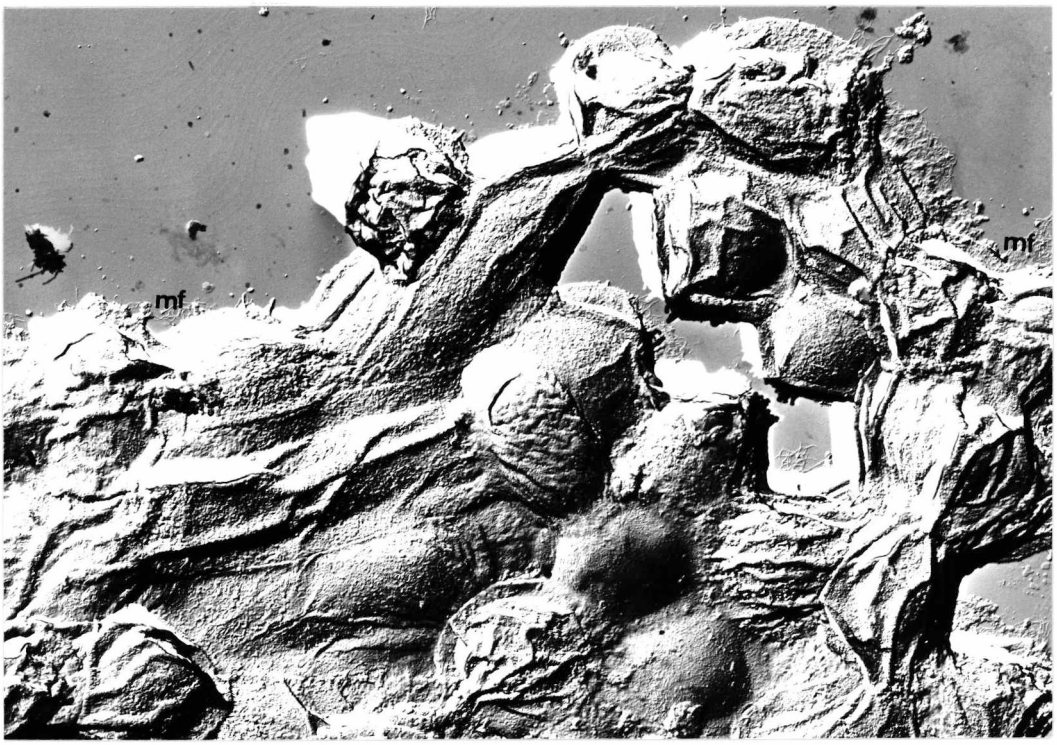
mf
mf

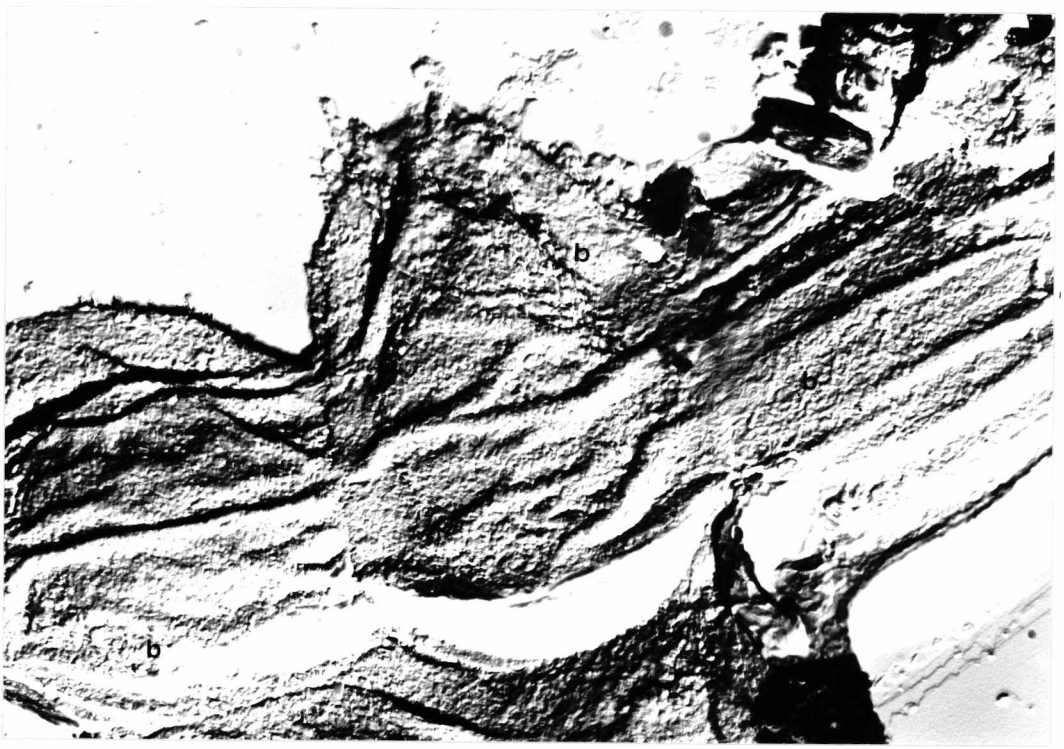
b
b
b

Fig. 73

SR of dormant spores after initial alkaline treatment (6h + 18h in 5% KOH), (x17500)

Fig. 74

SR of dormant spores after initial alkaline treatment. (x20000)


b


b

Fig. 75

SR of dormant spores after initial alkaline treatment (x24400)

Fig. 76

SR of dormant spore after initial alkaline treatment. Wrinkled bumps can be observed individually on the rugose wall layer of the spore (x37300)

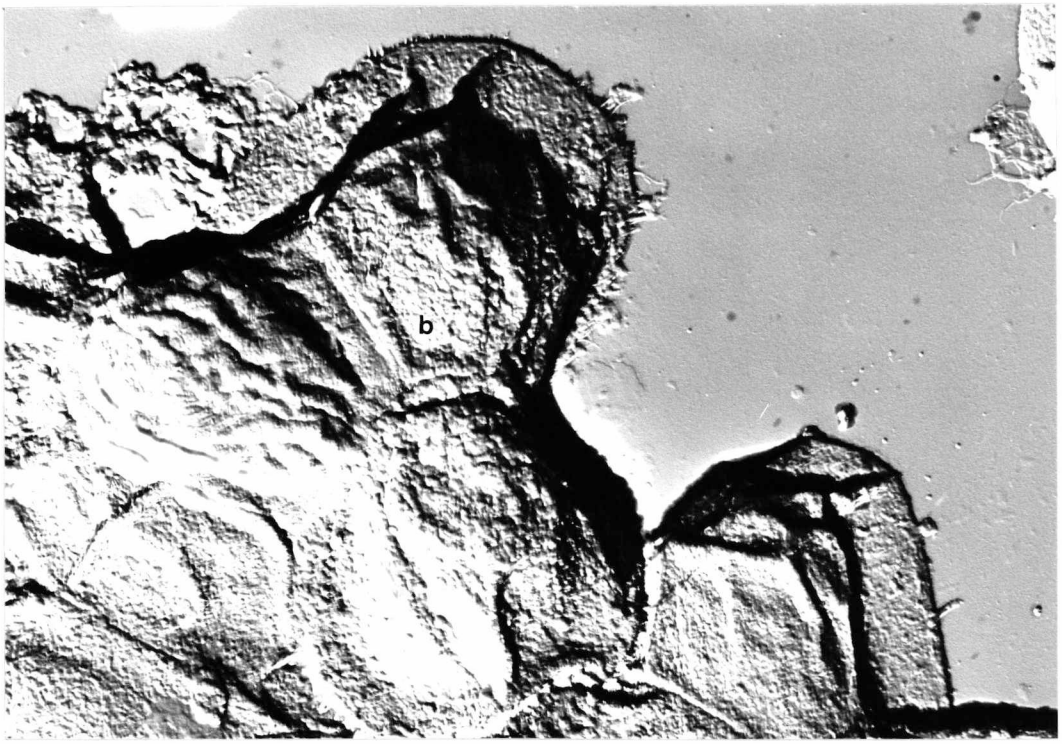
b


b

Fig. 77

SR of dormant spores after initial alkaline and autoclave treatments. Figures 77 - 79 show the "fried-egg" appearance of the spores, characteristic of spores at this stage in the chemical treatments (cf. Table 9). The layer of thick microfibrils can be seen as forming a tightly interwoven network of fibrils (x18200)

Fig. 78

SR of dormant spores after initial alkaline and autoclave treatments. Note the sheets of plate-like material (Figs. 77 - 84) covered with wrinkled bumps present in these preparations at this stage in the chemical treatments (x18100)

Fig. 79

SR of dormant spores after initial alkaline and autoclave treatments (x18000)

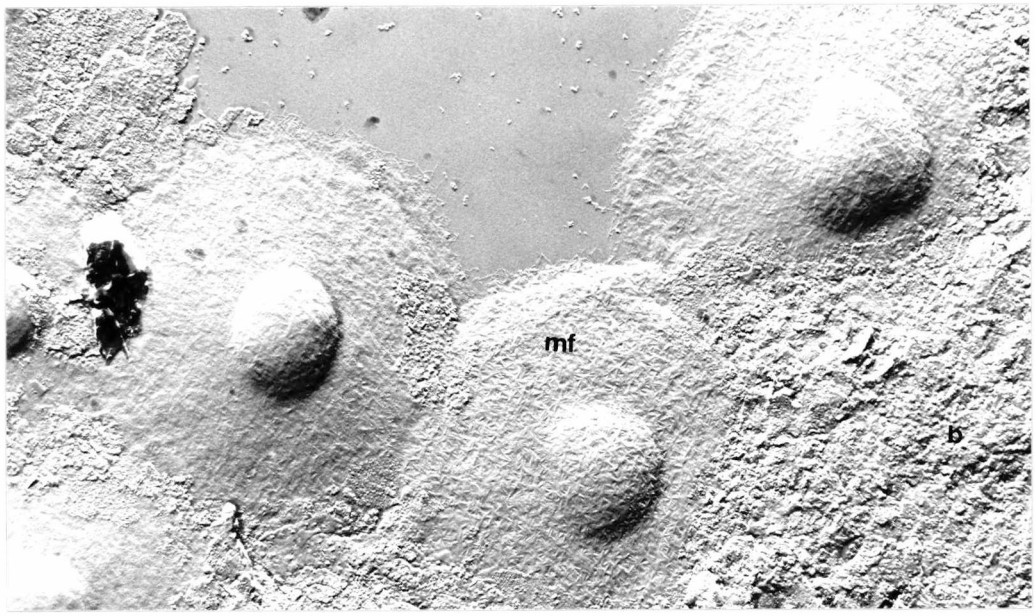
mf
b

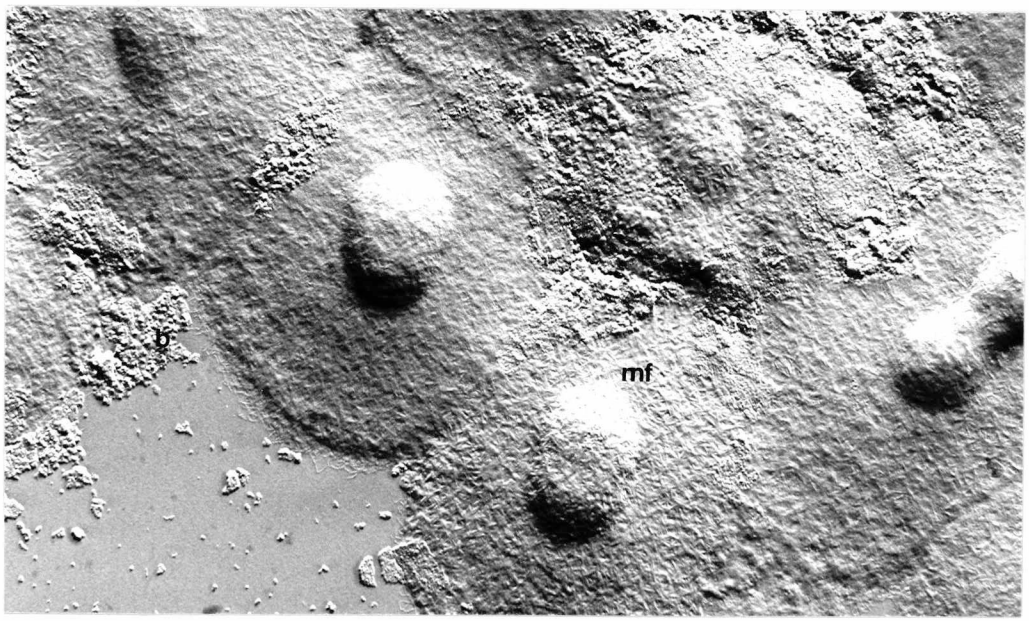
b
mf

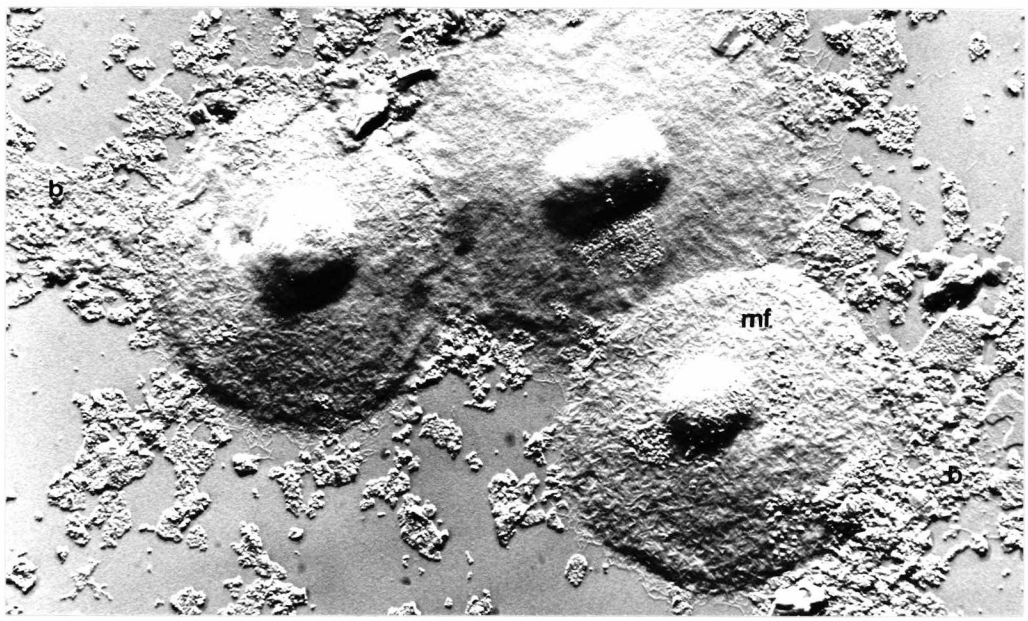
b
mf
b

Fig. 80

SR of dormant spores after initial alkaline and autoclave treatments. The thick microfibrils are masked by a layer of amorphous material in the spore on the left, whilst the thick microfibrils are seen as being embedded in an amorphous matrix in the spore on the right (x32000)

Fig. 81

SR of dormant spores after initial alkaline and autoclave treatments. A similar situation as seen in Figure 80 is observable in this micrograph (x31000)

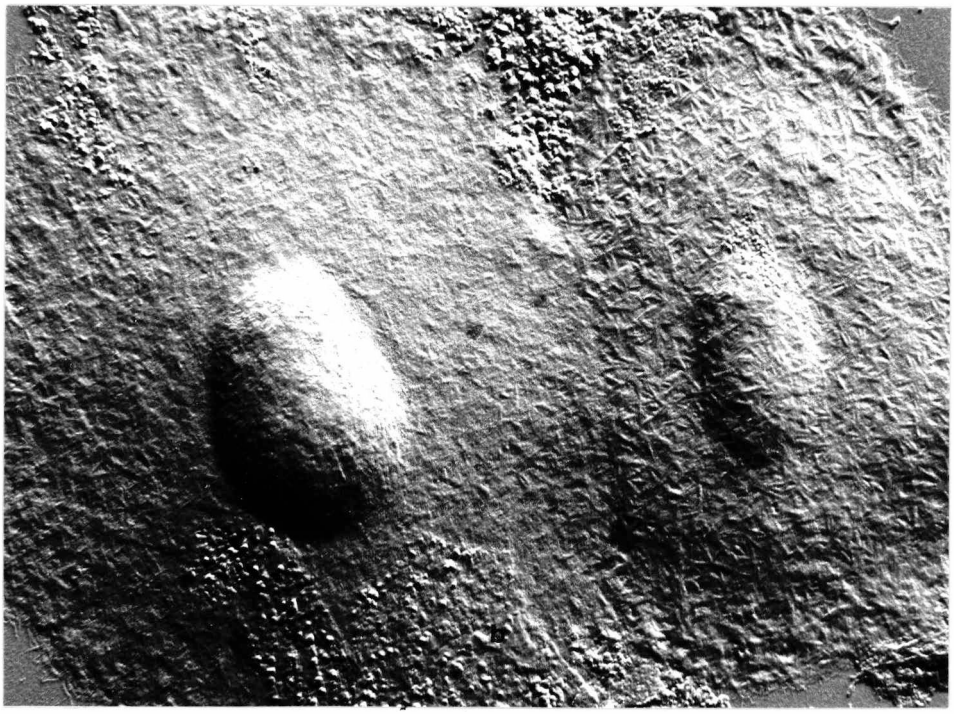


b

Fig. 82

SR of dormant spore after initial alkaline and autoclave treatments. Close examination of the thick microfibrils (Figs. 82 - 84) did not show that the thick fibrils were composed of smaller units (x31800)

Fig. 83

SR of dormant spore after initial alkaline and autoclave treatments (x31300)

Fig. 84

SR of dormant spore after initial alkaline and autoclave treatments (x31400)

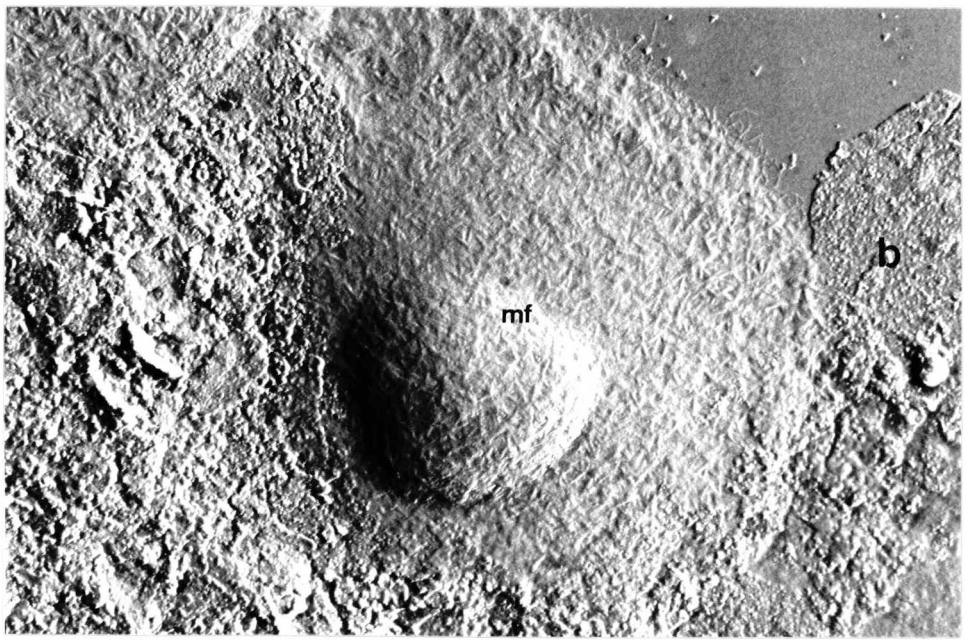
mf
b

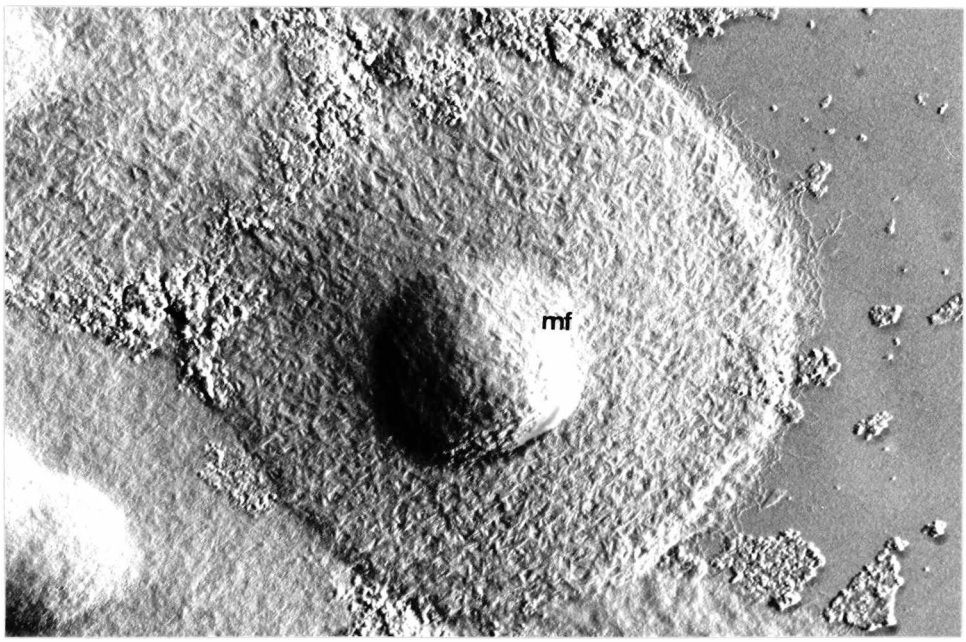
mf

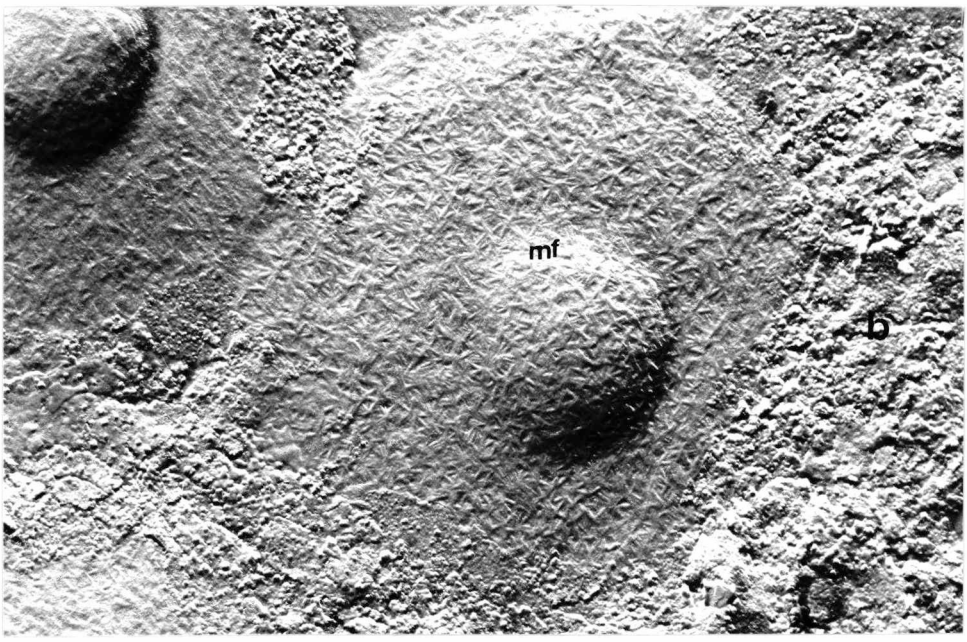
mf
b

Fig. 85

SR of dormant spore after initial alkaline and autoclave treatments. The criss-cross network of the thick microfibrils is clearly seen in both this and the following micrograph (x84400)

Fig. 86

SR of dormant spore after initial alkaline and autoclave treatments (x104000)

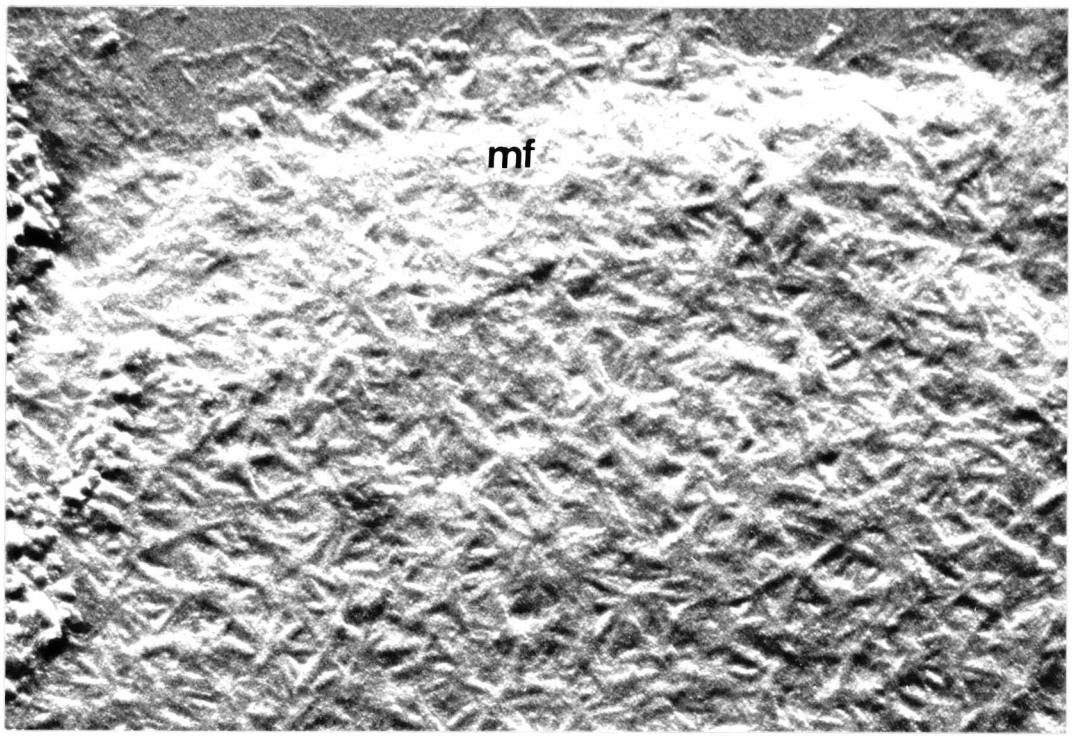
mf

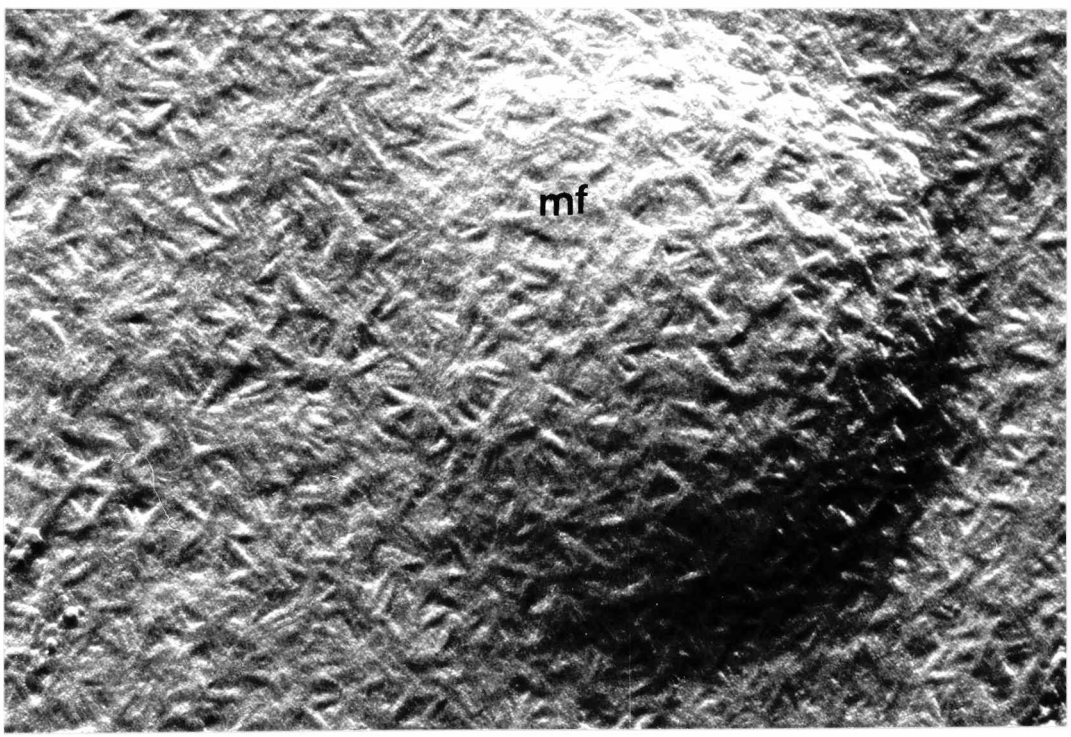
mf

Fig. 87

SR of dormant spore after initial alkaline and autoclave treatments. The sheet of material on the left-hand side of the micrograph is covered with numerous small, wrinkled bumps (x37100)

Fig. 88

SR of dormant spore after initial alkaline and autoclave treatments. Sheets of plate-like material covered with wrinkled bumps is seen as lying on top of the spore (x37300)

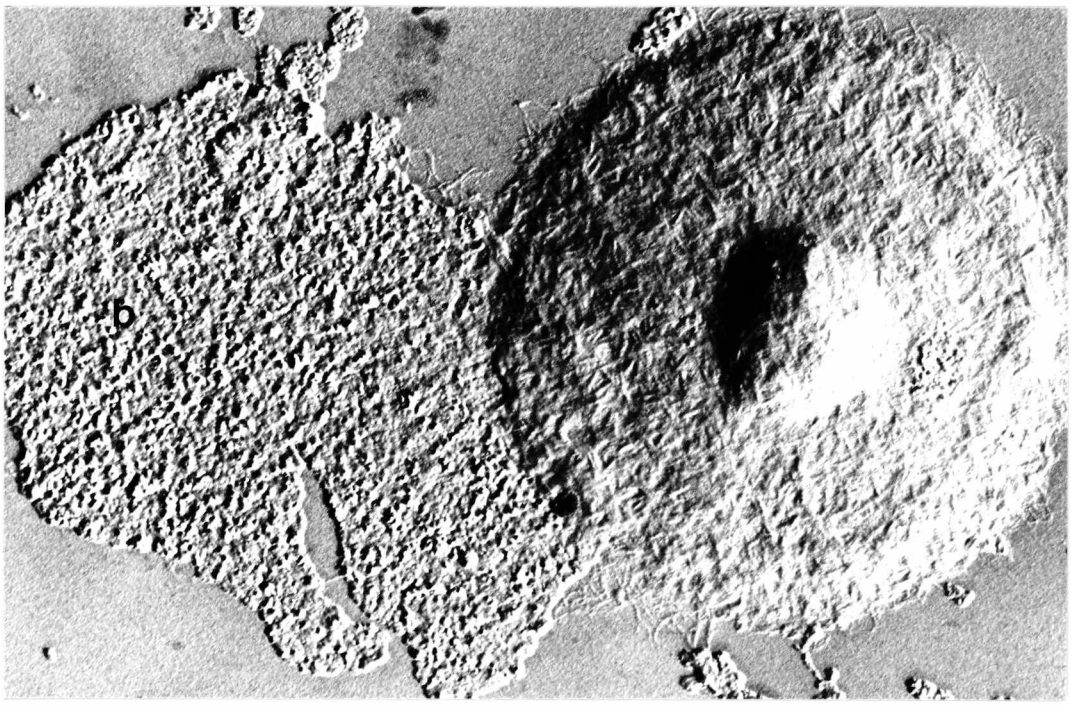
b

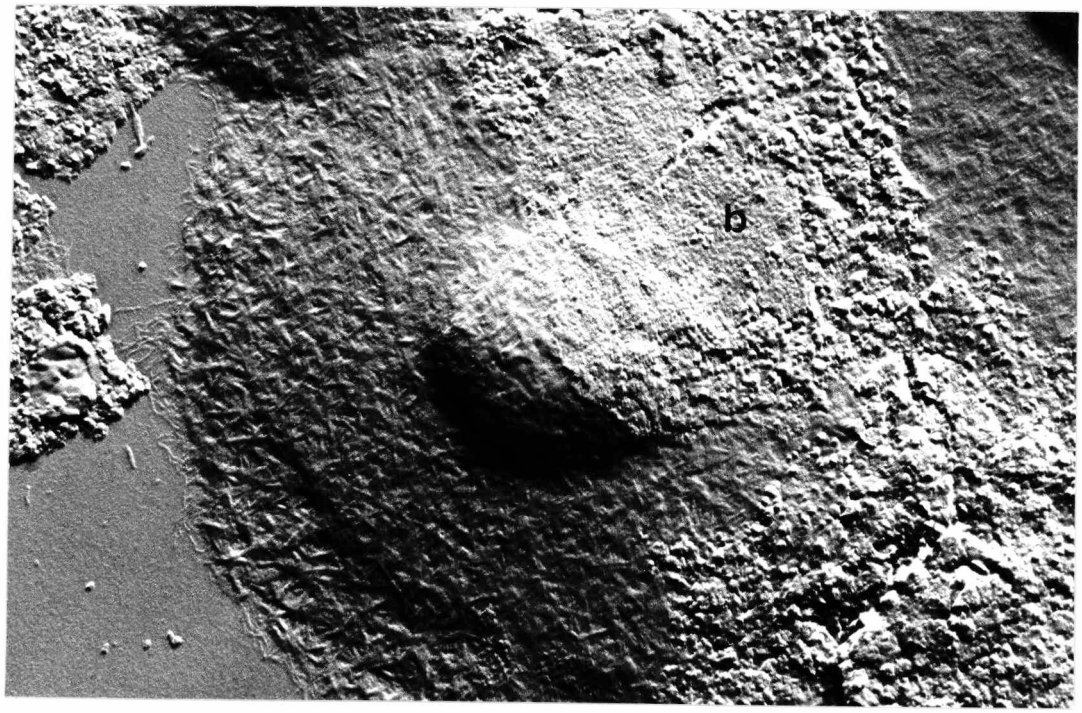
b

Fig. 89

MS of dormant spore after completion of all chemical treatments (cf. Table 9). The layer of thin microfibrils are composed of long fibrils criss-crossing an underlying microfibrillar mesh. (x20000)

Fig. 90

MS of dormant spore after completion of all chemical treatments. The longer microfibrils (arrows) can be seen more clearly. (x38400)

Fig. 91

MS of dormant spore after completion of all chemical treatments. The micrograph shows the criss-cross network of thin microfibrils with the overlying longer microfibrils (x38500)

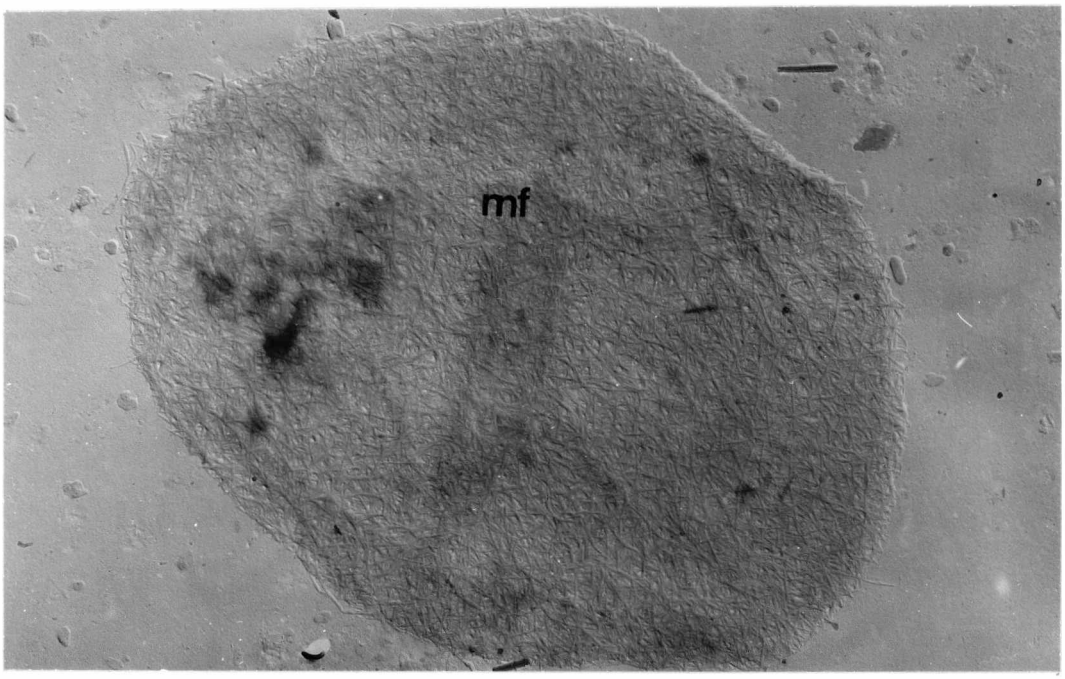
mf

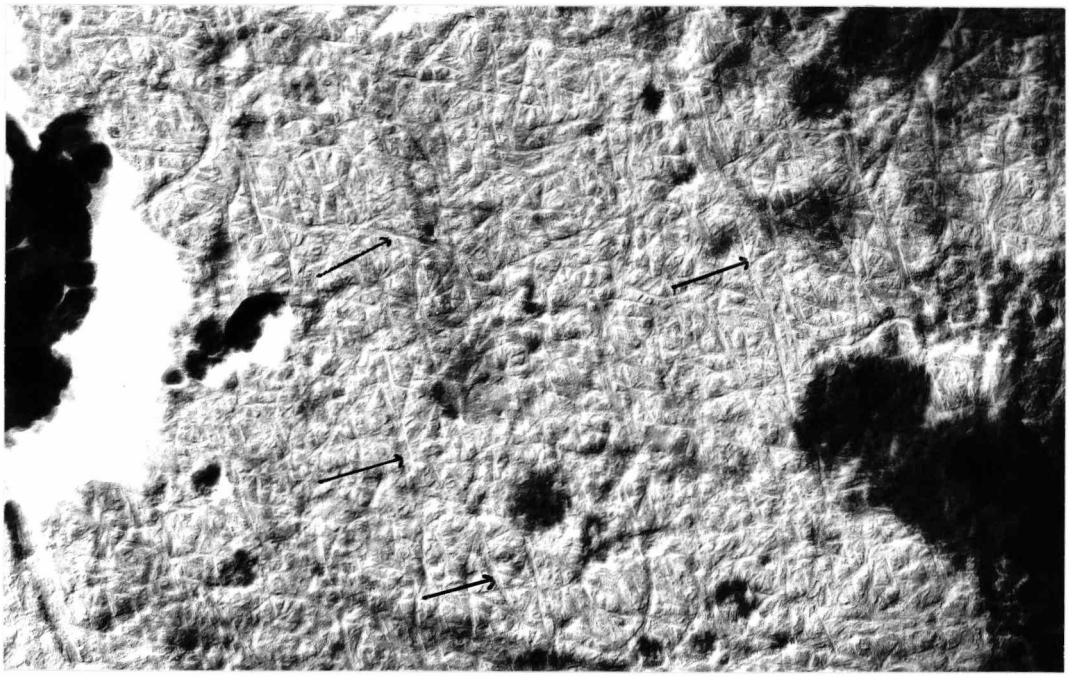

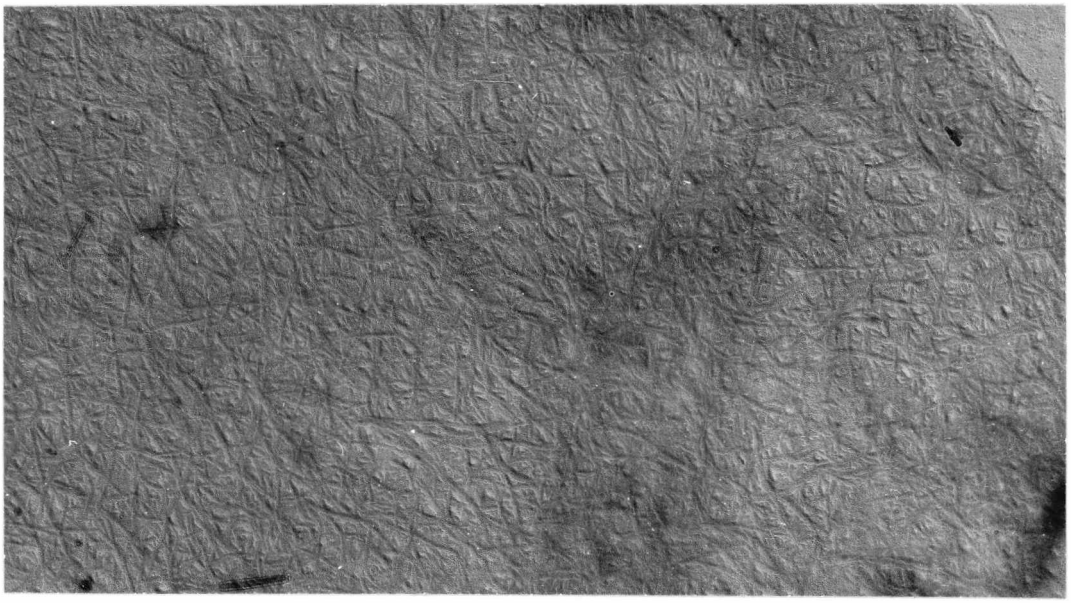

Fig. 92

MS of dormant spore after completion of all chemical treatments. Higher magnification of these longer microfibrils shows that they are probably composed of aggregates of several fibrils (mf). This can also be observed in the following micrograph (x54100)

Fig. 93

MS of dormant spore after completion of all chemical treatments (x59100)

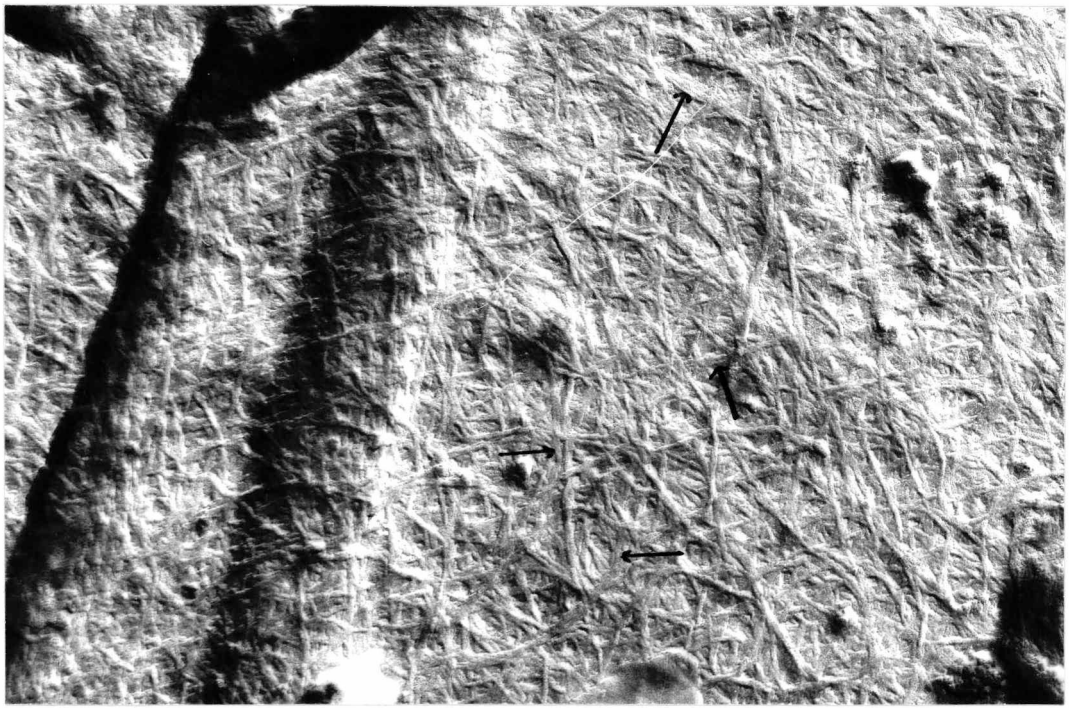

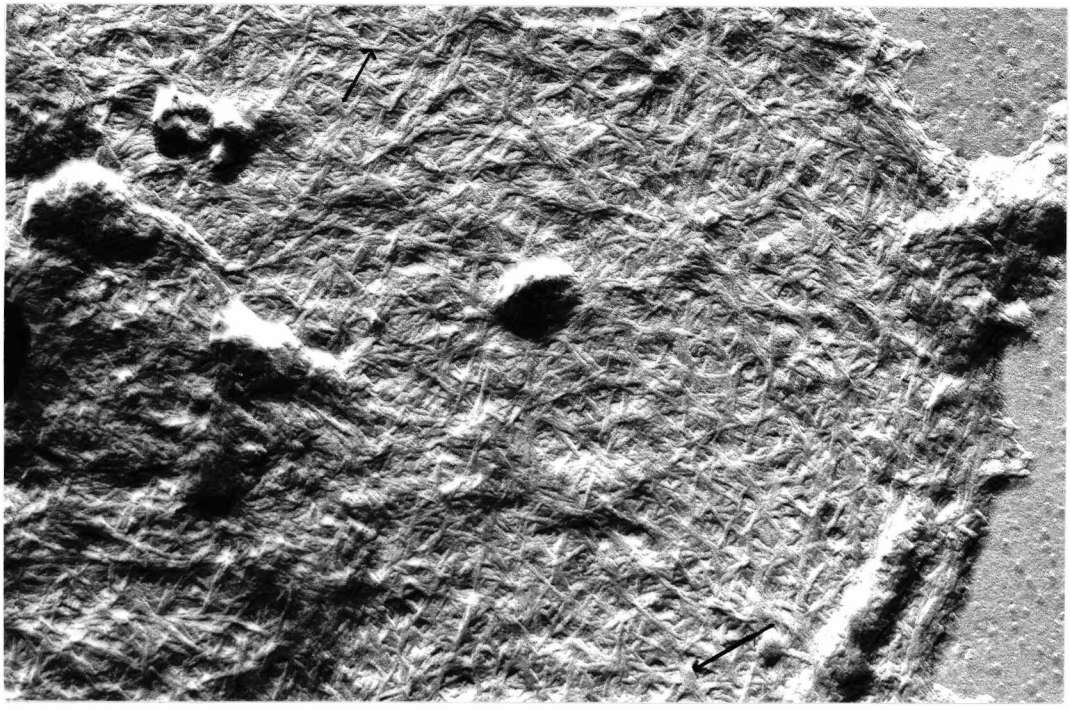

Fig. 94

TS of untreated dormant spore. The thick nature of the spore wall (W) is seen, as is the plasmamembrane (P), mitochondria (M) and nucleus (N), (x39000)

Fig. 95

TS of untreated dormant spore (x93100). The spore wall has three distinct layers:

A - an outer layer,

B - a middle layer,

C - an inner layer.

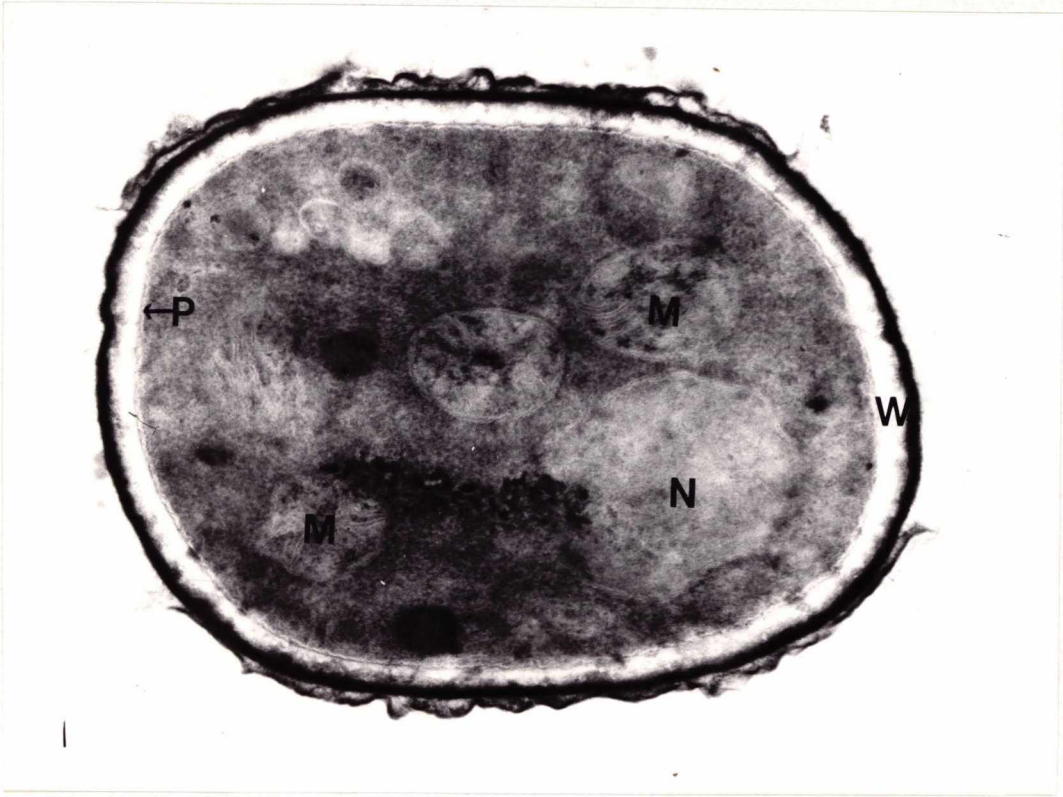
←P
M
W
N
M

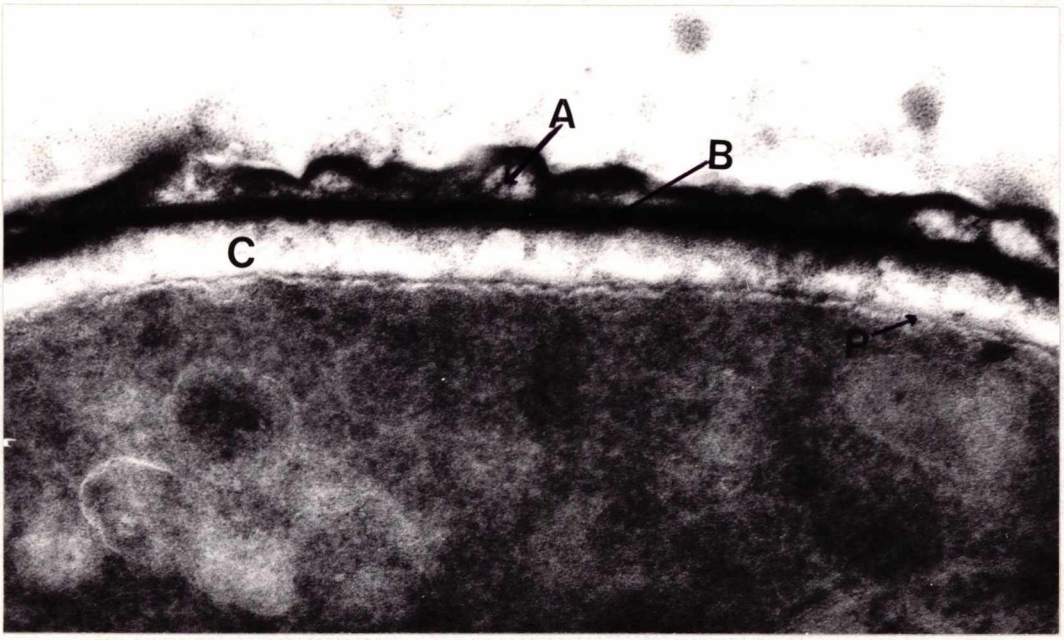
A
B
C
P

Fig. 96

Diagrammatic representation of sugar spots on chromatogram after total hydrolysis of the thick microfibril sample.

A - glucose

B - galactose

C - mannose

D - sample of thick microfibrils

E - galactose/glucose/mannose

F - glucose

G - mannose

H - galactose

I - glucose

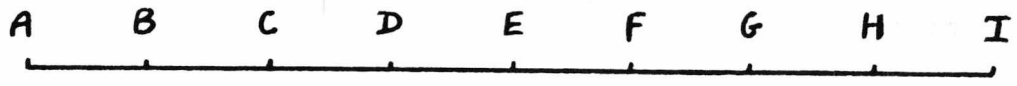
A
B
C
D
E
F
G
H
I

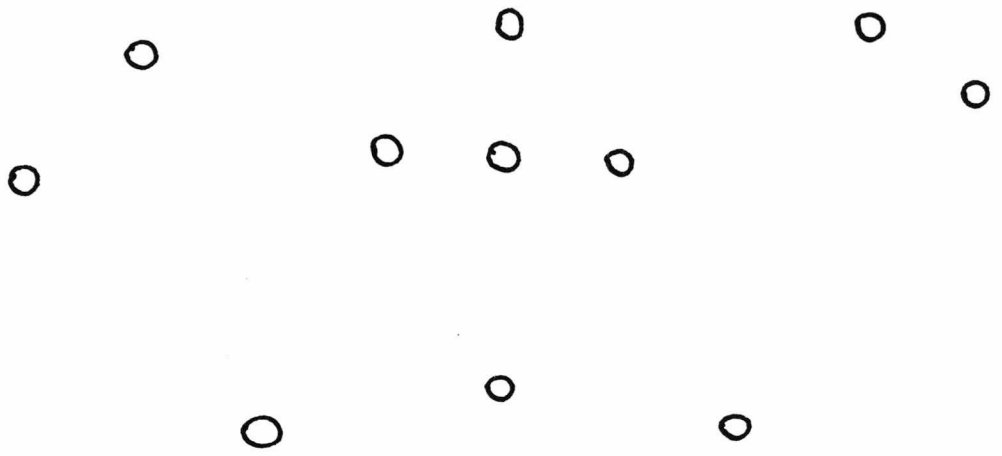

Table 11

R_G values, calculated from Figure 96, for the sugar spots obtained after total hydrolysis of the thick microfibril sample. R_G values were based upon the glucose spot run at E (Fig. 96).

SUGAR	R_G VALUE
A - glucose	1.07
B - galactose	0.88
C - mannose	1.40
D - thick microfibril sample	1.02
E - galactose	0.81
E - glucose	1.00
E - mannose	1.37
F - glucose	1.02
G - mannose	1.43
H - galactose	0.83
I - glucose	0.89

Fig. 97

Infra-red scans of the thick microfibril sample (A), of laminarin from Laminaria hyperborea (B), and a 1:1 (w/w) mixture of laminarin and protein (C).

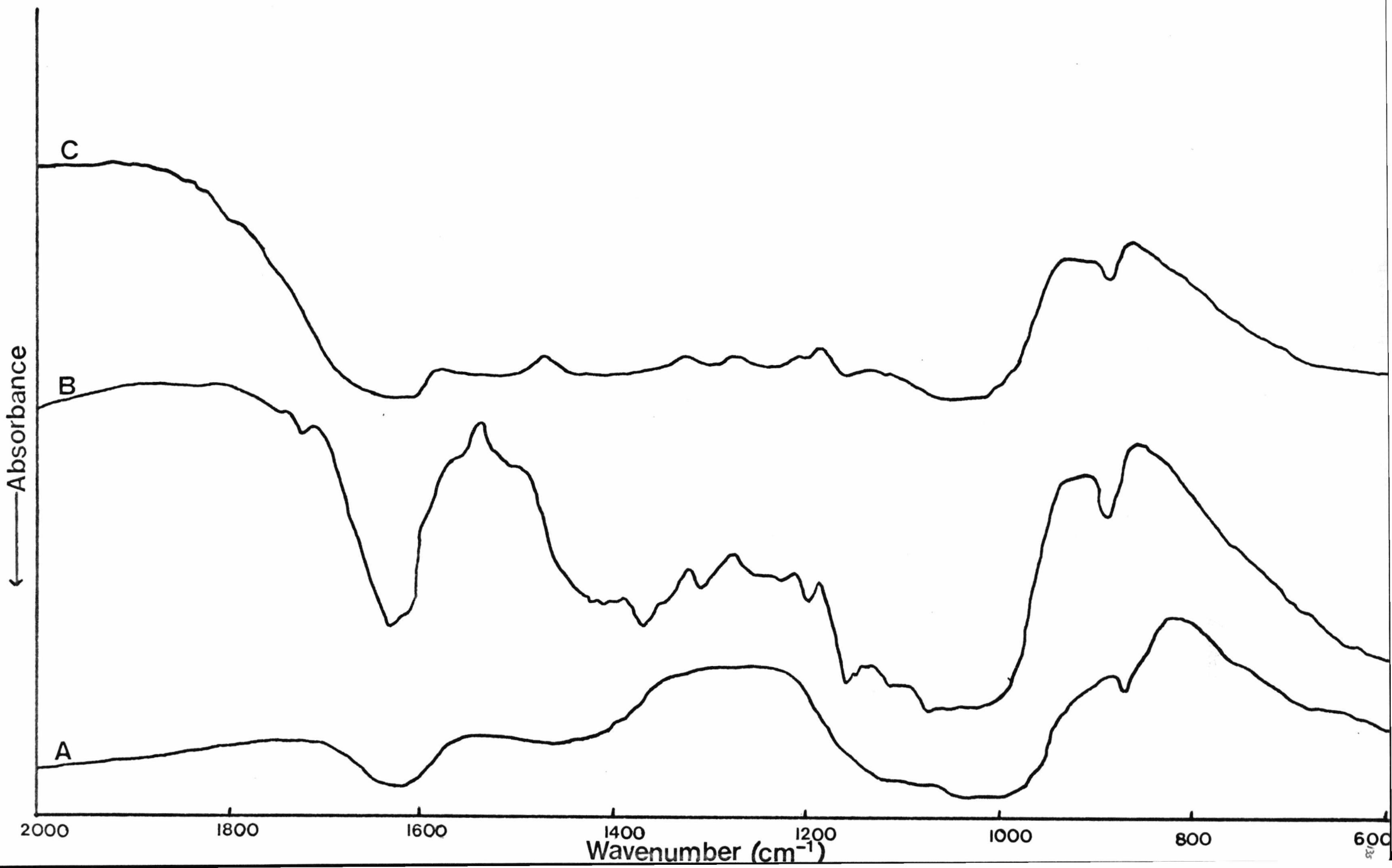
C
B
A
Absorbance
2000
1800
1600
1400
1200
1000
800
600
Wavenumber (cm⁻¹)

Fig. 98

Diagrammatic representation of sugar spots on chromatogram after total hydrolysis of the thin microfibril sample.

A - glucose

B - glucosamine

C - galactosamine

D - sample of thin microfibrils

E - galactosamine/glucosamine/glucose

F - galactosamine

G - glucosamine

H - glucose

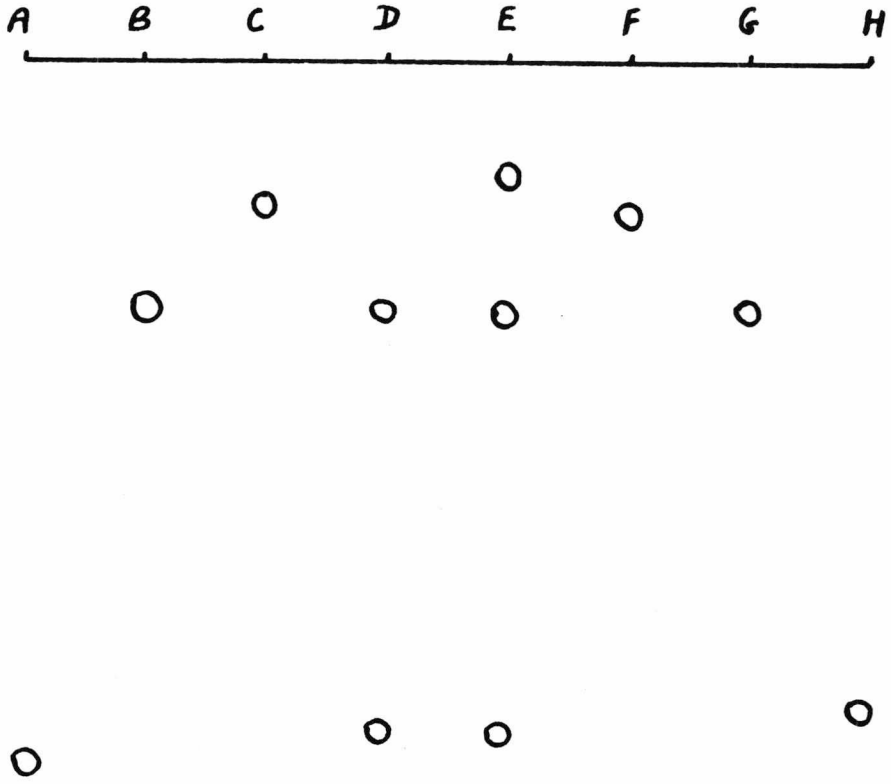
A
B
C
D
E
F
G
H

Table 12

R_G values, calculated from Figure 98, for the sugar spots obtained after total hydrolysis of the thin microfibril sample. R_G values were based upon the glucose spot run at E (Fig. 98).

SUGAR	R_G VALUE
A - glucose	1.05
B - glucosamine	0.36
C - galactosamine	0.21
D - thin microfibril sample	0.35/1.0
E - galactosamine	0.19
E - glucosamine	0.36
E - glucose	1.0
F - galactosamine	0.23
G - glucosamine	0.35
H - glucose	0.97

Fig. 99

Infra-red scans of the thin microfibril sample (A), and commercial chitin, B.D.H.Ltd, (B).

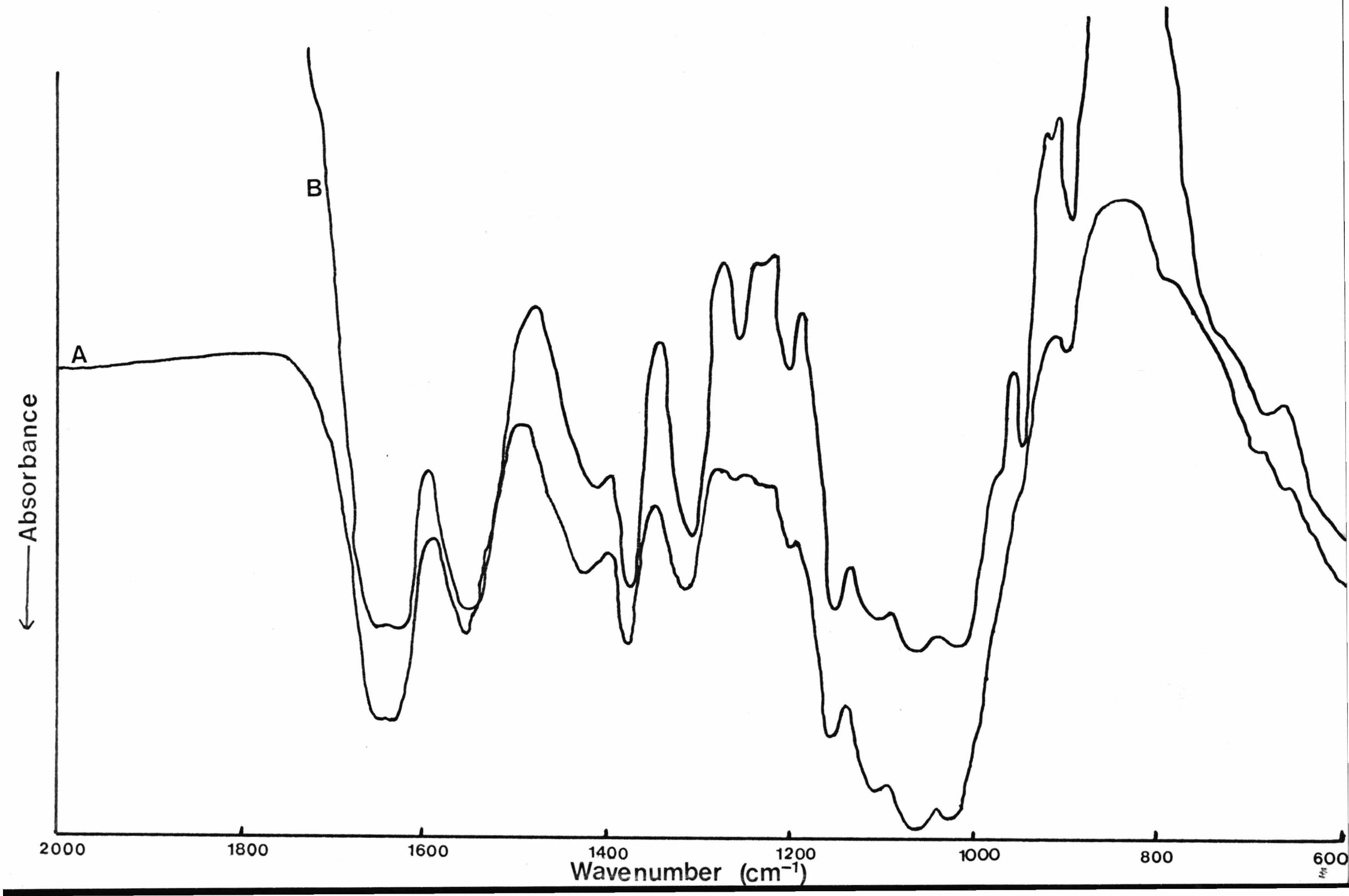
B
A
Absorbance
2000
1800
1600
1400
1200
1000
800
600
Wavenumber (cm⁻¹)

Table 13

Comparison of I.R. scans of chitin from different fungi:

A - *Syncephalastrum racemosum*; thin microfibril sample.

B - Commercial chitin (B.D.H.Ltd).

C - *Paracoccoides brasiliensis*.[1]

D - *Histoplasma farciminosum*.[1]

E - - chitin.[2]

F - *Aspergillus nidulans*.[3]

G - Commercial standard, crab chitin (Sigma).[4]

H - *Rhizophydium patellarium*.[4]

I - *Phylctochytrium arcticum*.[4]

J - *Choanephoria cucurbitarum*.[5]

K - chitosan.[2]

(1) San-Blas & Carbonell (1974).

(2) Michell & Scurfield (1967).

(3) Katz & Rosenberger (1970).

(4) Gerhart & Barr (1974).

(5) Letourneau, Deven & Manocha (1976).

WAVELENGTH (cm^{-1})

A	B	C	D	E	F	G	H	I	J	K
				3450		3440	3420	3420		
				3265	3260	3270		3270		
	3100	3150	3100	3105	3090	3110	3100	3100		
2900	2930	2920	2900	2960		2940	2920	2920		2960
	2880			2875		2870	2880	2870		2875
1645	1630	1640		1655	1650	1660	1660	1650	1655	1640
			1610	1620		1640	1620	1625	1624	
										1590
1555	1550	1575	1560	1550		1560	1550	1555	1550	
		1475					1480			
			1450				1455			1440
1425	1415			1420	1410			1420	1420	1400
1375	1375	1390	1370	1375		1380	1375	1380	1375	
1315	1310	1320		1310	1310	1320	1310	1315	1300	
1265	1260	1260	1250^{sh}	1260		1265		1260		1290
1200	1205			1210		1210	1200	1200	1228	
1155	1155	1150		1155		1160	1150	1150	1160	1150
1115^{sh}	1110	1120	1110	1115	1120	1120			1115	
1065	1065	1075	1060	1072		1060	1070	1070	1072	
1025	1020	1040	1025	1020		1030	1030	1025	1015	1040
	950	980	980	950	950	950	955	950	955	
900	895	894	894	894	890	900	900	900	895	900
P_t 12	16	13	12	19	8	18	17	18	13	9

Fig. 100

Pictorial representation of the dormant spore wall:

(1) TS of dormant spore; W, dormant spore wall.

(2) TS of dormant spore wall; A, outer layer; B, middle layer; C, inner layer.

(3) SR of surface rodlet layer (=A).

(4) SR of layer of amorphous material (=A).

(5) SR of rugose or plate-like layer (=B).

(6) SR of layer of thick microfibrils (=C).

(7) SR of layer of thin microfibrils (=C).

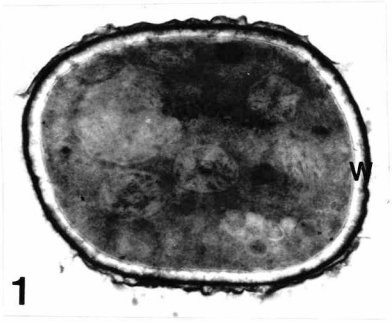
W
1

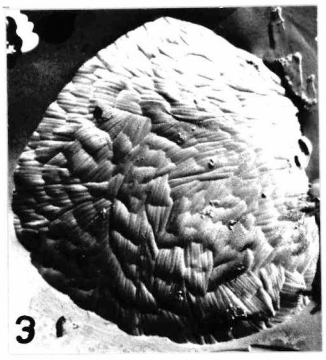
3

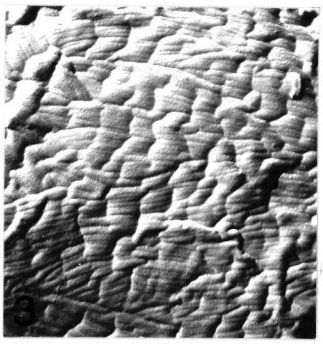
3


4


4

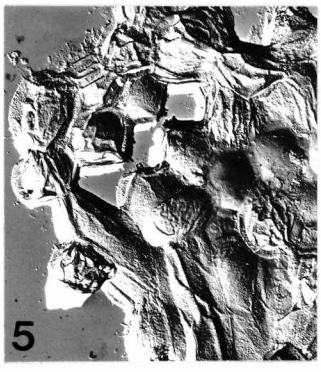
5

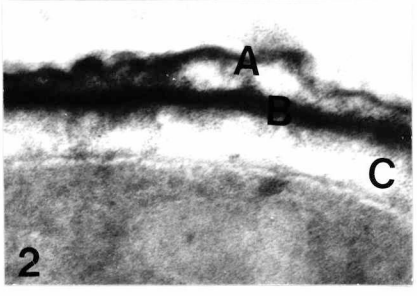
A
B
C
2

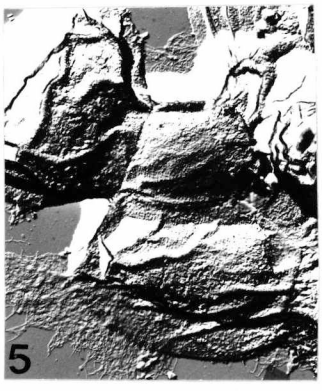
5

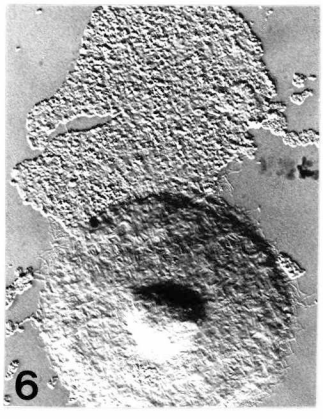
6

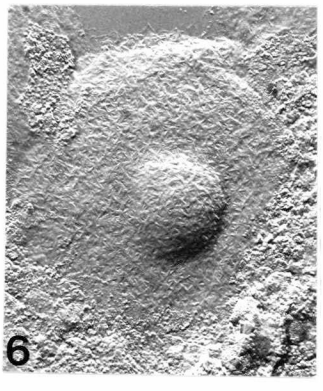
6

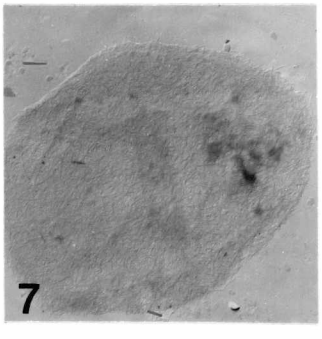
7

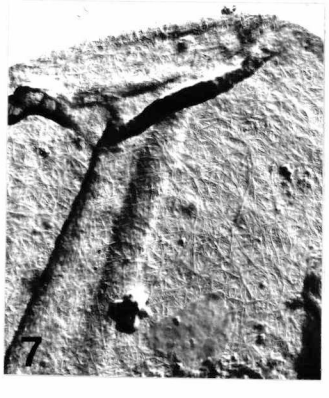
7

Fig. 101

Diagrammatic representation of the dormant spore wall:

(1) Surface rodlet layer.

(2) Amorphous base layer.

(3) Rugose or plate-like layer.

(4) Layer of thick microfibrils.

(5) Layer of thin microfibrils.

(6) Plasmamembrane.

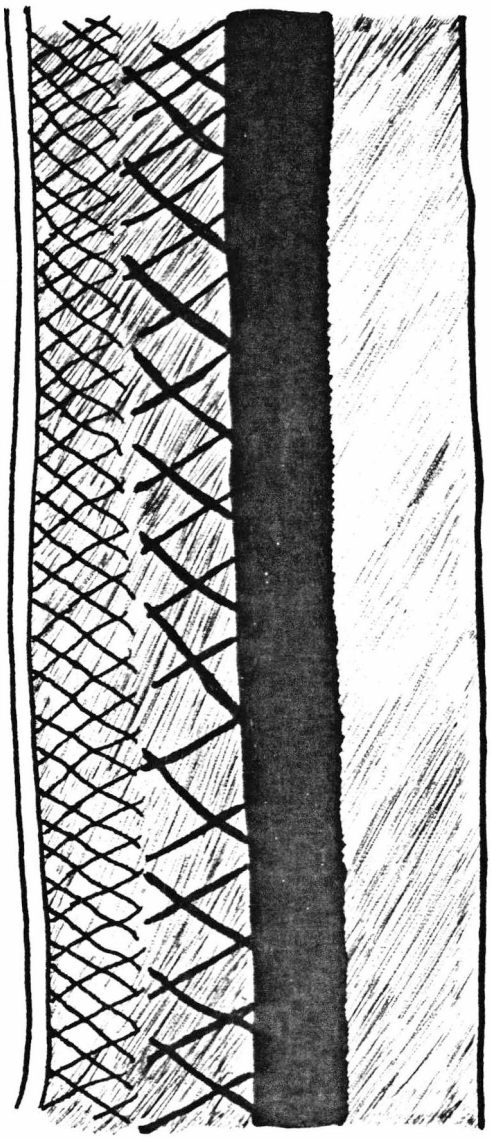

(6) (5) (4) (3) (2) (1)

CHAPTER SIX

Fig. 102

TS of dormant spore. A, outer wall layer; B, middle wall layer; C, inner wall layer. (x32300)

Fig. 103

T.S. of swollen spore with germ tube emergence just beginning. A new wall layer (D) has formed around the entire space. The breakpoint (X) between spore and germ tube is clearly seen. Mitochondria (M), nucleus (N) and nucleolus (R) can also be observed (x15300)

Fig. 104

TS of swollen spore. The new wall layer (D) has formed around the spore between the inner wall layer C and plasmamembrane (P). Cellular organelles are also seen (as in Fig.103), with many ribosomes present (x15300)

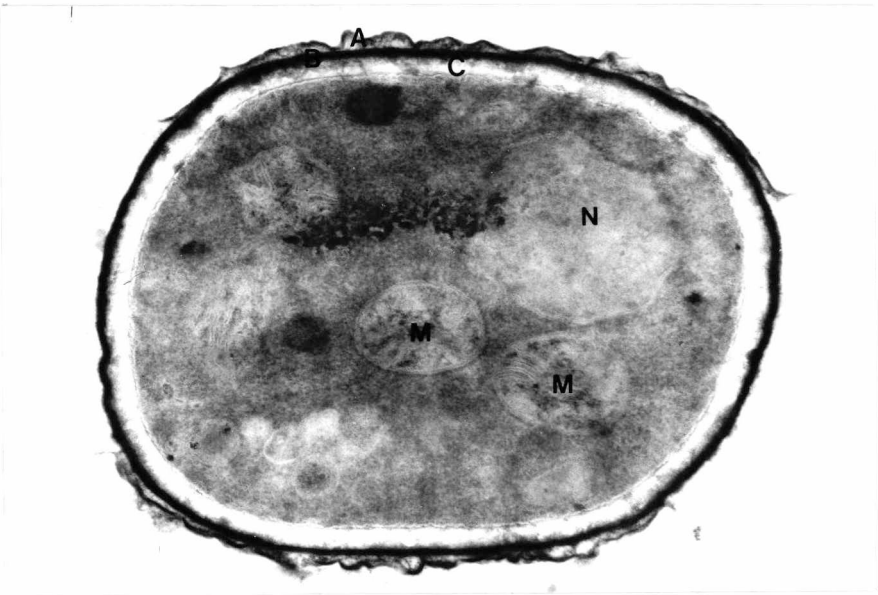
A
B
C
N
M
M

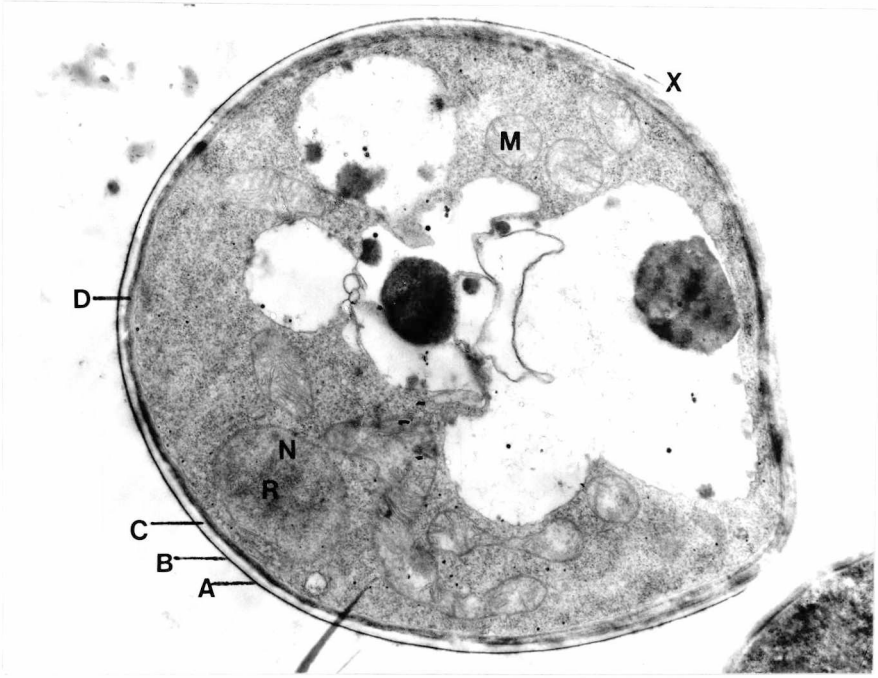
X
M
D
N
R
C
B
A

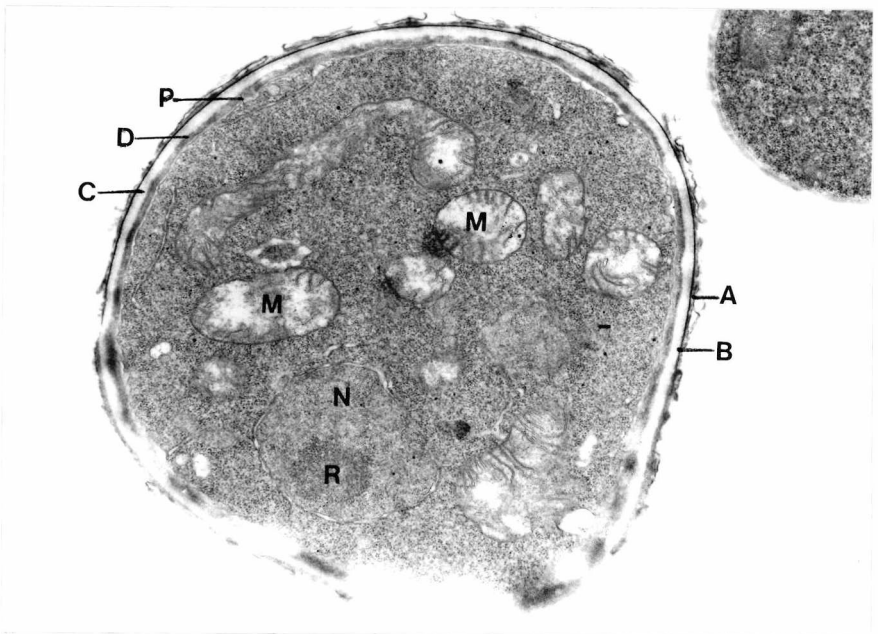
P
D
C
M
M
A
B
N
R

Fig. 105

TS of swollen spore with germ tube emergence just beginning. The breakpoint (X) is discernable as is the new wall layer (D) (x22300)

Fig. 106

TS of swollen spore with germ tube (germinated spore). The breakpoint (X) and new wall layer (D) are present. Layer (D) is seen as being continuous with the germ tube wall. (x13700)

Fig. 107

TS of breakpoint (X) between swollen spore (Sw) and germ tube (g). The wall layer D is composed of two layers (D_1 and D_2); only these two layers are present in the germ tube wall (x36900)

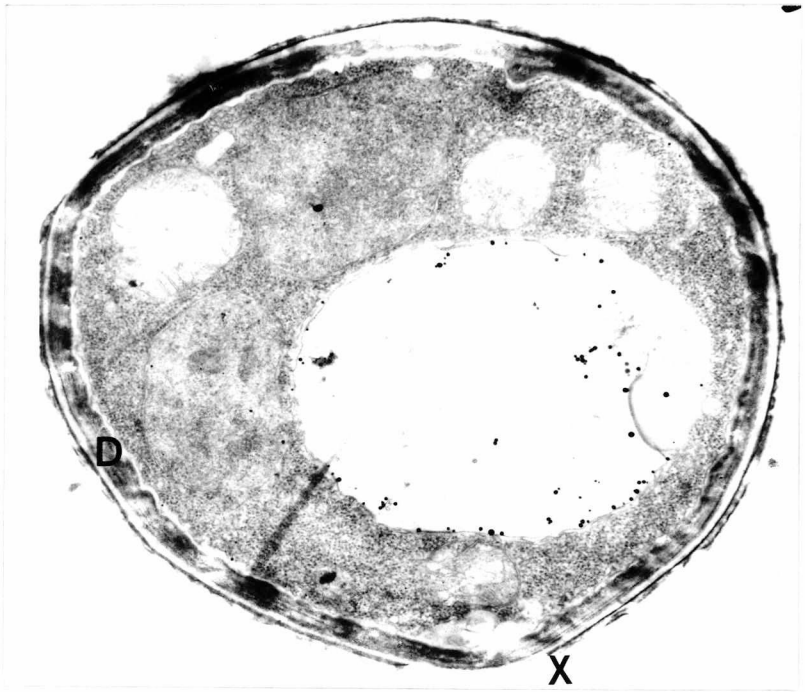
D
X

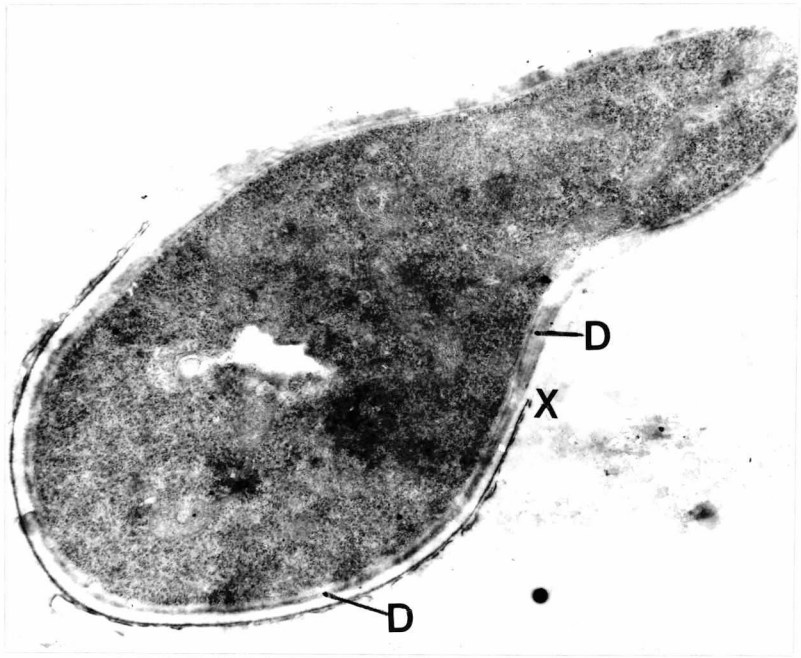
D
X
D

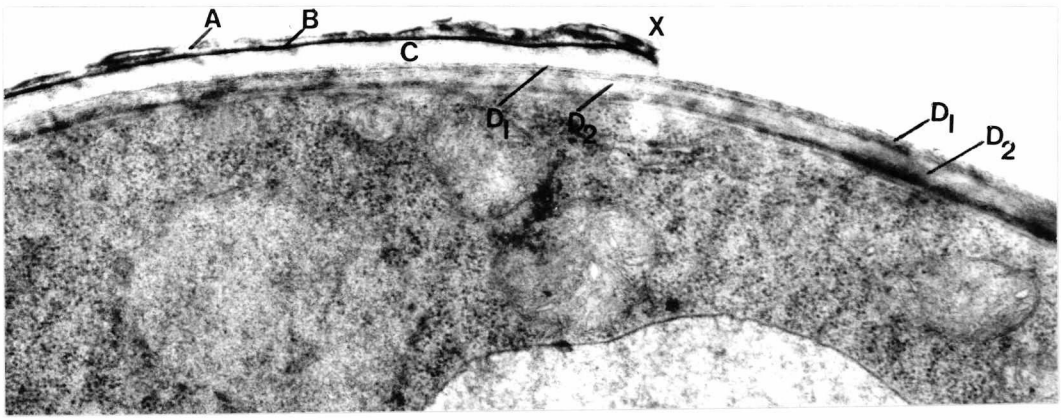
A
B
C
X
D1
D2
D1
D2

Fig. 108

SR of untreated germinated spore. In both this micrograph and the following one, the breakpoint (X) between the surface rodlet layer of the spore (S) and the smooth surface of the emergent hypha (H) is seen (x4500)

Fig. 109

SR of untreated germinated spore (x4400)

Fig. 110

SR of untreated germinated spore. From this spore two germ tubes have developed. They both have smooth outer walls, contrasting with the surface layer of rodlets on the spore (x14400)

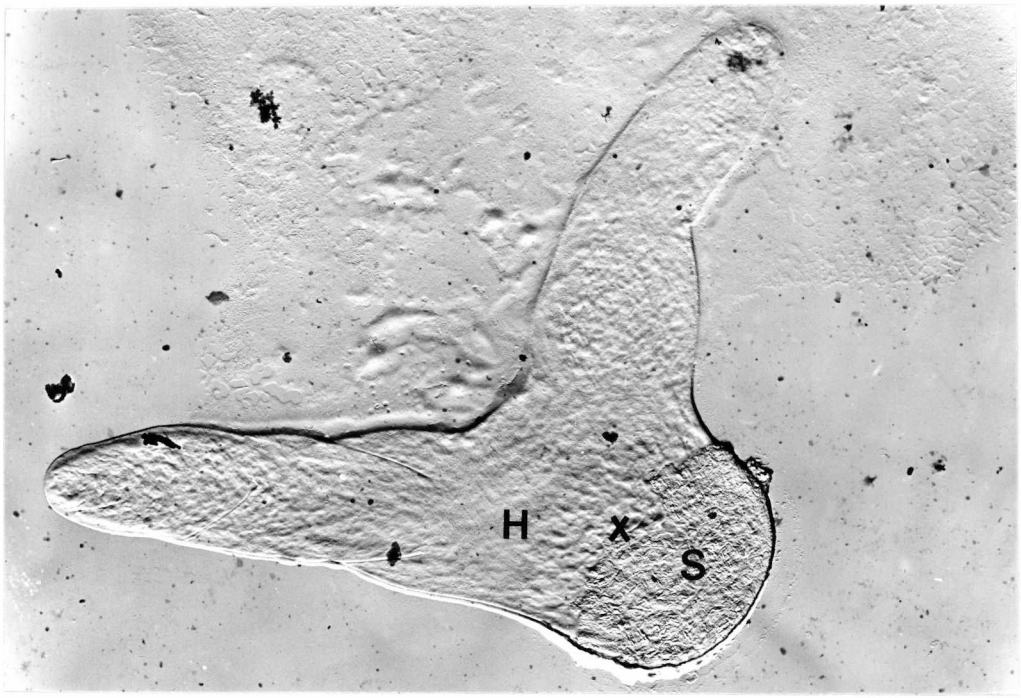
H
X
S

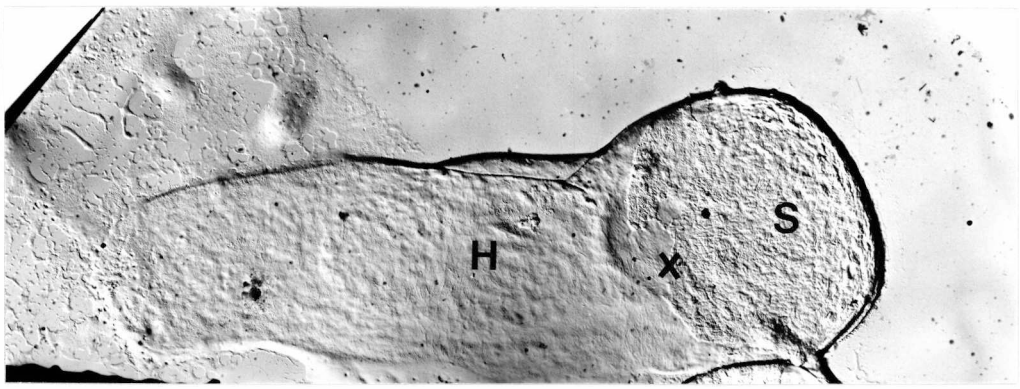
S
H
X

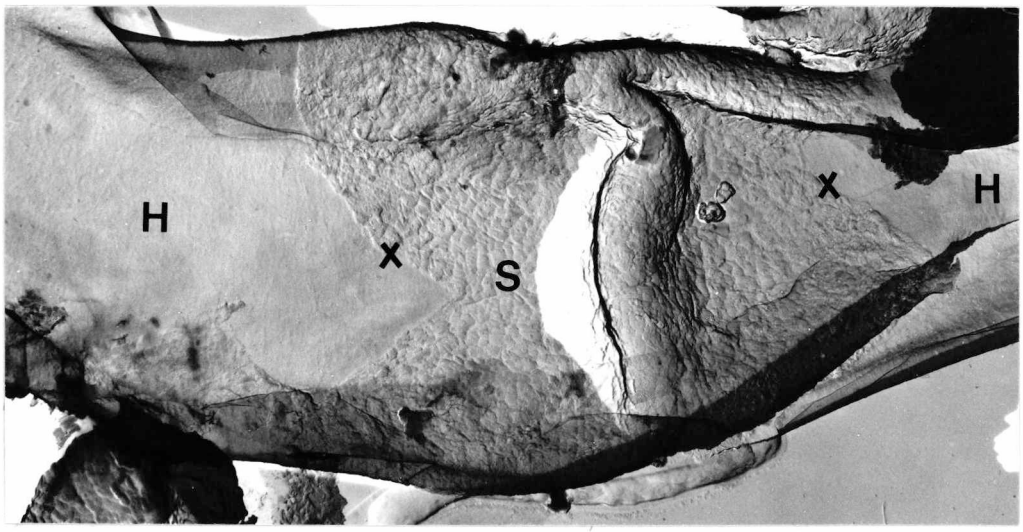
H
X
S
X
H

Fig. 111

SR of untreated germinated spore. The breakpoint (X) has a V-shape. The surface rodlets of the spore surface (S) contrast sharply with the smooth outer surface of the germ tube (H). This micrograph is a higher magnification of one of the breakpoints observed in Figure 110, (x40700)

Fig. 112

SR of untreated germinated spore showing a V-shaped breakpoint (x21600)

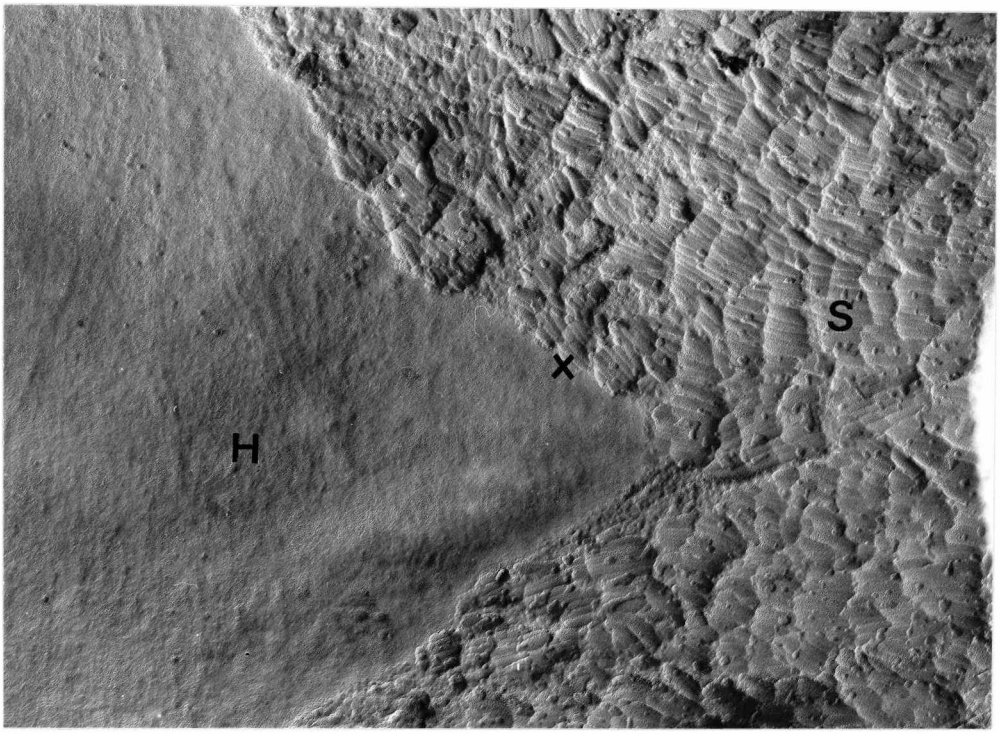
S
X
H

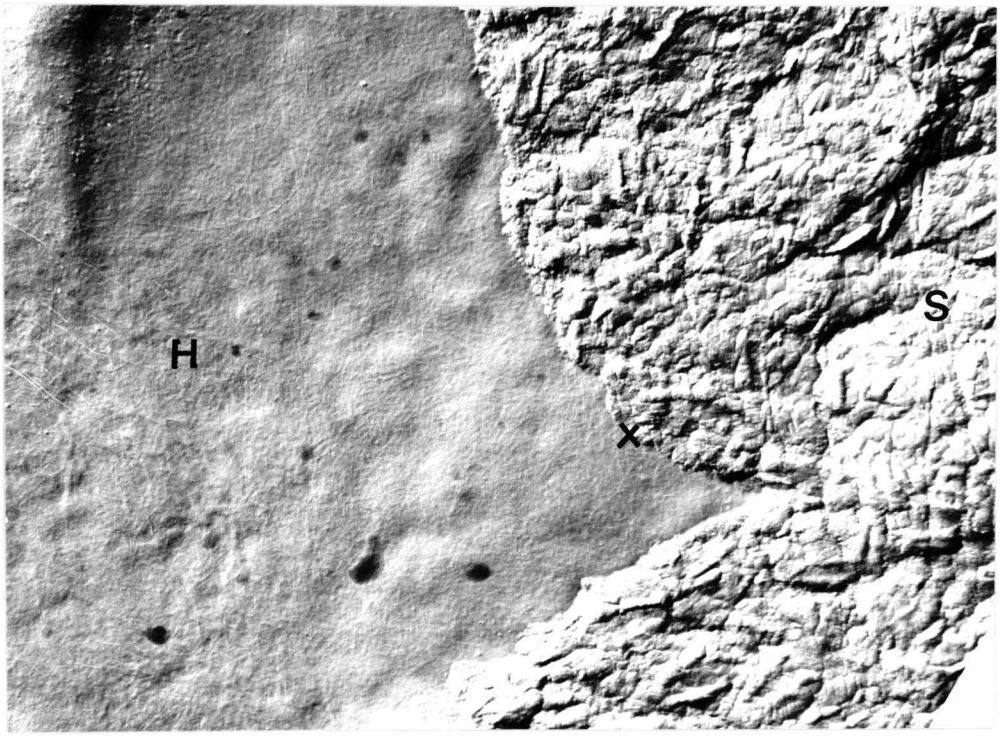
S
H
X

Fig. 113

SR of untreated swollen spore. The surface rodlet layer (S) is in disarray and the underlying amorphous layer (Am) is visible (x14400)

Fig. 114

SR of untreated swollen spore. The criss-cross pattern of surface rodlets is difficult to make out, and the rodlets appear to be arranged linearly (x15300)

Fig. 115

SR of untreated swollen spore. The cross-patched network of rodlets is in disarray (x11500)

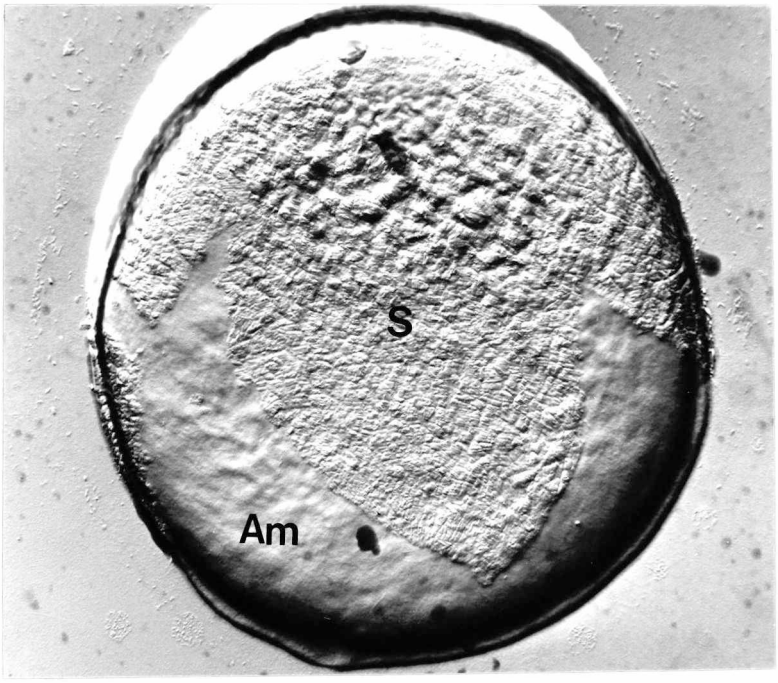
S
Am

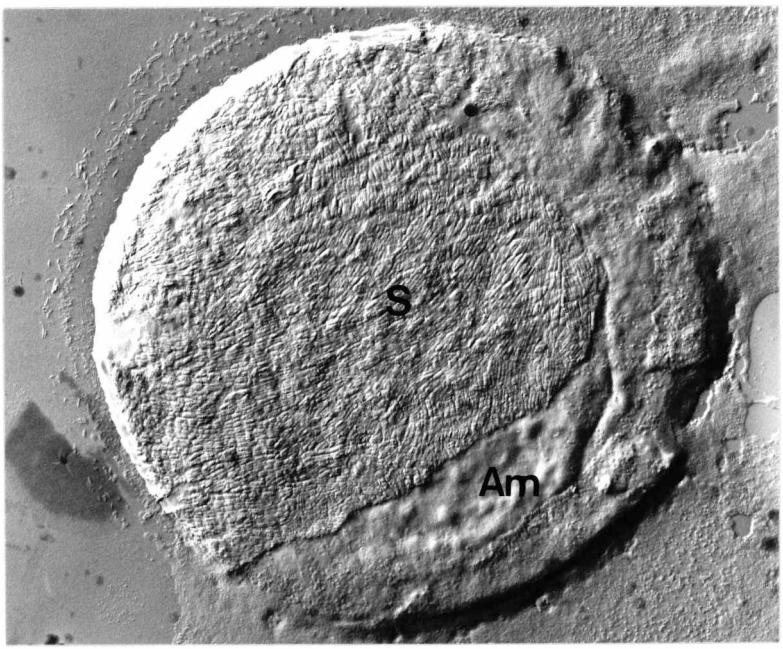
S
Am

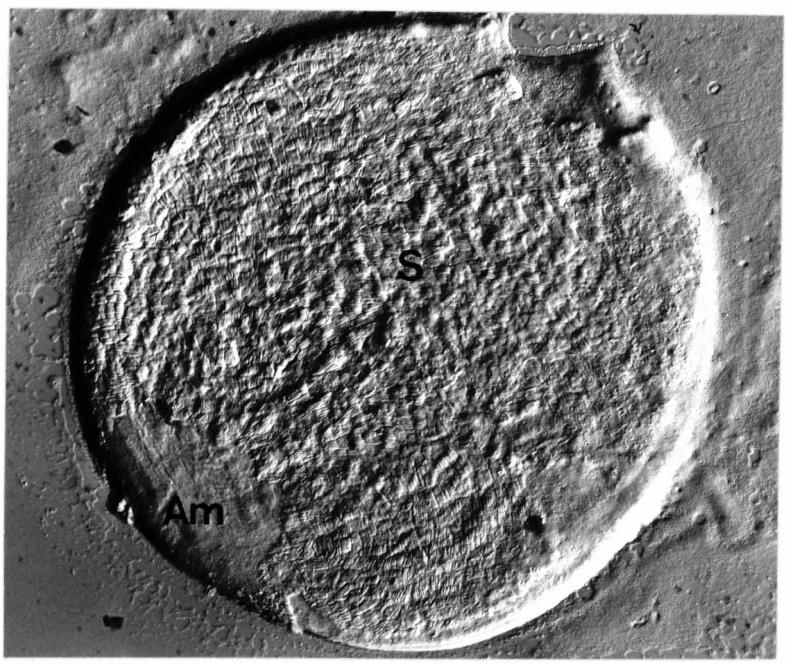
S
Am

Fig. 116

FF of untreated dormant spore. The cross-patched surface layer of rodlets contrasts very strikingly with the disorganisation of the surface layer observed in Figures 113-115, (x36200)

Fig. 117

SR of untreated germinated spore. The break-up of the cross-patched pattern of rodlets on the spore surface is seen even on germinated spores (x11500)

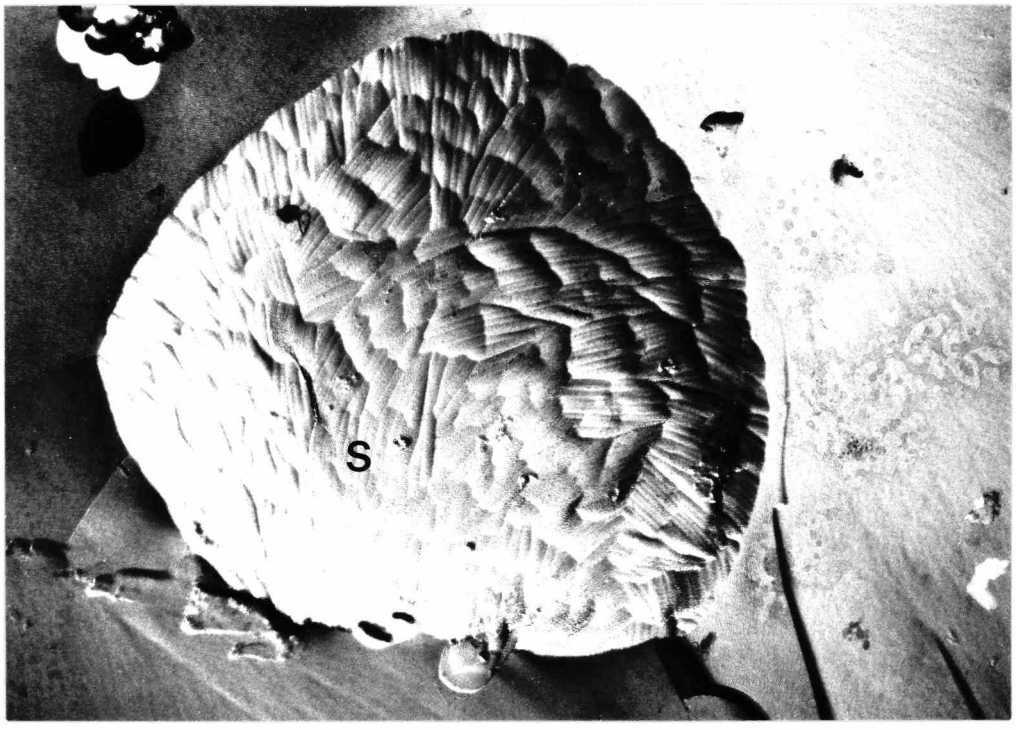
S


H
S
X

Fig. 118

SR of untreated swollen spore. The rodlets are so disarranged that areas free from rodlets have appeared, revealing the underlying amorphous layer (Am). Figure 119 also shows this phenomenon, (x16500)

Fig. 119

SR of untreated swollen spore (x12500)

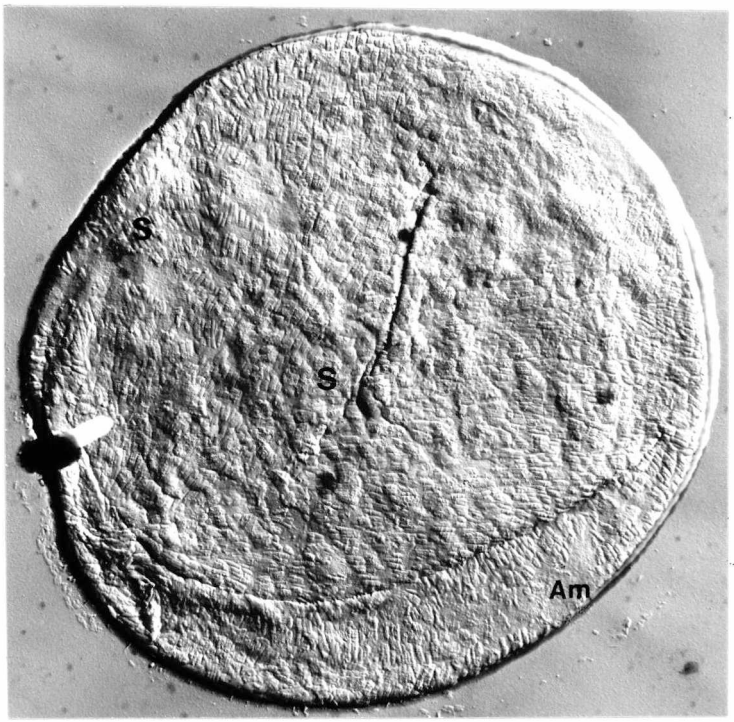
S
S
Am


S
Am
S
Am

Fig. 120

SR of germinated spores after 6h 5% KOH treatment. The surface rodlet layer of the spores has been removed and has revealed the plate-like layer covered with amorphous material (Am). The breakpoint (X) between spore and germ tube is seen, the emergent germ tubes having a smooth outer wall (x1900)

Fig. 121

SR of germinated spores after 6h 5% KOH treatment. The breakpoint (X) is present between the roughened surface of the spore and smooth germ tube wall (x4100)

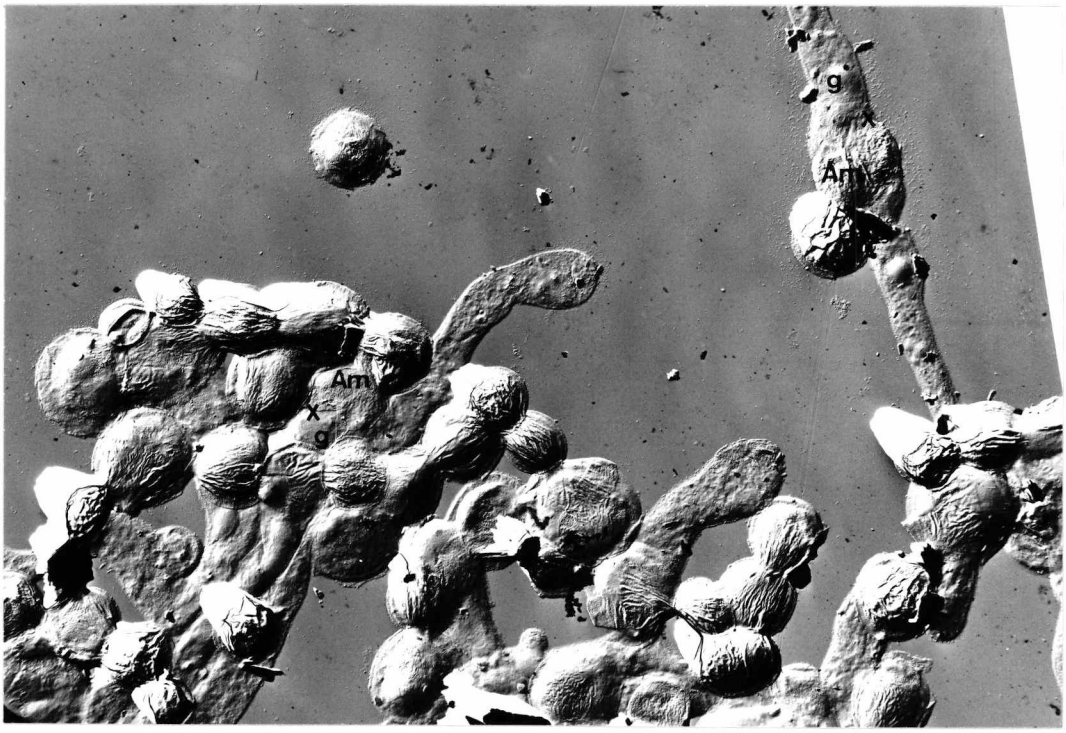
g
x
Am
Am
x
g

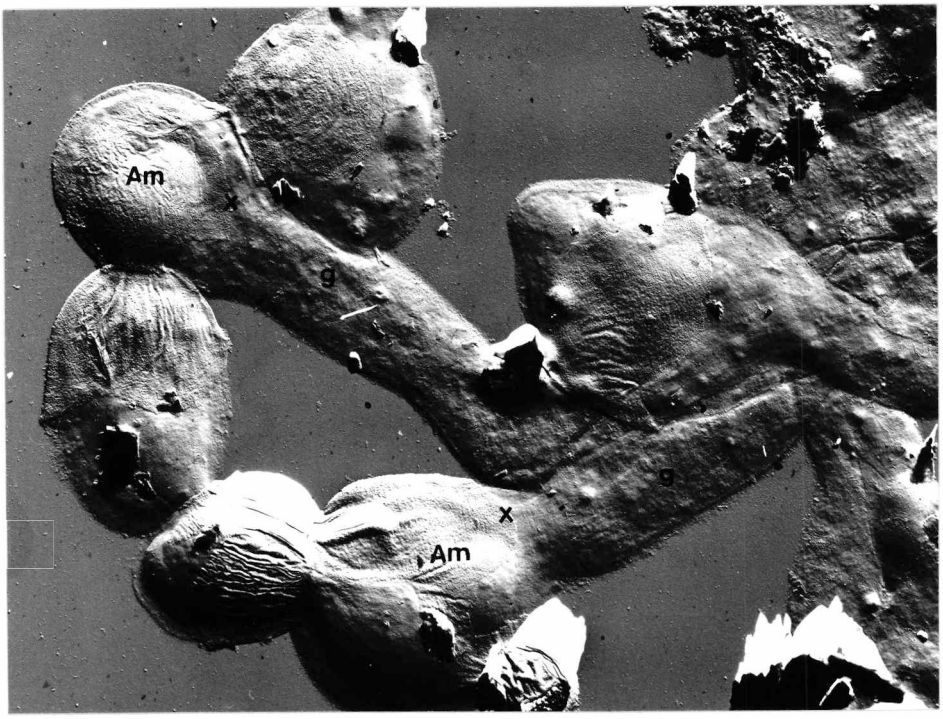
Am
x
g
g
x
Am

Fig. 122

SR of germinated and swollen spores after 6h 5% KOH treatment. On the left is a swollen spore, whilst on the right is a swollen spore with a young emerging germ tube (x7500)

Fig. 123

SR of swollen and germinated spores after 6h 5% KOH treatment. The two swollen spores are partly covered by a spore with a young emergent germ tube. The wall of the germ tube is smooth (x10200)

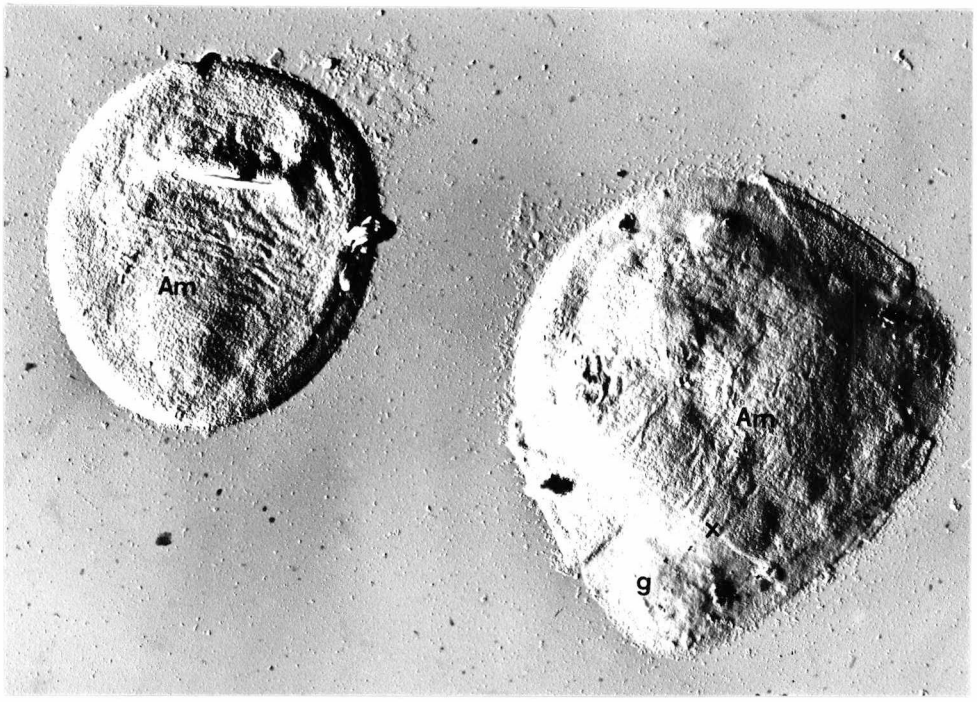
Am
Am
x
g

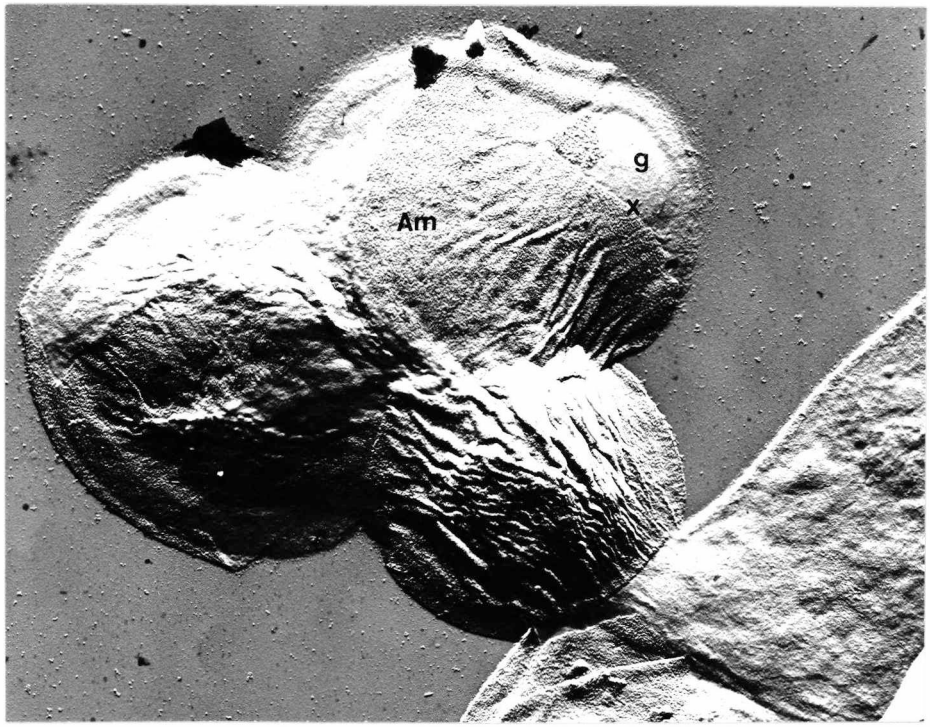
g
x
Am

Fig. 124

SR of germinated spore after 6h 5% KOH. In this and subsequent micrographs (Figs. 124-133), the breakpoint (X) (sometimes having a V-shape) delimits the smooth germ tube wall from the roughened wall of the spore (x3600)

Fig. 125

SR of germinated spore after 6h 5% KOH treatment (x5700)

Fig. 126

SR of germinated spore after 6h 5% KOH treatment (x6500)

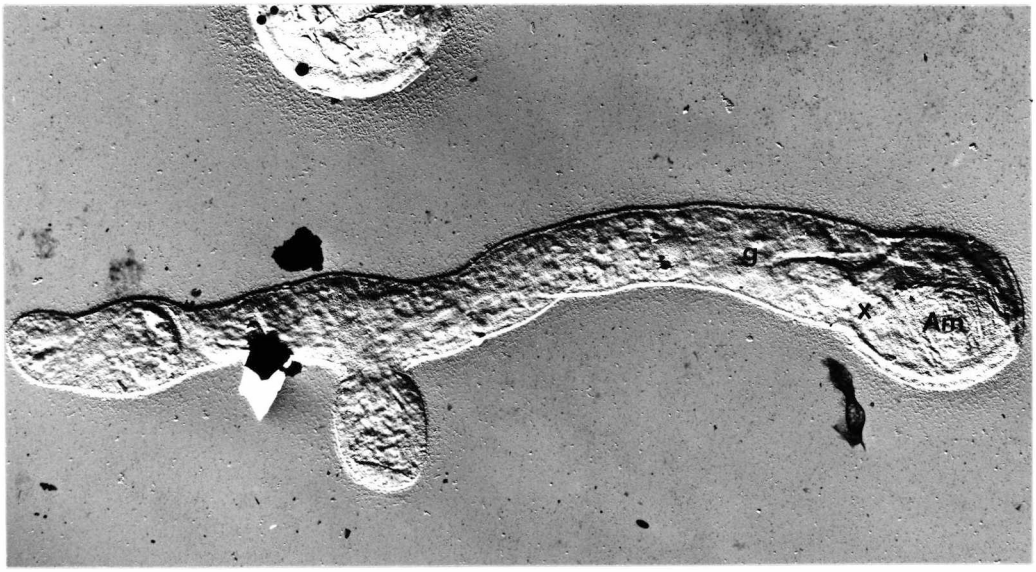
g
x
Am

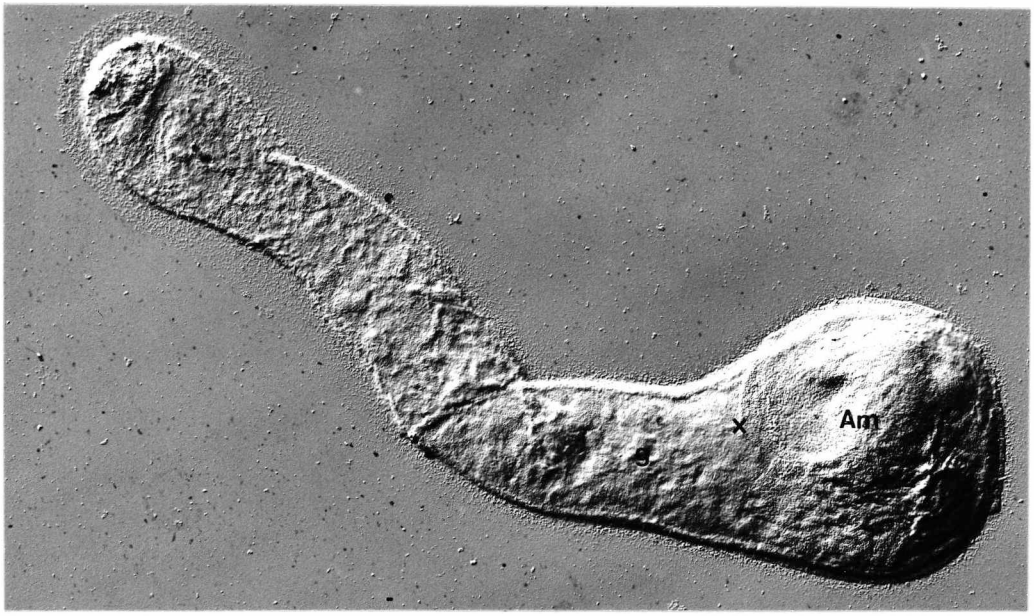
x
Am
g


Am
g

Fig. 127

SR of germinated spore after 6h 5% KOH treatment (x5600)

Fig. 128

SR of germinated spores after 6h 5% KOH treatment (x3900)

Fig. 129

SR of germinated spore, with two developing germ tubes, after 6h 5% KOH treatment (x9100)


g
Am

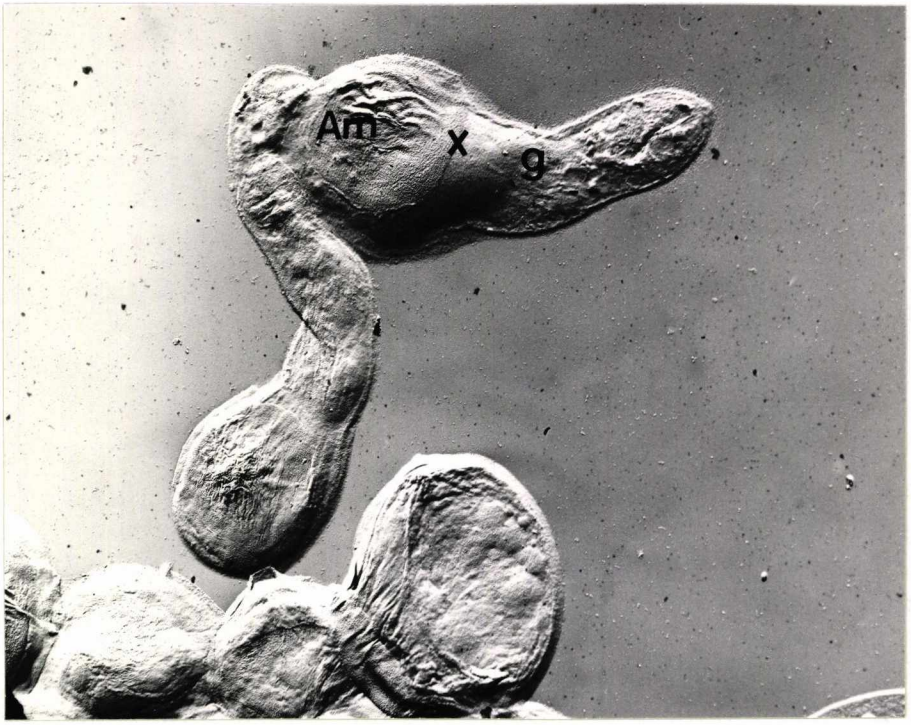
Am
x
g

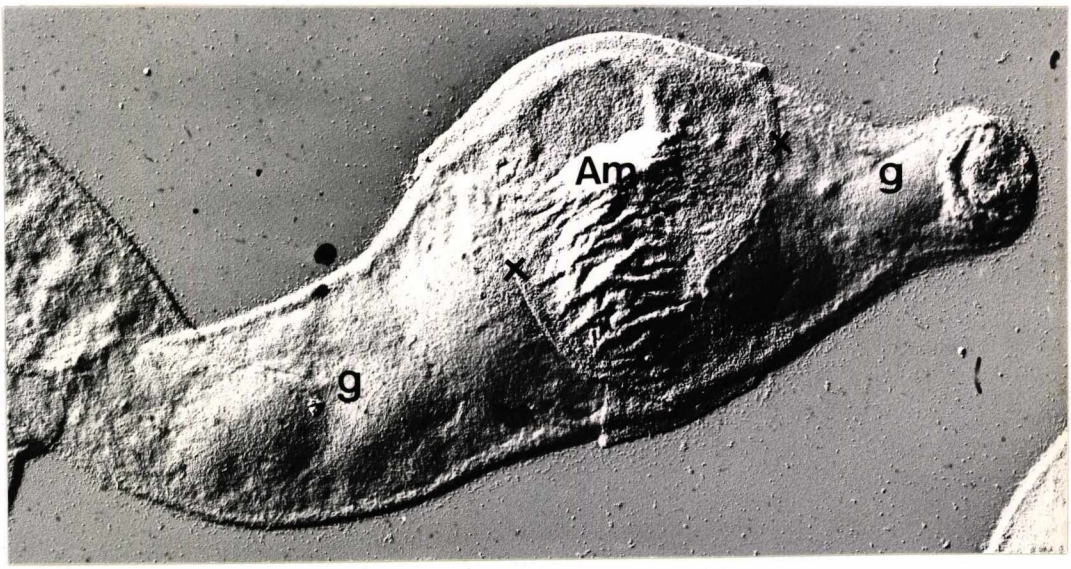
Am
g
x
g

Fig. 130

SR of germinated spore after 6h 5% KOH treatment. Here the germ tube has branched to give two young hyphae soon after emerging from the spore (x6500)

Fig. 131

SR of germinated spore after 6h 5% KOH treatment (x10300)

Fig. 132

SR of germinated spore after 6h 5% KOH treatment (x8200)

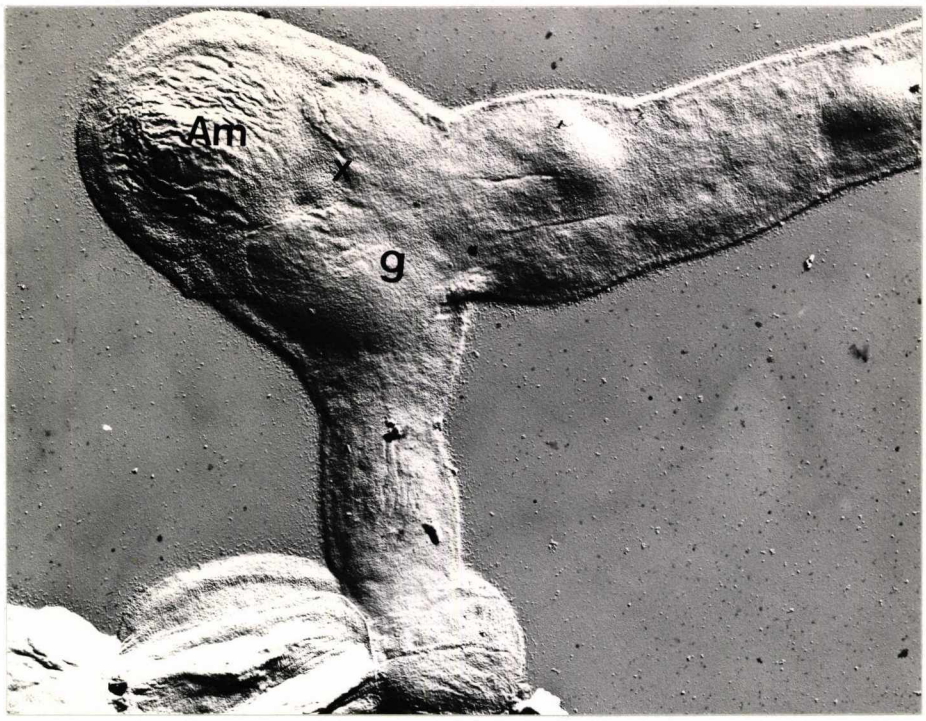
Am
x
g

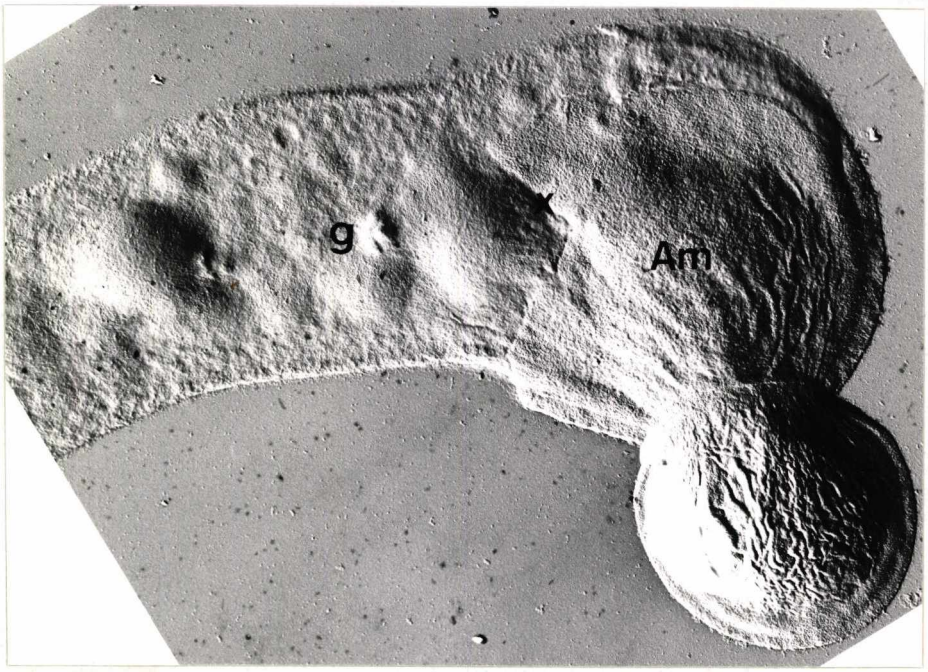
g
x
Am

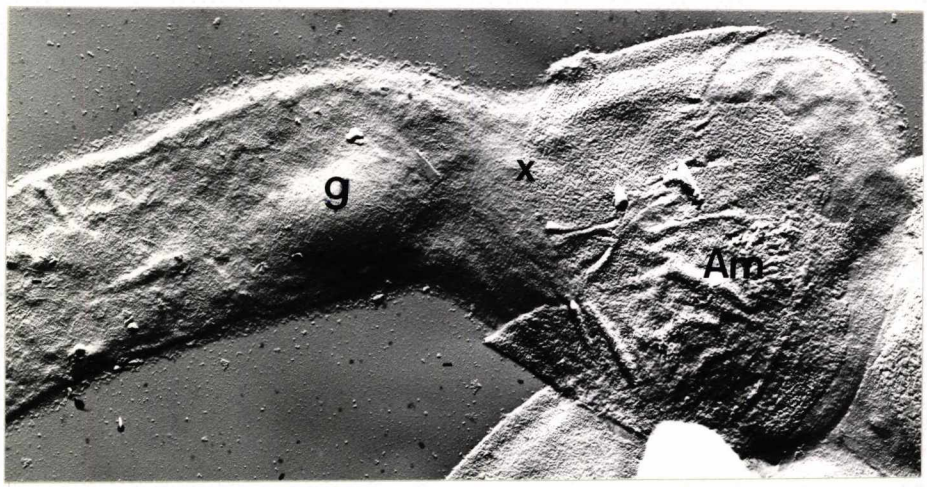
g
x
Am

Fig. 133

SR of germinated spore after 6h 5% KOH treatment (x8300)

Fig. 134

SR of germinated spore after 6h and 18h 5% KOH (initial alkaline) treatment. The breakpoint (X) is still visible (Figs. 134-136) between the rugose (rough surface) wall layer of the spore and the smooth outer wall of the germ tube. There is, however, some hint of an underlying microfibrillar layer (mf) in the germ tube (x8200)

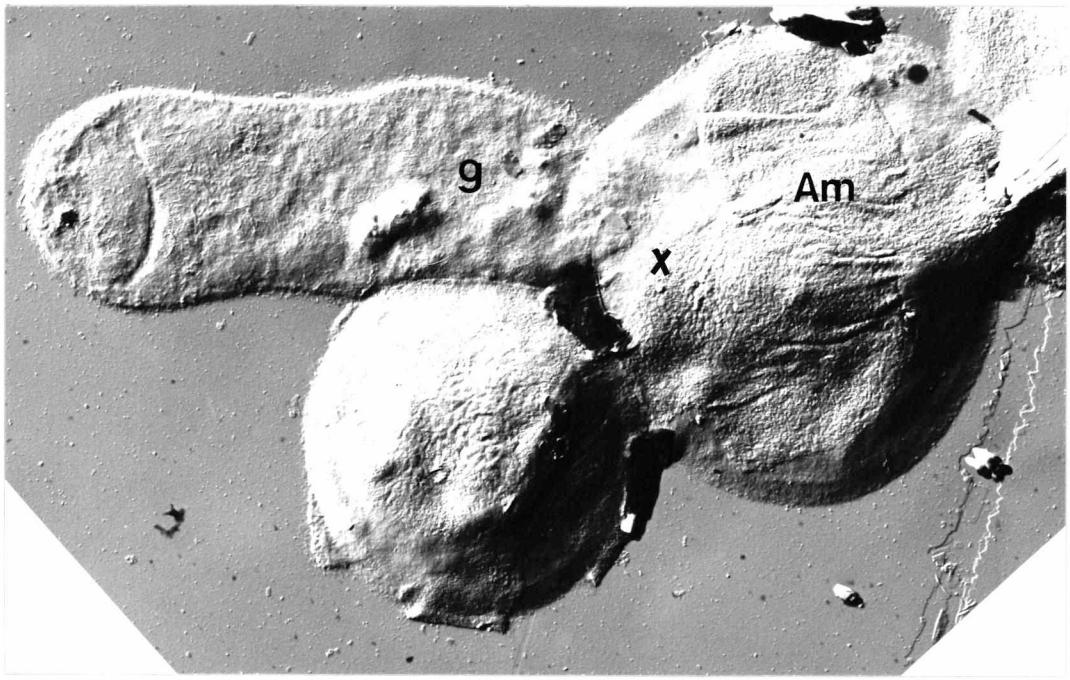
g
Am
x

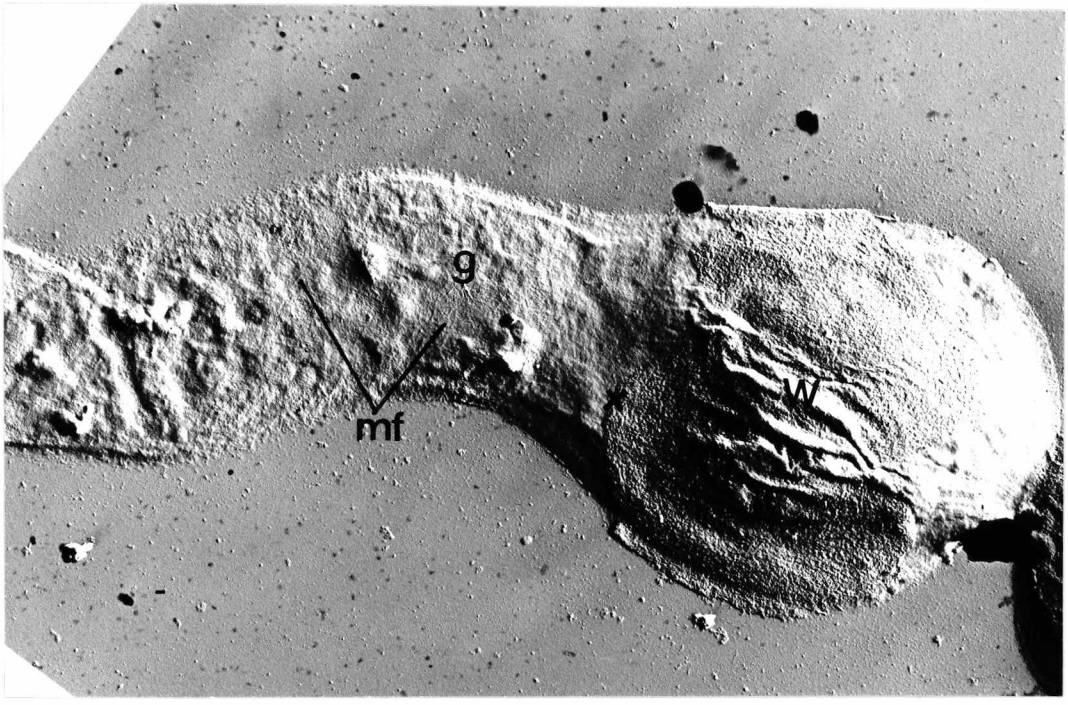
g
mf
W

Fig. 135

SR of germinated spore after initial alkaline treatment. Microfibrils are just visible beneath the outer amorphous layer of the germ tube (x8200)

Fig. 136

SR of germinated spore after initial alkaline treatment (x12900)

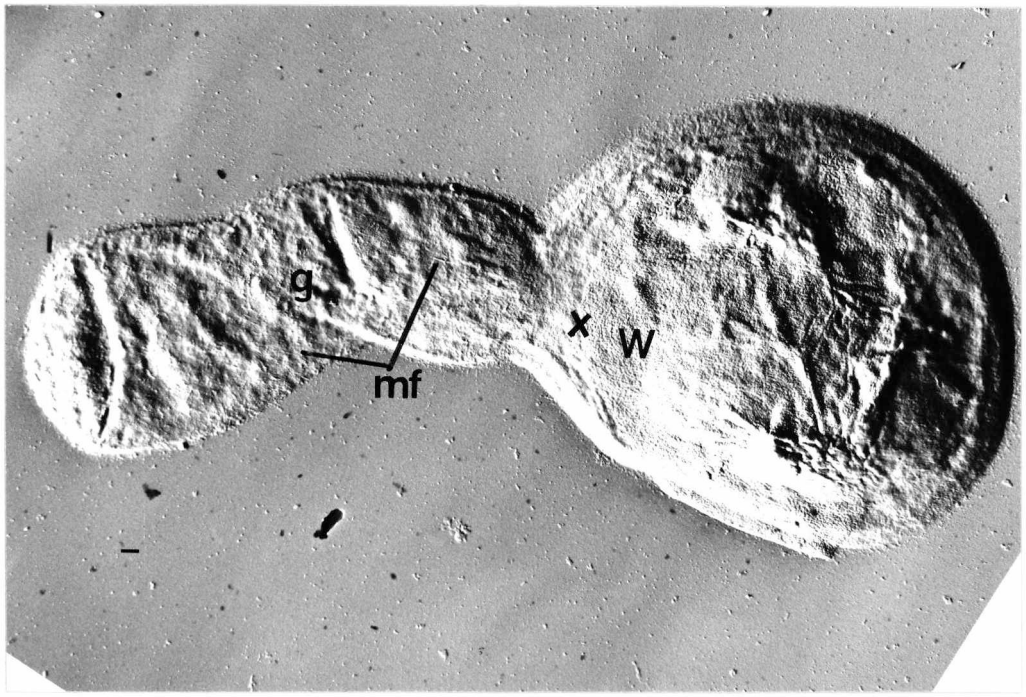
g
mf
x
w

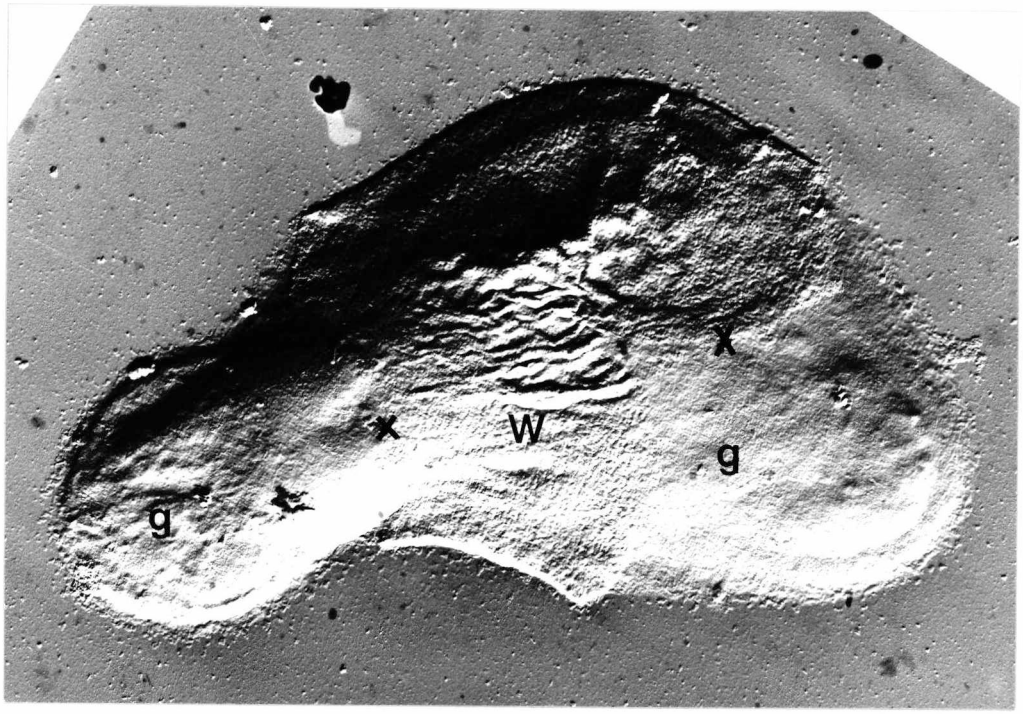
x
x
w
g
g

Fig. 137

SR of germ tube after (1) initial alkaline treatment and (2) autoclave procedure. The smooth, outer amorphous layer of the hypha has been removed revealing a layer of thin microfibrils (x20600)

Fig. 138

SR of germinated spore after (1) initial alkaline treatment and (2) autoclave procedure. No breakpoint is visible, only a layer of thin microfibrils of the spore wall which are continuous with the thin microfibrils of the germ tube (x8300)

Fig. 139

MS of swollen spore after completion of all chemical treatments. The innermost wall layer is composed of a randomly-orientated criss-cross network of thin microfibrils (x21200)

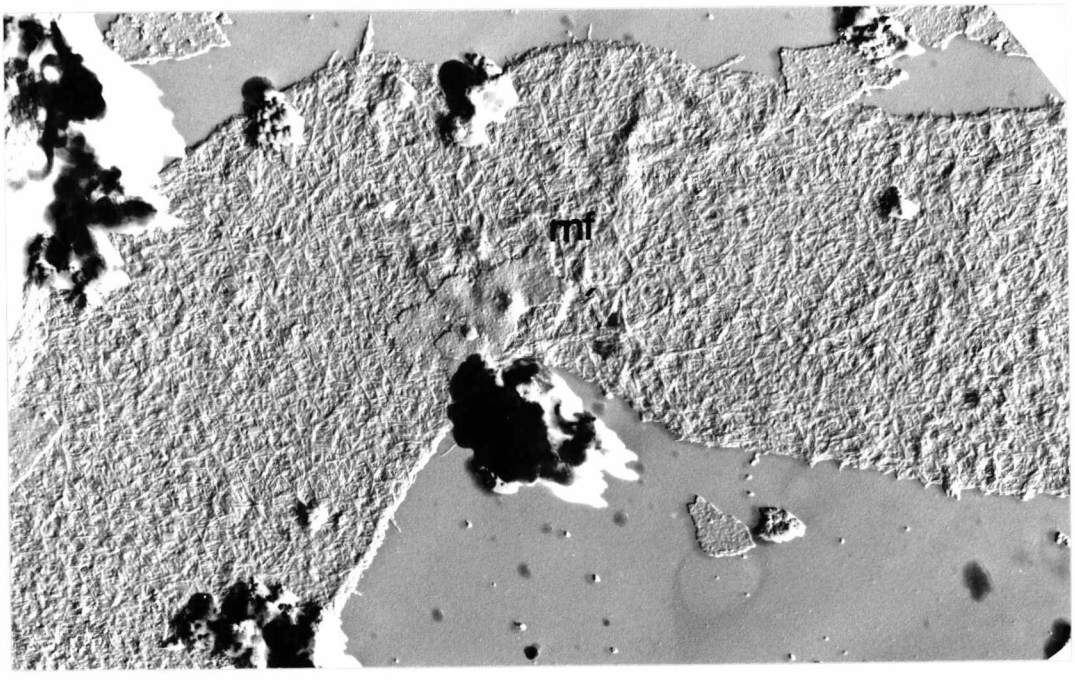
mf

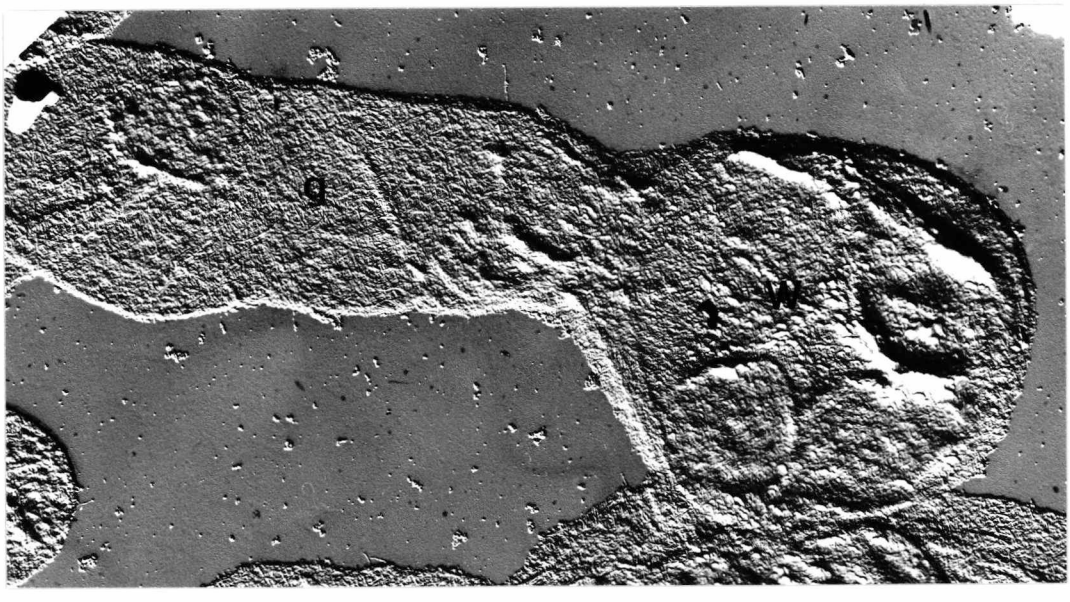
g

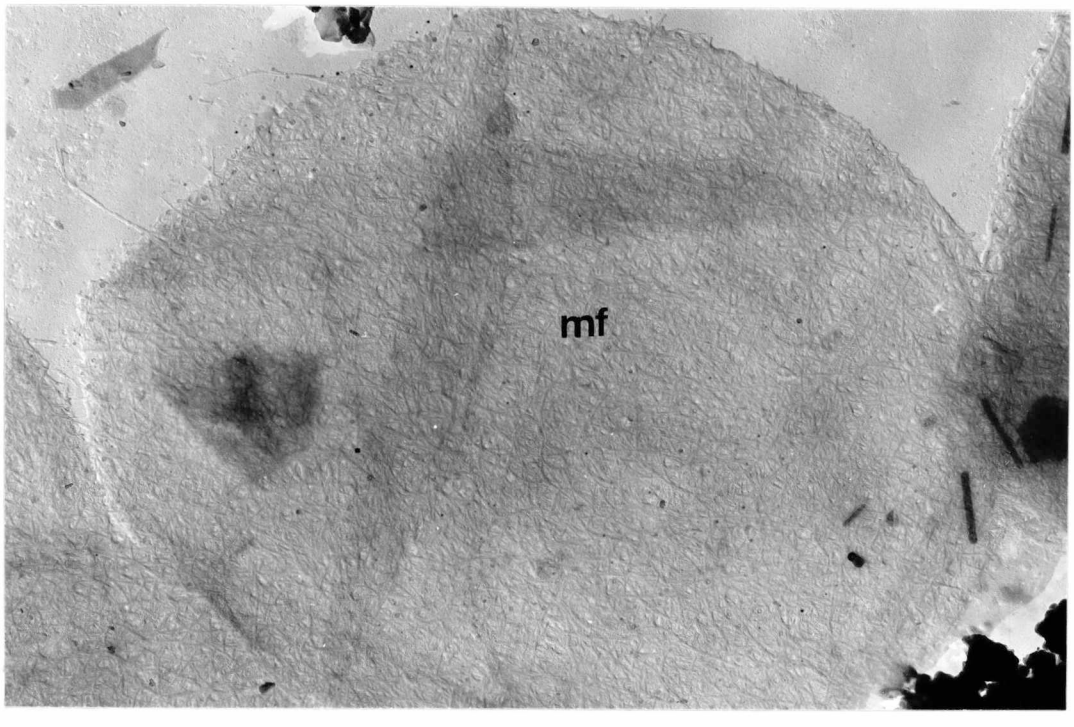
mf

Fig. 140

MS of germinated spore after completion of all chemical treatments. The thin microfibrils are present in both the swollen spore and germ tube. No breakpoint is noticeable (x12900)

Fig. 141

MS of germinated spore after completion of all chemical treatments. Higher magnifications of the point of attachment (Y) of germ tube to spore (Figs. 141, 142 and 144) show no breakpoint between spore and germ tube. Fibrils from spore and germ tube criss-cross over each other and run from one area to the other (x21600)

Fig. 142

MS of germinated spore after completion of all chemical treatments (x20000)

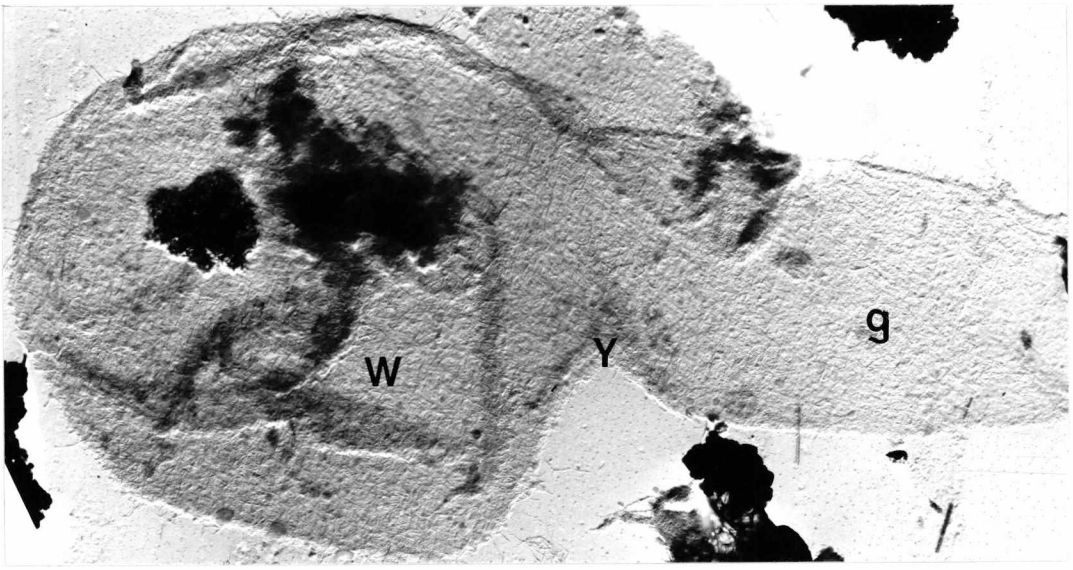
W
Y
g

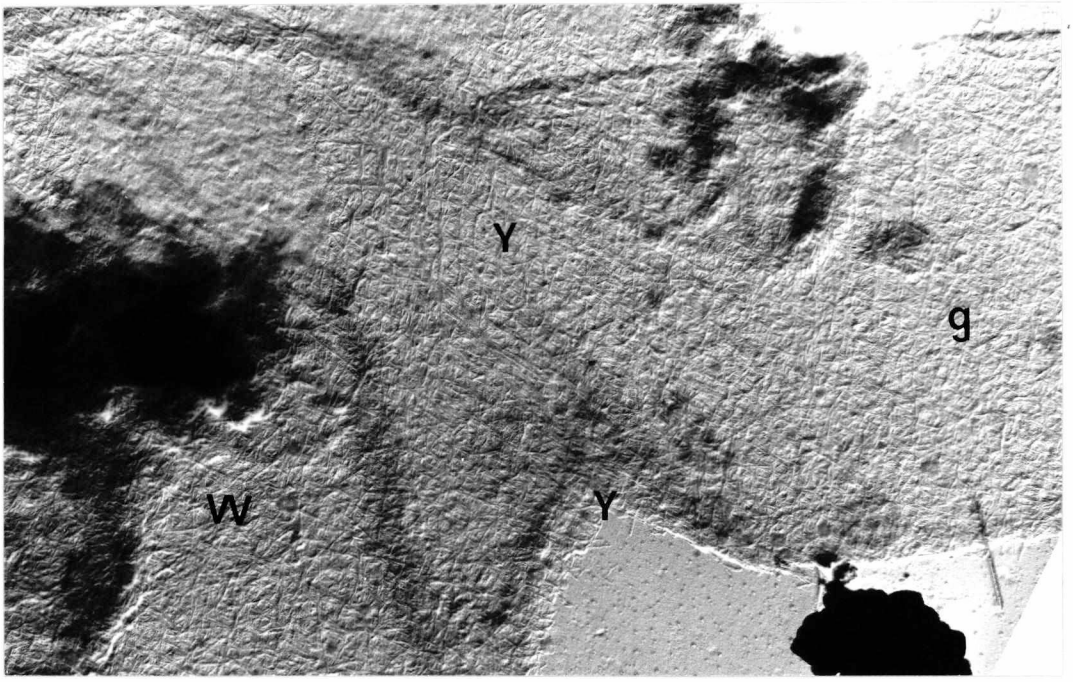
Y
g
W
Y

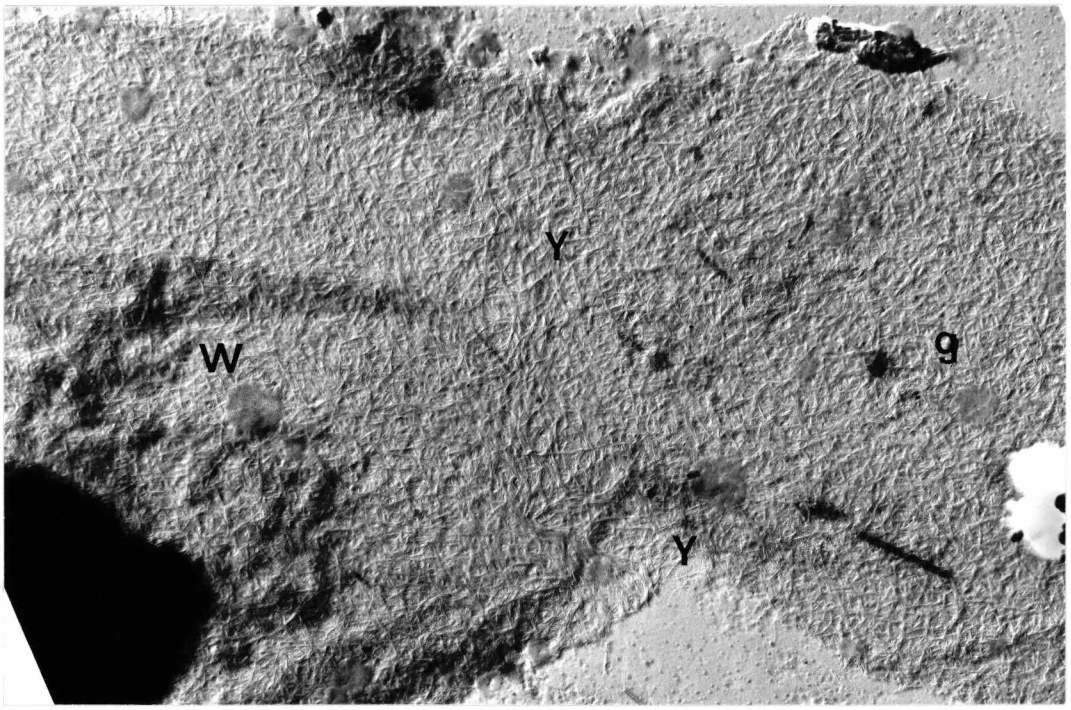
Y
W
g
Y

Fig. 143

MS of germinated spore after completion of all chemical treatments. The continuity of the spore and germ tube wall layer of thin microfibrils is emphasised by this micrograph (x19100)

Fig. 144

MS of germinated spore after completion of all chemical treatments (x29600)

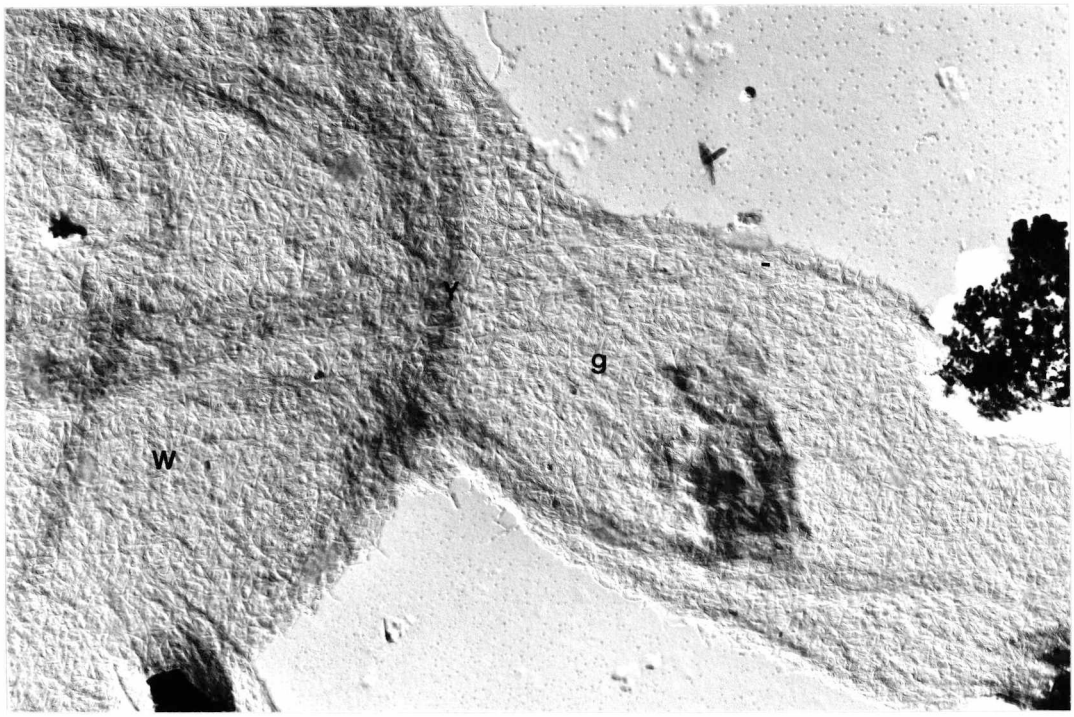
Y
g
W

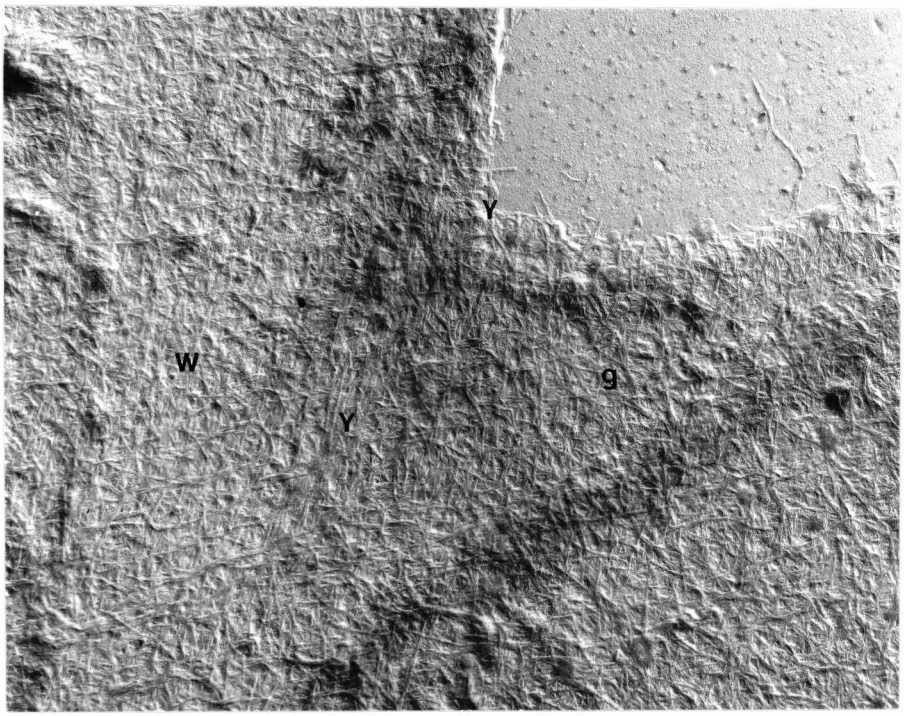
Y
W
g
Y

Fig. 145

Diagrammatic representation of spore wall changes during germination (cf. Figs. 100 and 101):

(1) Dormant spore wall.

(2) Swollen spore wall, (layer A is in disarray).

(3) Germ tube emergence.

(1)

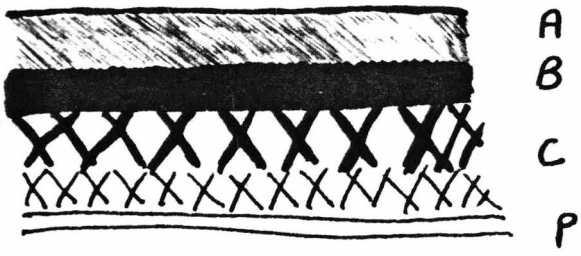

(2)

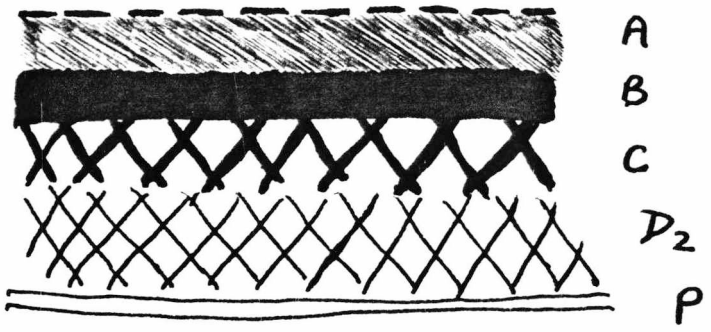

(3)

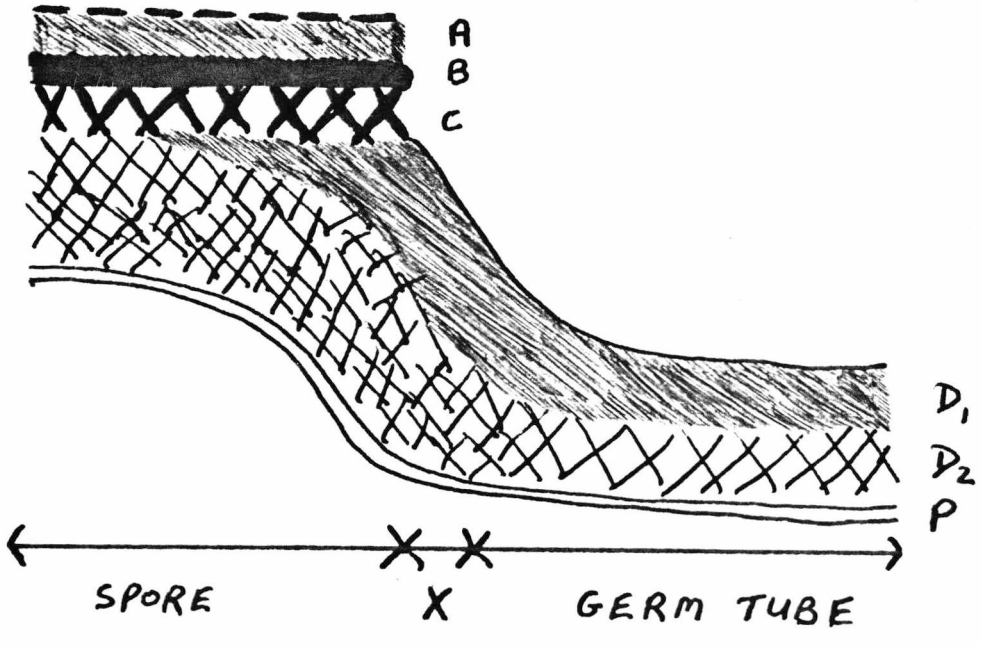

CHAPTER SEVEN

Fig. 146

FF of dormant spore (concave). The plasmamembrane is covered with an irregular pattern of large particles, some of which are arranged linearly into groups of three or four (arrowed), (x33000)

Fig. 147

FF of dormant spore (concave). The irregular pattern of large particles is arranged in groups of three in a few places (arrowed), (x33300)

Fig. 148

FF of dormant spore (concave), (x50200)


W

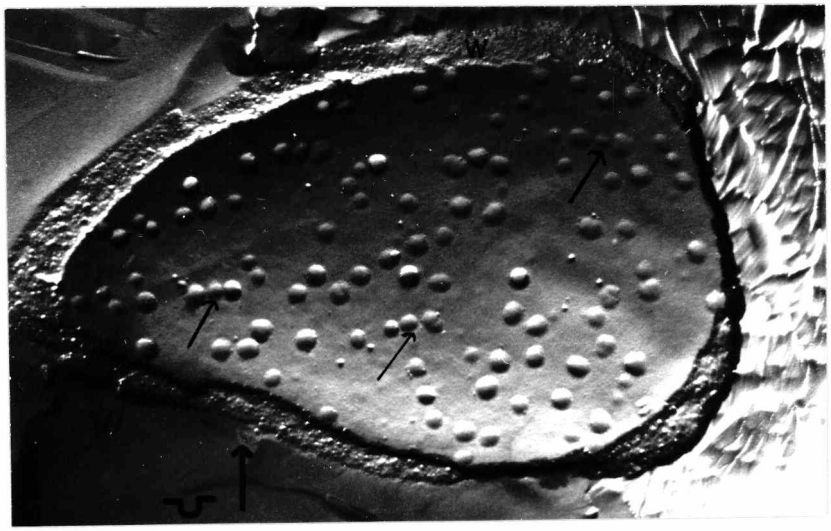
W

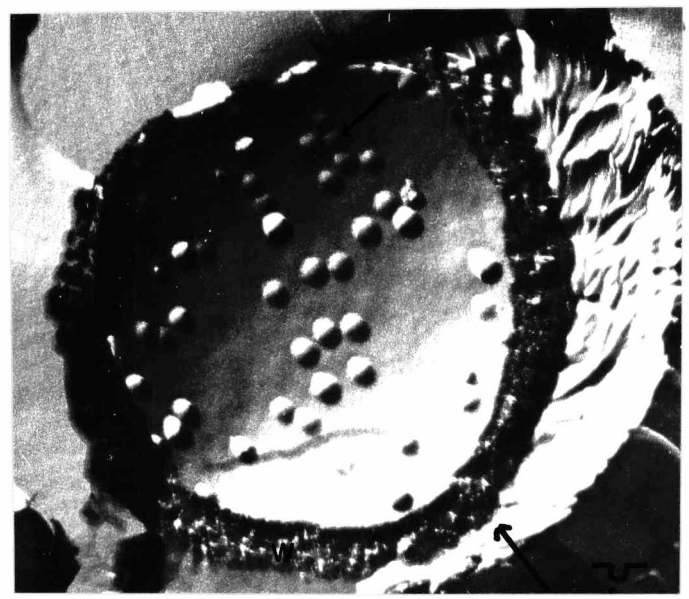

Fig. 149

FF of dormant spore (convex). The plasmamembrane is covered with numerous small particles and an irregular pattern of large depressions. In some places the large depressions are arranged linearly in groups of three (arrowed), (x50000)

Fig. 150

FF of dormant spore (convex). A higher magnification on the convex fracture face shows the numerous small particles and large depressions in greater detail (x98300)

Fig. 151

FF of swollen spore (concave). The plasmamembrane has a relatively smooth surface covered with numerous small particles (x41200)

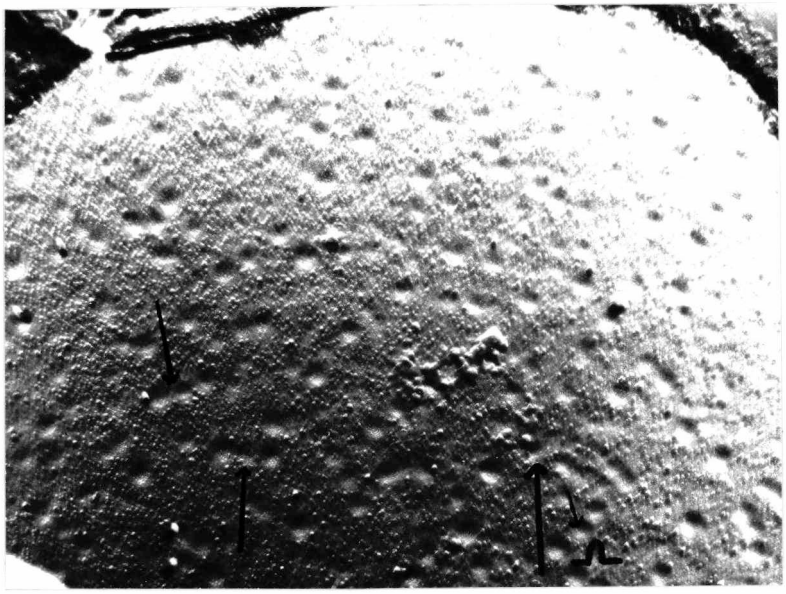

Fig. 152

FF of swollen spore (concave). Higher magnification of the smooth plasmamembrane surface covered with numerous small particles (x85200)

Fig. 153

FF of swollen spore (convex). The plasmamembrane is covered with numberous small particles (x48900)

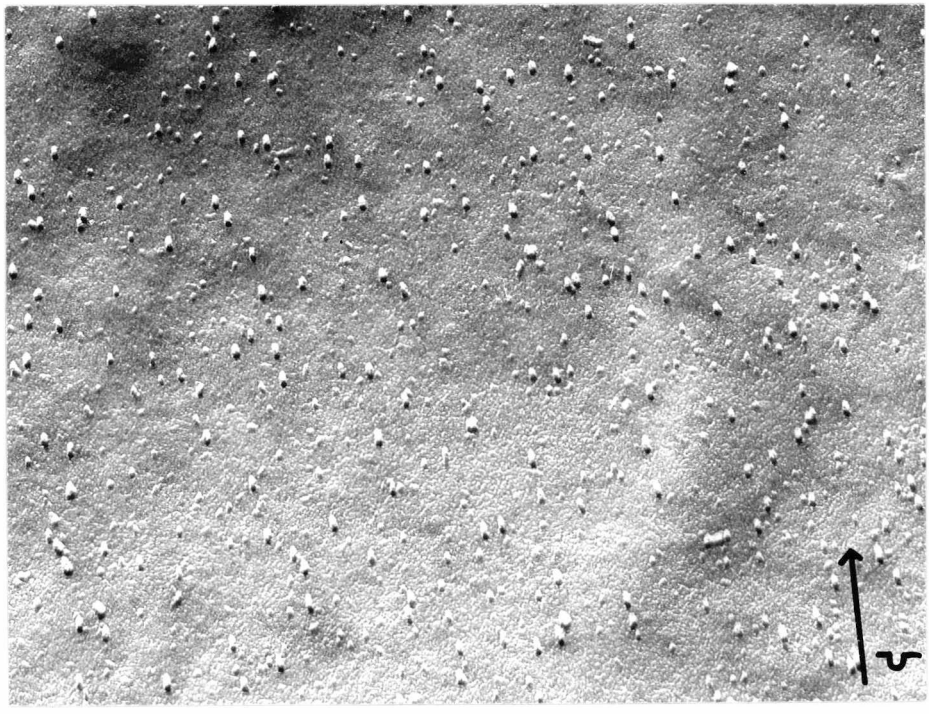

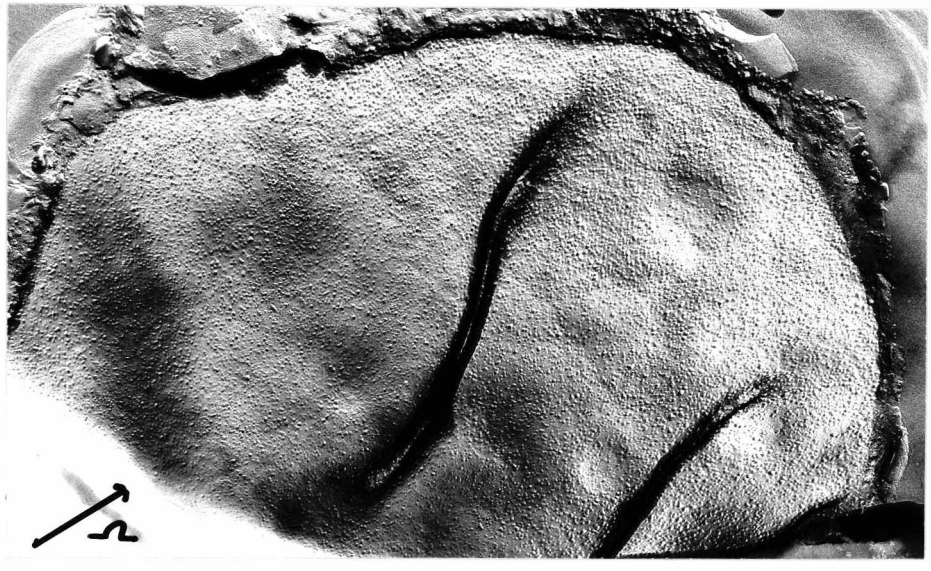

Fig. 154

FF of swollen spore (convex). Numerous small particles are seen on the plasmamembrane surface (x41000)

Fig. 155

FF of swollen spore (convex). Higher magnification of the plasmamembrane surface show it to be covered with numerous small particles and also intermediate particles (IP) arranged in an irregular pattern (x69800)

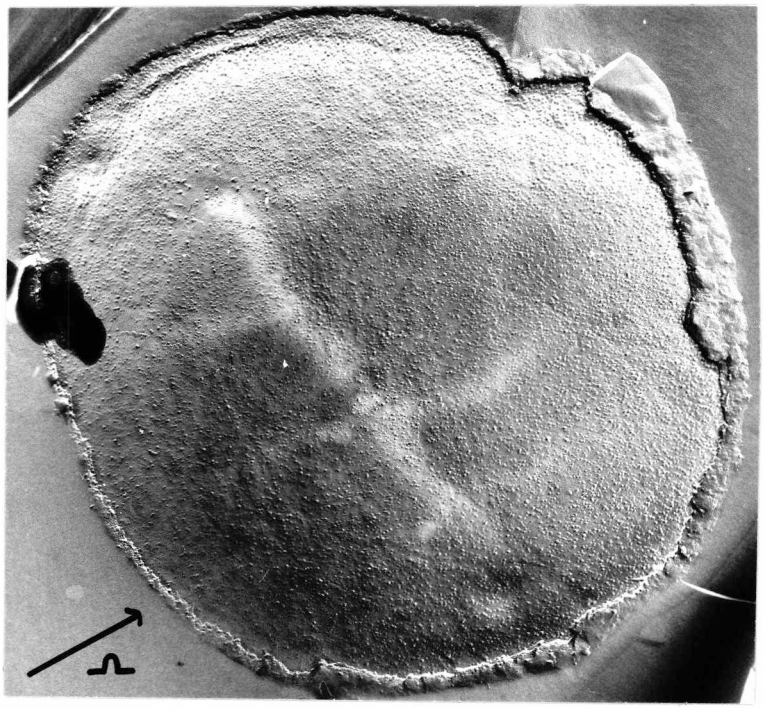


IP
IP

Fig. 156

FF of germ tube (convex). Numerous small particles can be seen on the convex fracture face of the germ tube plasmamembrane (x70200)

Fig. 157

FF of swollen spore with young emergent germ tube (convex). Numerous small particles and some intermediate particles are seen on the plasmamembrane surface of the young emergent hypha (x37500)

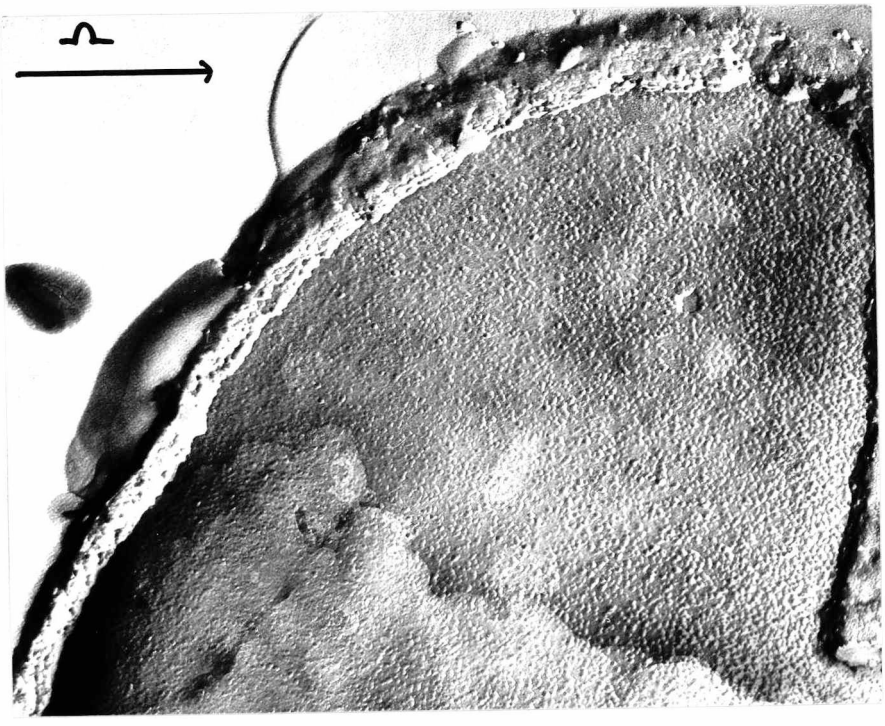


IP
Cv

Fig. 158

Diagrammatic summary of the freeze-fracture observations of (1) dormant, (2) swollen and (3) germinated spore plasmamembrane.

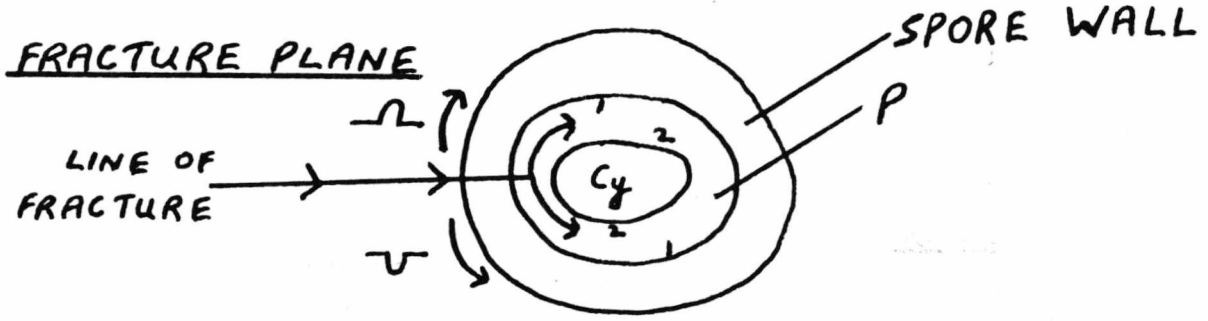

∪ CONCAVE FRACTURE REVEALS FACE 1.

∩ CONVEX FRACTURE REVEALS FACE 2.

(1).

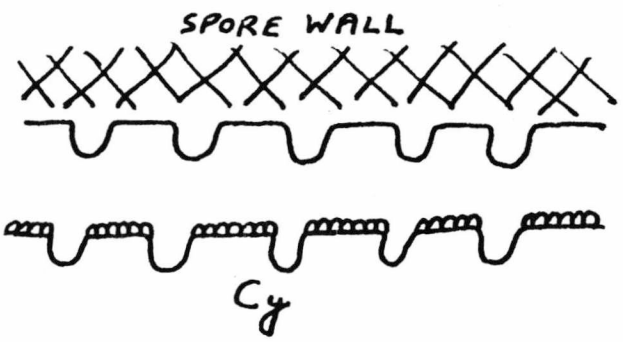

(1) ∪ LARGE PARTICLES

(2) ∩ LARGE DEPRESSIONS, SMALL PARTICLES

(2).

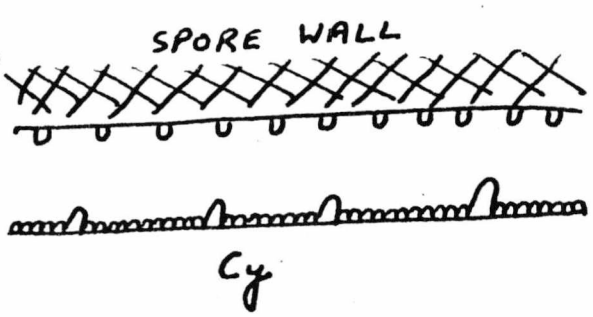

(1) ∪ SMALL PARTICLES

(2) ∩ SMALL PARTICLES, INTERMEDIATE PARTICLES

(3).

(2) ∩ SMALL PARTICLES

Fig. 159

Diagrammatic representation of the plasmamembrane in (1) dormant and (2) swollen spores, (cf. Malhotra and Tewari, 1973):

L - lipid bilayer

LP - large particles

SP - small particles

LD - large depressions

IP - intermediate particles

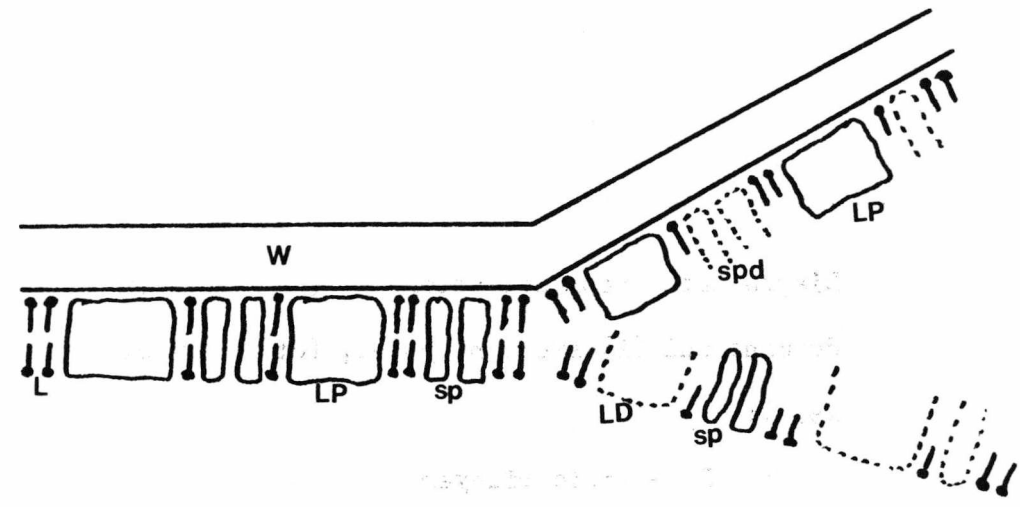

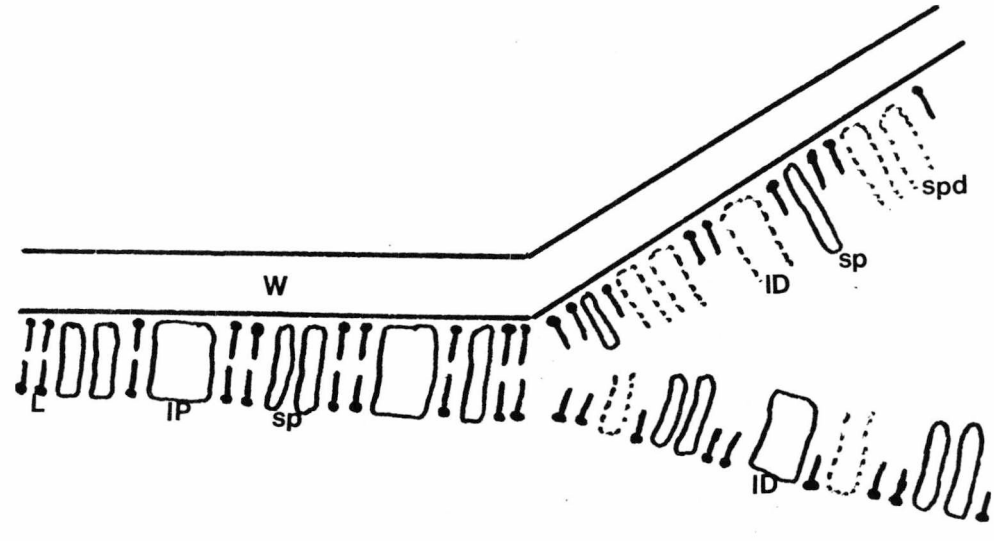

ID/spd – IP & sp depressions not seen in the EM.